DEMOKRITOS

Institute Of Nuclear and Particle Physics

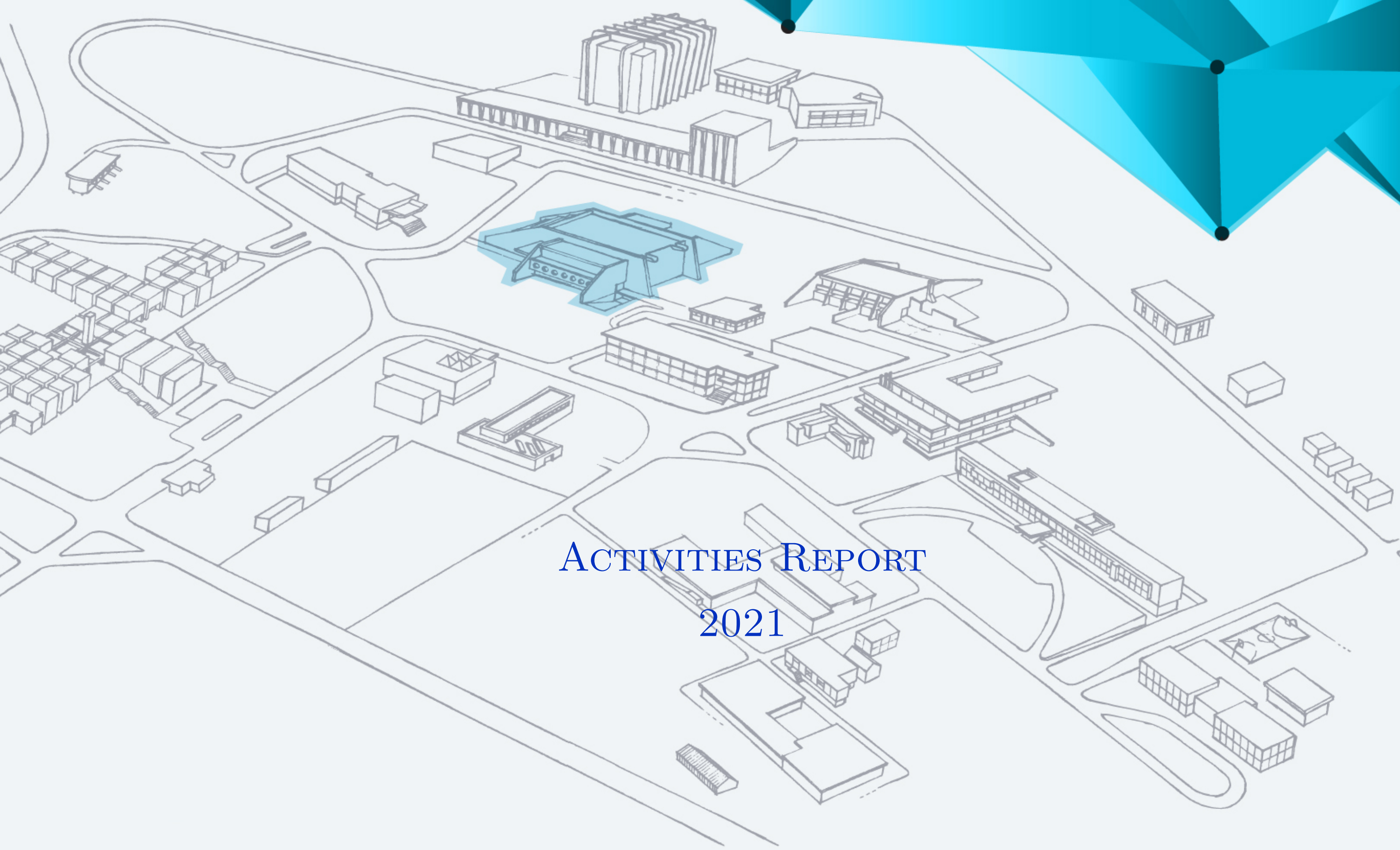

Activities Report

2021

Institute Of Nuclear and Particle Physics

National Center for Scientific Research "DEMOKRITOS"

Activities Report

2021

Editors:

C. Markou, M. Axiotis, G. Kareli

January 2021

Institute of Nuclear and Particle Physics,
NCSR "Demokritos"
Aghia Paraskevi, 15310, Athens, Greece

http://www.inp.demokritos.gr

Contents

Overview

The Institute of Nuclear and Particle Physics (INPP), at NCSR Demokritos, has as its mission the experimental and theoretical research, scientific excellence and innovation in High-Energy Physics, Nuclear Physics and Astro-Particle Physics as well as their applications in line with the National Research and Innovation Strategy for Smart Specialization.

The experimental and theoretical research in High Energy Physics focuses on the study of elementary particles and their interactions. INPP participates in the CMS and ATLAS experiments of the LHC at CERN. The Detector Instrumentation Laboratory (DIL) and the Data Acquisition, Monitoring and Analysis Laboratory (DAMA) of INPP, develop innovative detector technologies and instrumentation along with applications in science and innovation.

Nuclear Physics research focuses on Nuclear Structure, Nuclear Reactions, Nuclear Astrophysics and the study of interactions of X-rays with matter. The INPP hosts a 5.5. MV Tandem accelerator, a unique research infrastructure in Greece that is open to external users from Greece and abroad. The Tandem accelerator laboratory is an interdisciplinary open-access research infrastructure with innovative applications covering the fields of cultural heritage, environment, energy, human health and the development and testing of advanced materials and detectors. The XRF laboratory focuses on cultural heritage, environmental monitoring and biomedicine and offers technology transfer and on-site analytical services to museums, archaeological sites and other institutions.

The Astro-Particle Physics group participates in the development, deployment, data acquisition and data analysis of the kilometer cube underwater neutrino telescope in the Mediterranean, KM3NeT. The INPP hosts the Laboratory of Assembly, Testing and Calibration of the Digital Optical Modules, the basic units of the KM3NeT telescope. The INPP supports also the Deep-Sea Technology and Astro-Particle Physics Research Infrastructure in South-West Peloponnese (Kalamata, Pylos, Methoni).

Dr. C. Markou, Director INPP
tel. +302106503511
email: cmarkou@inp.demokritos.gr

Ms. G. Kareli, Secretary INPP
tel. +302106503512
email: gkarel@inp.demokritos.gr

Web-site: www.inp.demokritos.gr

Organizational Chart

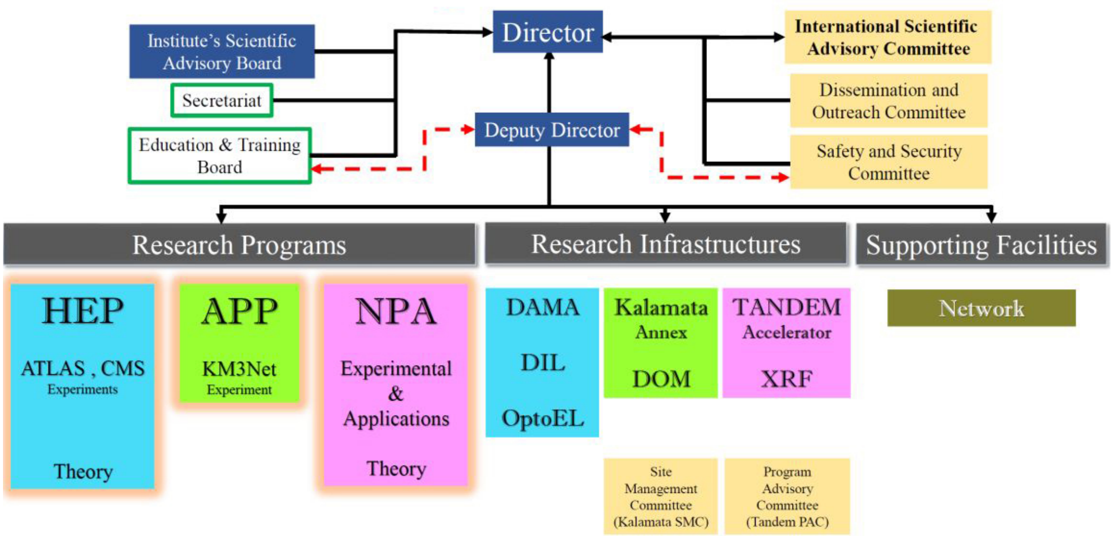

Director:	Dr. C. Markou
Deputy Director:	Dr. M. Axenides
Administration:	G. Kareli, Secretary M. Simantirakis, Administration
Institute Scientific Advisory Board:	M. Axenides (Chair) G. Anagnostou A. Karydas T. Geralis A. Lagoyannis
International Scientific Advisory Committee:	Prof. C. Bachas, Ecole Normale Superieure Prof. A. Bracco, University of Milan Prof. D. Charlton, University of Birmingham Prof. Y. Karyotakis, LAPP Annecy Prof. K. Kokkotas, University of Tübingen Prof. M. Lewitowicz, GANIL Prof. F. Linde, NIKHEF

Scientists in charge

High Energy Physics	Dr. T. Geralis: HEP-ATLAS & DAMA Dr. D. Loukas: HEP-CMS & DIL Dr. M. Axenides: HEP-Theory
Nuclear Physics & Applications	Dr. D. Bonatsos: Nuclear Structure Theory Dr. S. Harissopulos: Experimental Nuclear Physics & Applications – Tandem Dr. A. Karydas: XRF Laboratory & Applications
Astroparticle Physics	Dr. C. Markou: APP-KM3NeT

Personnel

The lists below reflect the INPP personnel as of the 31st of December 2021.

Researchers

Dr. Georgios **ANAGNOSTOU**	Senior Researcher	Exp. High-Energy Physics	anagnog@inp.demokritos.gr
Dr. Minos **AXENIDES**	Director of Research	Theoretical Particle & Astroparticle Physics	axenides@inp.demokritos.gr
Dr. Michail **AXIOTIS**	Researcher	Exp. Nuclear Physics	axiotis@inp.demokritos.gr
Dr. Dionysios **BONATSOS**	Director of Research	Theoretical Nuclear Physics	bonat@inp.demokritos.gr
Dr. Georgios **DASKALAKIS**	Director of Research	Exp. High-Energy Physics	daskalakis@inp.demokritos.gr
Dr. Evaggelia **DRAKOPOULOU**	Researcher	Astroparticle Physics	drakopoulou@inp.demokritos.gr
Dr. Theodoros **GERALIS**	Director of Research	Exp. High-Energy Physics	geral@inp.demokritos.gr
Dr. Sotirios **HARISSOPULOS**	Director of Research	Exp. Nuclear Physics	sharisop@inp.demokritos.gr
Dr. Andreas **KARYDAS**	Director of Research	Exp. Nuclear Physics	karydas@inp.demokritos.gr
Dr. Aristotelis **KYRIAKIS**	Director of Research	Exp. High-Energy Physics	kyriakis@inp.demokritos.gr
Dr. Anastasios **LAGOYANNIS**	Director of Research	Exp. Nuclear Physics	lagoya@inp.demokritos.gr
Dr. Dimitrios **LOUKAS**	Director of Research	Exp. High-Energy Physics	loukas@inp.demokritos.gr
Dr. Christos **MARKOU**	Director of Research	Exp. High-Energy & Astroparticle Physics	cmarkou@inp.demokritos.gr
Dr. Konstantinos **PAPADOPOULOS**	Director of Research	Theoretical Particle Physics	cgppdo@inp.demokritos.gr
Dr. Georgios **STAVROPOULOS**	Director of Research	Exp. High-Energy & Astroparticle Physics	stavrop@inp.demokritos.gr
Dr. Ekaterini **TZAMARIUDAKI**	Director of Research	Astroparticle Physics	katerina@inp.demokritos.gr

Special Scientific Officer

Ioannis **KAZAS**	Exp. High-Energy Physics	kazas@inp.demokritos.gr

Other Scientific Personnel

Stavroula **TSAGLI**	Physicist	tsagli@inp.demokritos.gr

INPP Administration

Emmanuel **SIMANTIRAKIS**	Administrator	msiman@inp.demokritos.gr

INPP Secretariat

Georgia **KARELI**	Secretary	gkarel@inp.demokritos.gr

Technicians

Vassilios **ANDREOPOULOS**	Electronics	andreo@inp.demokritos.gr
Panagiotis **BABOULAS**	Technician	baboulas@inp.demokritos.gr
Ioannis **KISKIRAS**	Electronics	kiskiras@inp.demokritos.gr
Emmanuel **TSOPANAKIS**	Workshop technician	mtsop@inp.demokritos.gr
Aggelos **VOUGIOUKAS**	Craftsman	vougioukas@inp.demokritos.gr

Support Personnel

Sophia **BAKOU**	General support	bakou@inp.demokritos.gr

Personnel under fixed term contracts

Miltiadis **ANDRIANIS**	Physicist	A. Lagoyannis	madrian@inp.demokritos.gr
Patric **ASENOV**	Physicist	D. Loukas	asenov@inp.demokritos.gr
Panagiotis **ASSIOURAS**	Physicist	D. Loukas	assiouras@inp.demokritos.gr
Dhimiter **CANKO**	Physicist	C. Papadopoulos	canko@inp.demokritos.gr
Maria **DASOPOULOU**	Chemist	C. Markou	mariadasopoulou1@gmail.com@inp.demokritos.gr
Constantinos **GEORGANTAS**	Accountant	A. Lagoyannis	georgadas@inp.demokritos.gr
Prodromos **HATZISPYROGLOU**	Physicist	C. Markou	prohatz@hotmail.com@inp.demokritos.gr
Constantinos **KARAKATSANIS**	Physicist	D. Bonatsos	kokaraka@hotmail.com@inp.demokritos.gr
Dimitrios **KATSINIS**	Physicist	M. Axenides	katsinis@inp.demokritos.gr
Zoi **KOTSINA**	Physicist	A. Lagoyannis	zkotsina@inp.demokritos.gr
Aggelos **LAOUTARIS**	Physicist	A. Lagoyannis	laoutaris@inp.demokritos.gr
Georgios **LINARDOPOULOS**	Physicist	G. Pastras	Linardopoulos@inp.demokritos.gr
Demetrios **MANOLOPOULOS**	Physicist	G. Pastras	manolopoulos@inp.demokritos.gr
Efthymios **MPISTEKOS**	Technician	A. Karydas	info@philonmodels.com@inp.demokritos.gr
Eleni **NTEMOU**	Physicist	A. Lagoyannis	ntemou@inp.demokritos.gr
Sofia **OIKONOMOU**	PR officer	C. Markou	oikonomou@inp.demokritos.gr
Stefanos **PAPAGIANNIS**	Physicist	A. Lagoyannis	papagiannis@inp.demokritos.gr
Georgios **PASTRAS**	Physicist	A. Axenides	pastras@inp.demokritos.gr
Archimedes **PAVLIDIS**	Network Engineer	C. Markou	apavlidis@inp.demokritos.gr
Maria Myrto **PRAPA**	Physicist	T. Geralis	prapa@inp.demokritos.gr
Dikaia **SARAGA**	Physicist	C. Markou	dsaraga@inp.demokritos.gr
Smaragda **SARANTOPOULOU**	Physicist	D. Bonatsos	sarantopoulou@inp.demokritos.gr
Dimitrios **STAVROPOULOS**	Physicist	C. Markou	dstavropoulos@inp.demokritos.gr
Nikolaos **SYRRAKOS**	Physicist	C. Papadopoulos	syrrakos@inp.demokritos.gr
Kalliopi **TSAMPA**	Physicist	A. Lagoyannis	tsampa@inp.demokritos.gr
Vasilios **TSOURAPIS**	Physicist	C. Markou	tsourapis@inp.demokritos.gr
Eleni **VAGENA**	Physicist	A. Lagoyannis	vagena@inp.demokritos.gr
Olga **ZORMPA**	Physicist	C. Markou	zormpa@inp.demokritos.gr

Mobility

During 2021, Dr. E. Drakopoulou was hired as Researcher Gade C' joining the Astroparticle Physics Group.

Dr. S. Harissopoulos was on leave of absence in the International Atomic Energy Agency, Vienna.

Dr. P. Dimitriou resigned in November 2020. Her resignation took in effect in February 2021.

Mr. G. Androulakis passed away in July 2021.

Funding Programs in 2021

Research in INPP was mainly funded by the following programs with funding sources including National funding initiatives, the Horizon 2020 E.U. program, European research agencies as well as a limited number of contracts with the private sector.

Prog. ID	Title	Principal Investigator	Starting Date	Finishing Date	Budget
10231	Non destructive analyses with x-rays	Andreas Karydas	1/4/1998	31/5/2027	80,000.00 €
10461	Support for INPP	INPP Director	28/7/1998	31/12/2024	58,000.00 €
10881	Detection devices systems	Dimitrios Loukas	1/12/2002	31/12/2021	35.000,00 €
11041	Technologies for education and development	Theodoros Geralis	11/12/2002	21/12/2021	50.000,00 €
11458	Particle Phenomenology	Kostas Papadopoulos	1/3/2007	28/2/2025	90,000.00 €
11551	Fusion – Radiation studies	Anastasios Lagoyannis	1/12/2008	31/12/2022	30,000.00 €
11776	KM3NeT support activities	Christos Markou	1/1/2013	31/12/2024	59,000.00 €
11893	LIBRA	Sotirios Harissopulos	1/9/2014	31/8/2023	200,000.00 €
11985	ENSAR 2 — H2020	Sotirios Harissopulos	1/3/2016	30/4/2021	60,000.00 €
12157	Analytic applications using synchrotron techniques	Andreas Karydas	10/3/2017	9/3/2021	15,000.00 €
12209	ESSnuSB (H2020)	George Fanourakis	1/1/2018	31/3/2022	64,953.00 €
12217	ORASY	INPP Director	1/4/2018	31/12/2022	282,000.00 €

12239	CALIBRA	Sotirios Harissopulos	1/1/2017	30/9/2022	3,422,000.00 €
12312	Detector Development and Technologies for High Energy Physics (DeTANet)	Theodoros Geralis	11/2/2019	10/2/2023	125.962,67 €
12335	GEANT4-based particle simulation facility for future science mission support	Anastasios Lagoyannis	1/4/2019	30/10/2022	120.935,00 €
12356	Access to Ion and Neutron Beams at NCSR "Demokritos"	Anastasios Lagoyannis	13/6/2019	12/6/2024	15.000,00 €
12386	Chaotic dynamics and black holes in the BMN theory	Minos Axenides	10/4/2020	9/8/2021	45.545,50 €
12390	High order corrections in QCD and applications in the High energy LHC experiments	Kostas Papadopoulos	1/4/2020	31/7/2021	37.037,00 €
12391	New generation of detectors and electronics for the upgrade of the CMS experiment at CERN	Dimitrios Loukas	17/3/2020	31/7/2021	41.041,00 €
12424	Nucleon separation energies	Dionysios Bonatsos	27/4/2020	27/8/2021	41.541,5 €
12429	Advanced System for collection and management of analytical data for documentation and conservation of large-scale paintings in an open laboratory	Andreas Karydas	28/7/2020	27/7/2023	155.311,00 €

12478	Intelligent, specialized, environmental observatory in Messinia	Christos Markou	1/5/2021	30/4/2023	400.000,00 €
12495	Development and Application of Ion Beam Techniques for Materials Irradiation and Characterization relevant to Fusion Technology	Michail Axiotis	1/5/2021	31/12/2025	15.000,00 €
12502	Silicon detectors and electronics	Dimitios Loukas	9/1/2021	31/12/2023	6.000,00 €

High Energy Physics

High Energy Experimental Physics - ATLAS

Researchers:	Theodoros Geralis (Team Leader)
	Georgios Fanourakis (Researcher Emeritus)
	Georgios Stavropoulos
PhD students:	Maria Myrto Prapa
	Olga Zormpa
Master students:	Foteini Faidra Trantou
Practical work students:	From Univ. of Patras
	Eleni Androutsou
	Dimitrios Giannakopoulos
	Theodora Remoundou
Technicians:	Ioannis Kiskiras

Introduction

The INPP ATLAS group is a full member of the ATLAS experiment since October 2017. The group activities are within the ATLAS New Small Wheel (NSW) Muon Upgrade project for Phase I and also on the Muon Software related to parallel threading and the detector alignment. The group starts activities on Physics Analysis in preparation for Run3. By the time of writing this report we have already started analysis on the precision Z mass measurement using Run2 data.

NSW is currently the largest Upgrade project among the LHC experiments and will be part of the Muon end cap ATLAS detectors. In December 2021 both Wheels were lowered to the ATLAS cavern and by the time of writing this report the NSW Wheels are connected in ATLAS. The NSW is required to cope with the increased luminosity of the LHC of about ($5 \times 10^{34} cm^{-2} sec^{-1}$) and will withstand high occupancies including the HL-LHC. This also affects the Trigger and data acquisition systems (TDAQ) as the decision to select the events of interest (rejection or acceptance) is made every 25 ns. This is a huge challenge, as the 25 ns decision time is too short for such a complex system with millions of detection channels while also considering that high detector performance must be maintained. The aim of the NSW is to reduce the fake triggers by providing tracking and triggering capabilities to allow pointing of the muons from the outer muon detectors (Big wheels) to the interaction point (IP) with a precision of 1 mrad. The final result will be reduced P_T muon thresholds, higher selection purity and lower rates. Two detector technologies were selected, the Micromegas and the sTGCs (small strips Thin Gap Chambers) that can cope with even higher rates than the ones expected (about $20kHz$) and be radiation resistant in the HL-LHC environment.

Fully completed projects in the previous years (2020) are: 1) The testing of a large number of electronic cards (L1DDC for Micromegas and for sTGC subdetectors) and ADDC for the Micromegas Trigger, 2) The full production of the serial and the LVDS repeaters (about 1000 electronic boards with their shieldings) 3) The official database handling for recording the whole history of the electronics components, 4) Porting of the whole Muon software to parallel threading mode.

The sTGC Repeater boards - the largest project of the group - started in 2018 and it was completed in 2020 with the commissioning of all the modules. Integration to the NSW continued and was completed in 2021, following the progressive integration of Wheel A and Wheel C. Our group has undertaken responsibility of the full sTGC Trigger Commissioning which by the end of 2021 was in advanced state. Both Wheels were lowered in ATLAS and were moved into the run (operation) position in January 2022.

In the activities subsection we describe the following items on which the ATLAS Demokritos team played leading role during 2020:

1. sTGC Repeaters
2. sTGC Trigger Slice setup
3. sTGC Trigger Commissioning
4. sTGC Detector integration
5. Muon and NSW software activities
6. sTGC testbeam analysis

Activities

sTGC Repeaters

The sTGC Trigger system operation is based on the proper transmission of the data from the Front End (FE) cards (pFEBs and sFEBs) to the Pad Trigger and subsequently to the Routers (electronics hosted in the Rim crate) and the Trigger Processor. The large distance between the FE cards and the Rim crate and the attenuation over these large distances necessitated the building of repeaters cards to reinstate the signals levels. The serial repeaters (SRL1R) restore signals from the pFEBs to the Pad Trigger (4.8 Gbps) while the LVDS repeaters (LVD6R) restore signals between the Pad Trigger and the sFEBs)640 Mbps). In 2019 the design of the repeaters, the design of their host cages which act also as Faraday cages and their cooling were performed. Detailed studies concerned their performance in data integrity as well as the effectiveness of the cooling. In the case of the LVD6Rs active cooling was necessary using a cooling bar that was integrated in the NSW cooling system.

Serial Repeaters - Final Production. In 2020 we have launched the final production of the serial repeaters SRL1Rs. NSW requires 768 SRL1Rs for both Wheels, so the final production was 850 boards. The boards and their shielding metallic boxes were manufactured in Greece.

Assembly of the SRL1Rs as well as configuration of the boost parameters took place in January 2020. The boards were tested in the Test Bench that was developed by our group with an acceptance higher than 99%. In 2021 all the repeaters were passivated with capton and were integrated in the sTGC sectors.

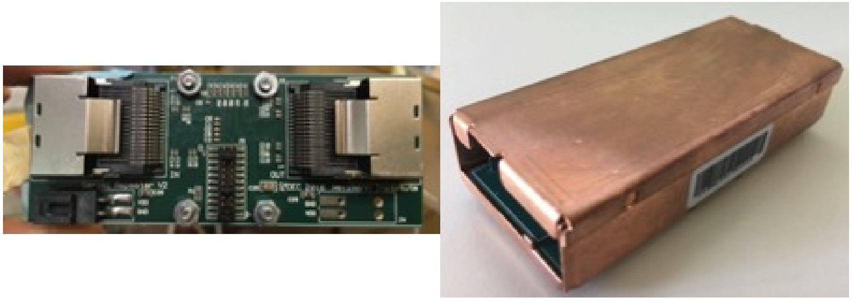

Figure 1: A Serial Repeater SRL1R (left) in its Faraday cage (right)

A serious electronic noise problem of the large sectors was cured by modifying the grounding scheme of the serial repeaters.

LVDS Repeaters - Final Production. The production of the LVDS repeaters was performed in two stages. Half of the LVD6Rs (70 boards) were produced in November 2019, because of delays to purchase the repeater chips but also the miniSAS connectors. The rest of the production was possible to perform in February 2020. The assembly of 70 LVD6Rs took place in February 2020. Cooling bars were produced for mounting the LVD6R boards as well as the aluminum Faraday cages. Full production of the LVD6Rs and the aluminum cages took place in Greek companies.The mounting of the remaining 70 LVD6R boards took place in October 2020 and all those devices were the first to be placed in Wheel C. This time marked the completion of the Repeaters Project by our group. By the time of writing this report, the repeaters are used extensively at the integration and the commissioning of the sTGC system and no problem has appeared in their operation.

Figure 2: LVD6R cooling bar with four mounted boards (left), one full LVD6R bar with four boards enclosed on the aluminum shielding mounted on Wheel A (middle) and LVD6Rs mounted on Wheel A indicated by red circles

sTGC Trigger Slice setup

In February 2020 our group completed a major task, to build a complete Electronics, Trigger and Readout System corresponding to one full sTGC wedge. The aim was to dispose an autonomous sTGC Trigger Slice system that would allow development, testing and commissioning of the full system. The system was ready just before the lockdown due to the pandemy, and was proven to be extremely useful as development on all activities continued during that period as well, through remote access.

The System corresponds to a fully equipped sTGC wedge: Front End boards: 12 sFEBs and 12 pFEBs, One Rim-Crate, 1 Pad Trigger board, 1 RimL1DDC board, 4 Routers, 8 L1DDCs boards, 2 LVD6Rs and 10 SRL1Rs repeaters, 1 Trigger Processor unit, 1 Felix system, 1 Software swROD system.

The system is hosted in two racks, the Analog and the Digital ones. A special mechanical support was machined in order to support the 24 front end cards. All connections were done with exactly the same cable and fiber lengths in order to reproduce an identical system as the on detector system. Almost all the components require cooling: 1) All FE boards were placed on copper pads and attached to it with thermal pads, 2) The L1DDC were placed in their cooling frame, 3) The LVDS repeaters on their cooling bars and 4) The Rim crate was cooled via the special backplane. A chiller with a custom made distribution system was setup to provide cooling through 3 different circuits. The temperature is kept to its nominal values i.e. temperature no higher than 23^0C. The system components can be powered on and off remotely and a booking system is serving for efficient sharing of the system among different groups. The system that our group has guilt is used by all team of the Trigger group i.e. Univ. of Technion, Weizmann Institute of Science, INFN Rome, University of Michigan, University of Massachusets, Harvard University and our group ATLAS/Demokritos. By the time of writing this report the whole Vertical Slice laboratory is under the responsibility of the Demokritos group. Apart the setups for the sTGC and the MM trigger and DAQ commissioning, the laboratory is equipped with a conditioned storage place were all NSW electronics spare components are kept.

sTGC Trigger Commissioning

NCSR Demokritos group in ATLAS is involved with sTGC TDAQ system. In 2021 four main projects on sTGC Trigger Commissioning, were running in parallel.

- Wheel-A and Wheel-C trigger Commissioning
- The sTGC Stage-0 trigger commissioning
- Measurements of the NSW trigger latency
- Fake Sector Logic
- The Alti pattern generator
- The sTGC detector test beam analysis

In the following schematic 3, NSW trigger electronics are presented. The upper part of this schematic shows sTGC trigger electronics. Four different ASICs (VMM, ROC, TDS and SCA) were designed and manufactured, to produce customized electronic boards for all the stages of the system, from the Front End boards to the data concentrators, the trigger and finally the readout systems.

Wheel-A and Wheel-C trigger Commissioning

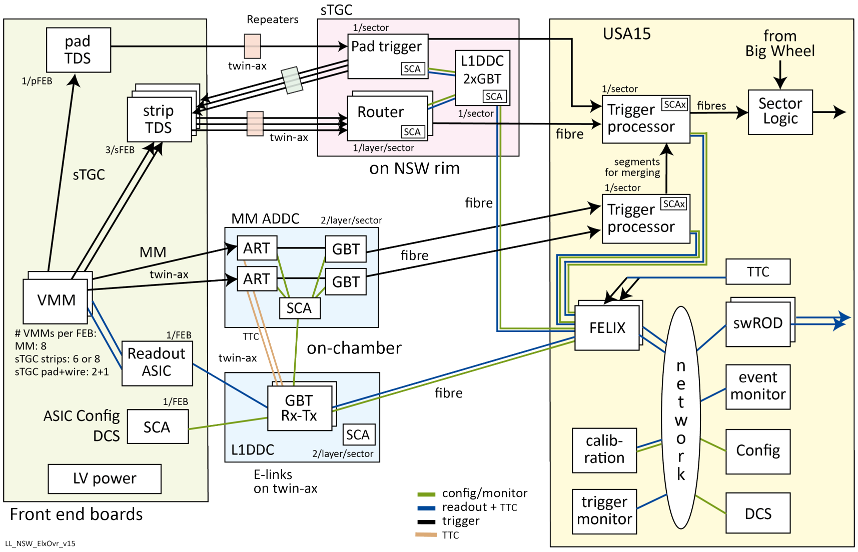

Figure 3: General Schematic of the NSW trigger electronics

Wheel-A Commissioning started in 2020 at CERN Meyrin site, Building 191 (B191) when the detectors started to gradually arrive from the construction sites. Both Wheels A and C were completed by the end of 2021 and were lowered to the ATLAS cavern. Wheel-A and Wheel-C have been installed in this building, before 2020, together with all the accompanying equipment (DAQ computers, TTC computers, cabling etc). In December 2019 the first Small Sector was installed and after this point a long list of tests was developed to validate connections and operation for every sectors. Among those tests, the sTGC trigger team developed tests that could validate the operation of sTGC trigger system. The tests were designed to serve two purposes. Firstly, to check the connectivity of the boards that belong to the trigger path and secondly to test that the data transmission to every path is without errors. The responsibility of NCSR Demokritos group was to develop and conduct these tests in all 16 sectors of Wheel-A. The test list to validate the proper operation of each sector is:

Connectivity Tests:

- PFEB Connectivity (PFEB/PT)
- SFEB Connectivity (PT/SFEB)
- Router Connectivity (QS1 SFEB/Router)
- Router VIOs test (QS1, QS2, QS3 connections)
- TP ILAs test (SFEB/Router/TP)

Data Quality Tests

- PFEB-PT IBERT/Eye Diagram Scans
- SFEB-Router IBERT/Eye Diagram Scans
- Router-TP IBERT/Eye Diagram Scans
- PT-TP IBERT/Eye Diagram Scans

The Connectivity tests were conducted by designing and then running a series of calibrations that tried to simulate the normal flow of the data in the trigger chain. The Data Quality Tests were using the FPGA utilities to test the data transmission by sending/receiving Pseudo-Random Binary Sequence - PRBS data.

In January 2022 both Wheels were installed in the ATLAS cavern. Before moving to their final run position, a part of the above tests performed in building 191 was repeated in place to verify the proper operation of the system after the NSW transfer from building 191 to the cavern.

Validation of Stage-0 trigger

sTGC Stage-0 trigger is a simplified version of sTGC trigger. It includes a smaller path that allows to get a fast decision on whether there is a valid trigger, meaning an event of interest. Stage-0 includes the pFEBs (pad front-end boards) the Pad Trigger board and the Trigger Processor board. The pFEB boards are receiving data from the sTGC detector'92s pads, which are larger areas that the detector is split. The pads from one layer are not totally aligned with the ones from the next layers, but staggered. This staggering facilitates the creation of a tower, a possible hit path of a muon., in every layer. Pad Trigger board has a look-up table stored in its FPGA that includes all possible towers. Using that look-up table can decide about whether there is an event of interest, in order to send this information to the Trigger Processor. The validation of Stage-0 was a milestone that was achieved, in 2020 but also a further step had been made. When the Trigger Processor receives the data from the Pad Trigger, meaning an event of interest has been found, it executes its algorithm and produces a pulse that can be used to trigger the rest of the system (remaining trigger electronics or Micromegas detectors). The produced pulse needed adjustments and shaping in order to be used by the TTC system, but this was soon resolved, and this tool became available for further studies.

Measurements of the NSW trigger latency

The trigger latency refers to the time interval that lapses after a pp collisions at the IP to the time a decision is taken concerning the acceptance or rejection of that event. The ATLAS trigger and also the NSW trigger part are designed to have fixed latencies the length of which defines the detectors buffer capacity to keep all events included in the time interval between collision and decision. It is critical to know the exact latency and also to minimize it as much as possible. The NSW latency includes the muon time of flight, the detector response time, the FE electronics signal processing and subsequently the transmission through cables and fibers and processing in the different trigger units.

Using the Trigger slice at the VS setup we have performed measurements for the part from the FE signal using test pulses to the decision taken by the Trigger Processor. We measure, using test pulses, the latency for the Stage-0 trigger i.e. the trigger that uses only the pad information. Because of possible delays in delivering the full trigger functionality this was the initially adopted strategy. By the time of writing a slightly different scheme has been adopted that includes the sTGC Pads and the Micromegas segments for triggering. Figure 4 shows the checkpoints of the latency measurements: the crossing of the test pulse threshold (t_0), the arrival of data in the Pad Trigger t_1, the decision and transmission of data from the Pad Trigger to the sFEB and the TP t_2, the reception of data from the TP t_3, the execution of the TP algorithm t_4 and the arrival of the decision data to the Sector Logic (t'_4). Most of the measurements were performed using an oscilloscope and probed the signals at the proper nodes (see Figure 4) and some

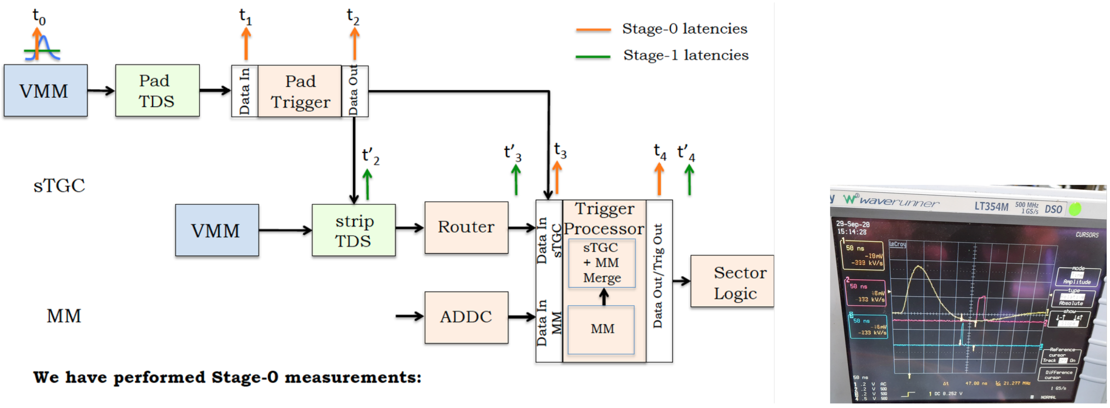

Figure 4: Latency measurements checkpoints on the NSW Trigger schematic (left) and screenshot of the Pad Trigger latency measurement with the oscilloscope at the corresponding checkpoints (right).

were measured internally in the FPGAs.

The total Latency measured for the Stage-0 NSW Trigger was found to be around 880 ns, well below the estimated maximum allowed of 1075 ns. Beyond this limit the NSW will be contributing more than any other detector to the global ATLAS Latency. This work was continued in 2022 and final NSW latency measurements will be presented in next year' report.

Fake Sector Logic

The Fake Sector Logic (FSL) design for the ATLAS Muon Trigger system is a Sector Logic emulator that processes data from the detectors and provides information and measurements. This architecture is being developed for the Kintex Ultrascale FPGA on the Trigger Processor board, which is part of the NSW Electronics. Inputs to the FSL consist of merged data from both the sTGC and MM detector FPGAs and are handled by firmware that both supports fiber optic connections and process them to a more compressed format. Outputs are exported via 10G Ethernet to a local Network Interface Card (NIC) via point-to-point connection. Data will be received on the NIC side using a software script and can be further optimized to facilitate and expedite testing procedures.

This design consists of the following parts, as well as any extra logic that ensures the smooth propagation of data between them:

- Input Transceivers and fiber optics connections.
- Processing and compression of data
- 10G Ethernet with UDP implementation- also contains Output Transceivers
- Software to receive and store data from the NIC

The firmware design has been completed in 2021 and there remained to be completed the readout part.

<u>Inputs and fiber optics connections.</u> Input data have a fixed format illustrated in the image and consist of packets hereafter called segment records. Each segment record contains a double comma character for the serialization of data, data of 4 segments, the sector ID, and Bunch Crossing ID. Segments contain data for their resolution and location in the detector. The most important field in the segment

data for the Fake Sector Logic is the $\Delta\theta$ field, which defines if a segment is valid and contains information that will be processed by the logic.

Segment records have been produced in different ways for testing purposes. So far, they appear as inputs following one of two different modes below:

Test Pulse Mode: 1 segment record packet consisting of 4 valid segments comes in per 3563 segment record packets. The rest of the packets are empty or invalid.

Playback Mode: segment record packet contents change per second. This means that regardless of the segment content, the same segment record packet will be input for 1s before changing to a different packet.

The full implementation of the input transceivers with a line rate of 6.4G has been completed in 2020. This part of the design makes full use of the Ultrascale features, provides the best connectivity options on the board while maintaining easy access to additional transceivers and availability of resources.

Processing and compression of data Input data are stored and are processed based on the selected mode of data as well as their content. Invalid segments are identified through $\Delta\theta$ and counted prior to data propagating to the branch of the architecture that is appropriate for the selected type of inputs. The firmware equivalent of a multiplexer is included to combine the simultaneously calculated results of two fibers to the single input of the 10G fiber.

The test pulse mode is based on a compression by three scheme; for every 3 invalid segments, a valid segment with its Sector ID and BCID is exported as output. The playback mode logic processes multiple inputs, compares them to stored previous values and currently exports counter results that indicate the number of identical segment records.

This part of the design has been completed in 2020. Both modes of the design feature a straightforward architecture of processing layers that can be easily modified to accommodate future testing requirements. The resource consumption is being minimized by taking advantage of the repetitive patterns that occur in the serial inputs and reusing logic and memory elements. Conditional statements and internal validity signals provide a stable data flow among the layers, while concurrently processing multiple fibers.

10G Ethernet The 10G Ethernet implementation uses the UDP/IP and MAC protocol to package and export processed data, effectively turning the FPGA into a NIC. A clock domain crossing FIFO is used to connect the two sides of the design. This part of the architecture consists of several sequential layers of code that adds headers, as well as the transceiver and fiber optics connection. The foundation has been laid in 2020 for this side of the project, in order to introduce the 10G Ethernet core components and to achieve a simplified and 10G compliant version of the UDP.

sTGC Detector integration

Our group has participated with one full time technician for the whole of the year 2020 and up to September 2021. We list below major works on which we played leading role in design and construction of systems that were necessary for the integration were: 1) The cooling frame for the sTGC L1DDC boards, 2) The Cooling system of the sTGC integration cite, 3) The assembly of the Faraday cages of the sTGC wedges, 4) the sTGC Sectors Assembly and 5) The design and manufacturing of many mechanical parts in the workshop that greatly helped accelerate the completion of the work of the sTGC integration

The cooling system of the sTGC L1DDC boards. sTGC data concentrator boards L1DDC require active cooling. Our group took part in adapting the cooling for a more efficient cooling. Our technician invented a mechanical mold that accelerated the manufacturing and helped build the frames faster. During the 2020 pandemy lockdown about half of the production was performed in Kalamata, in the INPP premises. In total 128 frames were built which are shown in 5.

The Cooling system of the sTGC integration cite. We have participated in the design and have built the whole Cooling system in building 188 at CERN where the sTGC integration of all the Sectors took place. The system was operated for the whole period without any problems providing 5 different lines of cooling circuits for the integration in parallel of two sectors and the full electronics chain. In 5 you can see the whole cooling system.

The assembly of the Faraday cages. The sTGC wedges (half of a sector) are enclosed in Faraday cages in order to reduce externally induced RF noise. We have taken part in the assembly of the Faraday cage which was composed from metallic parts made out of copper. Special care had to be taken for proper soldering and for avoiding leaks of the CO_2 envelop. In 5 you can see the assembly of the Faraday cage.

The sTGC Sectors Assembly. Every Sector is composed by two wedges (4 sTGC layers) and every wedge is split in three quads (Q1, Q2 and Q3). The quad were manufactured in the construction centers in Chile, Canada, Israel and Russia and were shipped to CERN for assembly. Our technician contributed to the assembly of the whole wedges and Sectors. The work took place in the Clean Room of B180 at CERN. Many intervention allowed the acceleration of the assembly of the sTGC detectors. In 5 you can see the team having assembled one sTGC Sector.

Manufacturing of mechanical parts. Many mechanical parts were manufactured in the machine workshop that allowed faster execution of the assembly operations (see 5).

ATLAS Local Trigger Interface

An upgrade to the current Timing, Trigger and Control (TTC) system at the ATLAS experiment will be the ATLAS Local Trigger Interface. ALTI is a new electronic board, designed to integrate the functionality of the four existing TTC modules and replace them with a single VME module. The primary function of ALTI is to provide the interface between the Central Trigger Processor (CTP) and the TTC optical broadcasting network.

The CTP is part of Level-1 Trigger system at the ATLAS Trigger and Data Acquisition system. It is responsible for making the initial trigger decision (Level 1 trigger accept signal) by identifying interesting particle candidates coming from the Level-1 calorimeter and Level-1 muon trigger systems. The L1A trigger signal,

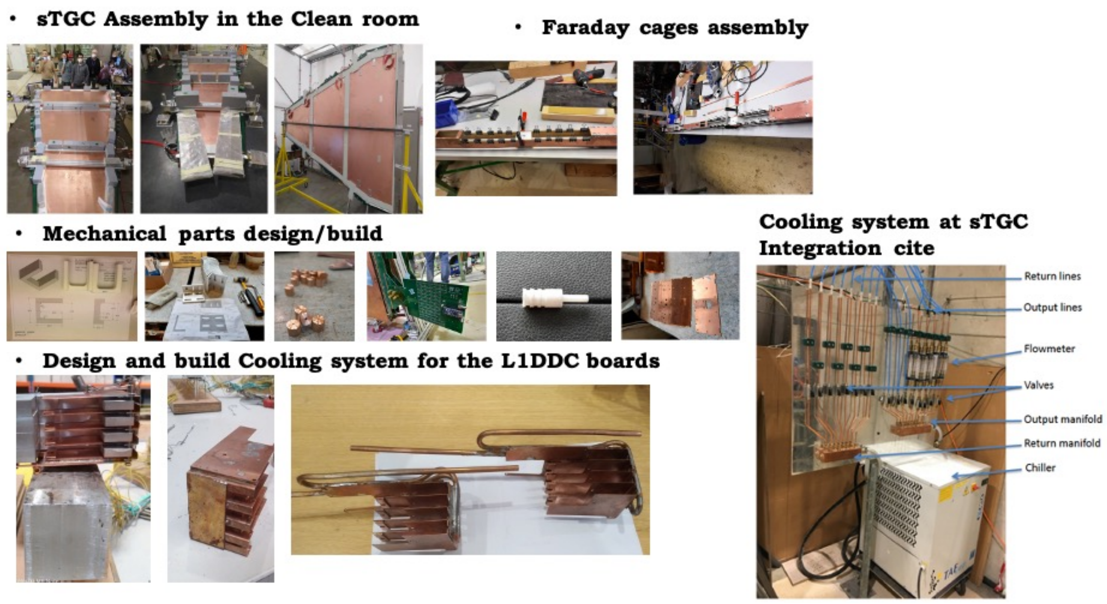

Figure 5: Photos from the integration cite works performed by our group

along with timing and synchronization signals such as the LHC 40 MHz clock (BC clock), are distributed to the sub-detector electronics via the TTC system.

The ALTI pattern tool

During LS2, no communication between the CTP and ALTI can be established. Therefore, NCSR Demokritos group developed a tool, using Python as a programming language and ROOT data analysis framework, in order to drive ALTI. The tool provides the generation of pulse pattern files that implement the TTC information (6). Additionally, it applies important parameters, electronic hardware restrictions, trigger rules and mechanisms on the generation of these patterns which are being used by the CTP in normal operation.

The motivation behind this tool was to utilize ALTI in order simulate real-time trigger conditions, and study the response of the Trigger System for the New Small Wheel muon detector electronics. This procedure facilitated developments related to the Trigger System validation and contributed to the verification of its operation and data readout process.

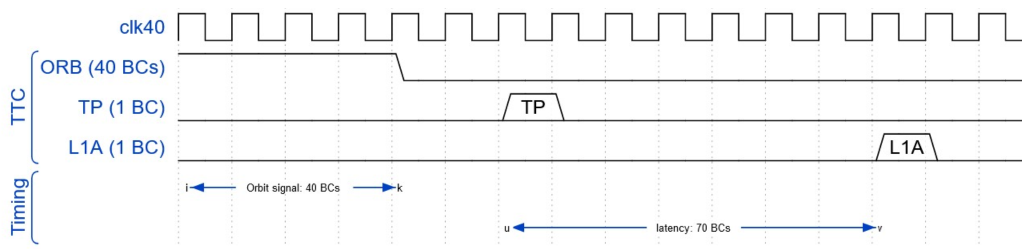

Figure 6: Time diagram of an ALTI pattern file (clock out of scale). An orbit signal represents one LHC turn, followed by a test pulse signal and the L1A signal that corresponds to it 70 Bunch Crossings (BC) later.

Analysis

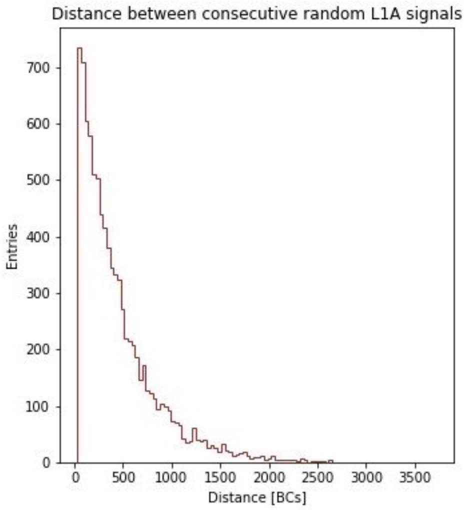

Figure 7: Histogram for random trigger type generated at 100 kHz, 70 BC test pulse 96 L1A signal latency.

ALTI was configured with pattern files at different rates, both for clocked and random trigger type. NetIO publish/subscribe system used was used to obtain distributed data from the NSW sTGC trigger path. The required time differences (or distance in BCs) were observed while transmitting TTC signals through ALTI to the individual electronics. The following histogram is produced from sending pulse patterns with random triggers to the sTGC Pad Trigger (Figure 3). It depicts the probability of a bunch crossing to occur, which decreases exponentially over time.

sTGC testbeam analysis

In order to understand the sTGC detector behavior in realistic conditions, a testbeam was performed in October 2021 at the Gamma Irradiation Facility (GIF++) at CERN. A layout of the building can be seen in Figure 8 (left). A quadruplet of an sTGC detector was placed vertically to the SPS H4 beam and it was irradiated with photons from a $^{137}Cesium$ source. The full setup including the Micromegas quadruplet that was also participating in the testbeam is shown in Figure 8 (right. The aim was to measure the muon detection performance at the presence of irradiation fluxes similar to the LHC ones during pp collisions at 14 TeV.

The INPP ATLAS group studies the efficiency of the sTGC pads. To do so, events triggered by a 4 scintillator coincidence were analyzed. The 4 scintillator coincidence was carried out by adding 2 small scintillators together with the GIF++ large scintillators pair, covering the area of a 4-layer, trigger tower, on the sTGC quad (Figure 9 left).

The calculated pad efficiency with respect to the background rate can be seen in Figure 9 (right). The background source rate was calculated to be $(13kHz/cm^2)$. In Figure 9 is shown that the pad efficiency is decreased with the increase of the background rate, for all 4 layers, but the minimum efficiency is 45%, with layers 4 and 7 having lower pad efficiency compared to inner layers.

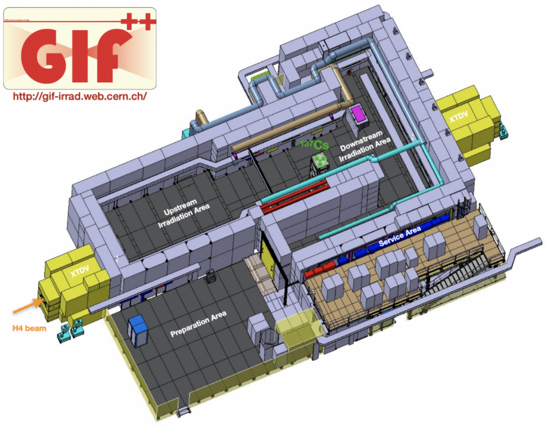

Figure 8: Gamma Irradiation Facility, CERN (left). Test Beam setup (right).

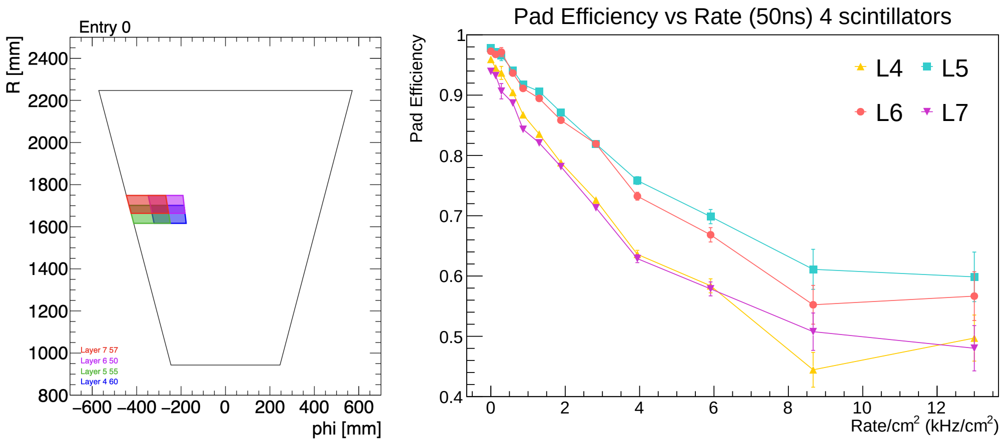

Figure 9: Trigger Tower under the 4-scintillator coincidence area. The pads of interest are shown with different colors, for each layer (left). The distribution of sTGC pad detection efficiency for muons with respect to the underlying background. The data were recorded with peaking time of 50 ns and a 4 scintillator coincidence. (right).

Muon and NSW software activities

The muon spectrometer is made up of several thousand chambers and is the outermost layer of the ATLAS detector. It identifies and measures the momentum of muons that fly out of the collision point. Key to this is a precise understanding of the muon spectrometer'92s geometry.

Measuring and recording the chambers' as-built geometrical parameters, translated to discrepancies with respect to the nominal (according to design) chamber geometry, is the first step towards precisely understanding the muon spectrometer'92s geometry.

At small scales, the geometry of the muon spectrometer is almost constantly changing, albeit slowly. Small temperature variations make the chambers and their support structures contract, expand and deform. Further, some of the chambers are mounted on the ATLAS toroid magnets, which themselves can occasionally move and deform.

The muon spectrometer is therefore equipped with an optical alignment system that monitors in real time the positions of chambers relative to each other and to calibrated reference objects in the detector, as well as their deformations. This information can be combined with data from muon tracks in order to fully understand the muon spectrometer'92s position.

The, precisely specified, muon spectrometer's geometry is implemented into the ATLAS software frame through the Detector Description software. It relies on a database technology and a standard set of geometrical primitives common to all ATLAS subsystems. The Muon Detector Description provides a unique and coherent geometry source for the simulation and reconstruction algorithms. ATLAS has adopted 3 sets of parameters to describe the discrepancies between the "actual" geometry with respect to the "nominal" one.

1. As built parameters: construction sites measurements translated to discrepancies w.r.t the nominal (according to design) chamber geometry.
2. Alignment of Stations / A Lines: 6 time dependent parameters meant to describe deviations w.r.t nominal positions.
3. Deformations / B Lines: 11 time dependent parameters meant to describe the deformation effects.

The upgraded NSW of the ATLAS muon system consists of two types of gas detectors (sTGC and MicroMegas), the precise geometry of which has to be introduced into the Muon Detector Description software. The INPP-ATLAS group has undertaken the responsibility to implement the, aforementioned, NSW sets of parameter in the ATLAS offline software. All the necessary tools for storing and retrieving these parameters into the relevant databases have been implemented, tested successfully and included into the official ATLAS software. Furthermore, various tools that correctly calculate the various geometry parameters have been developed and included in the official ATLAS software frame, to be used by other ATLAS packages such as simulation, reconstruction and graphics.

In October 2021 the ATLAS Demokritos group undertook the respnsibility of coordinating the work of the ATLAS Muon Software Group, which involves more than 40 scientists from more than 20 Institutes worldwide. The ATLAS Muon software is developed in a multi-threaded C++/OO and Python environment and is organised in the following thematic areas

- Data Access (Byte-stream Conversion and Cabling).
- Detector Description and Alignment.
- Conditions Databases and DCS.
- Detector Specific calibration procedures.
- Simulation.
- Modelling of the Detector Response (Digitization and ́93local'94 Reconstruction).
- Track Reconstruction and Muon Identification.

- Trigger.
- Offline Data Quality.

The highest priority of the muon sw group during 2021 was the support of the Run 3 data and the proper integration of the new detectors (NSW, BIS78) in the ATLAS main software frame (Athena).

Funding

Some equipment and personnel (PhD) was funded by the DeTANet infrastructures program with an amount of about 50 kEuros for the ATLAS group for the period Feb. 2019 to Feb. 2023. The INPP program ORASY also provided small personnel support. The main support came from the ATLAS NSW project which provided support for 2.7 FTE for the whole of 2021. The table 10 below present the two INPP sources.

Table 10: Funding through the infrastructures DeTANet program and the ORASY within INPP

Prog. ID	Title	Host Institution	Principal Investigator	Starting date	Finishing date	Budget (€)
12312	DeTANet	INPP	T. Geralis	10/02/2019	10/02/2023	125,962.67
	ORASY.	INPP	C. Markou	01/01/2015	31/12/2021	20,000.00

Outreach

Because of the Covid pandemic the Outreach activities were practically suppressed. Our Lab usually participates in many events like the Researcher's Night in which we provide demonstration with Cloud Chambers, exhibition of particle detectors, microscope inspection of micro pattern detector structures etc. Also we take part in the Master Classes program for high school pupils.

Overview

The year 2021, despite the pandemic problem, has been very productive for our group. We recapitulate the main research activities below:

- Integration of the sTGC Repeaters in the NSW
- Maintenence of the sTGC Trigger Slice setup
- Demokritos group is the driving force for the sTGC Trigger Commissioning on the Wheels
- Very significant contribution to the sTGC detector integration, providing technical support

- Major contribution to the Muon and NSW software activities
- Very important contribution in the developments for the sTGC Trigger processor like the project of the Fake Sector Logic and also the Alti Pattern generator that are extremely useful tools for the collaboration.
- Measurement of the Stage-0 NSW trigger latency
- Participation in the sTGC testbeam and data analysis

Responsibilities

The members of the ATLAS Demokritos group have gradually undertaken important responsibilities, given the short time we participate as full members in the ATLAS Collaboration. Below we give a list of responsibilities and participation in important bodies within ATLAS:

G. Stavropoulos: ATLAS Muon Software Coordinator, which is a major responsibility and achievement for our group. **T. Geralis: Coordinator of the sTGC Trigger Commissioning T. Geralis**: Member of the NSW Steering Group **T. Geralis**: Member of the Muon subdetector Institutes Board **T. Geralis**: Member of the NSW Electronics Coordination Group **Presentations in the ATLAS internal meeting in 2021 Presentations:** The members of the INPP ATLAS group have been organizing internal ATLAS meetings in the frame of their responsibilities, mainly within NSW but also the Muon community. Members of the group account for more than 100 presentations in 2021, in thematic meetings, in the Muon Weeks, in the parallel but also in plenary sessions.

High Energy Experimental Physics - CMS

Researchers:	G.Anagnostou
	G.Daskalakis
	A.Kyriakis
	D.Loukas
PhD students:	P.Assiouras
	A. Papadopoulos
	A.Stakia
Diploma students:	D.Papafilippou
Engineers:	I. Kazas (ELE)

Introduction

In 2020 the INPP CMS group entered in full swing into the preparation of components and modules for the Phase II upgrade of the CMS in the HL-LHC, in parallel with the physics analysis program and maintenance of the CMS apparatus.

The physics program of the CMS experiment aims at answering fundamental questions in particle physics. What is the origin of elementary particle mass? What is the nature of the dark matter we observe in the universe? Is a common framework for the unification of the fundamental forces? Do matter and antimatter have different properties? How strong forces behave under extremes conditions? Until the end of 2018 LHC has delivered 203 fb^{-1} to CMS. This data has yield a vast quantity of physics results summarized by the CMS collaboration in more than 1050 publications. The highlight has been the observation in 2012 of a new particle that has been identified as the Higgs Boson, a cornerstone of the standard model of elementary particles. In addition to this discovery, CMS and ATLAS were able to begin detailed studies of its properties to consolidate that it was indeed the Higgs boson.

Precision Higgs studies and the search for new physics provide a powerful motivation for higher luminosity. The High Luminosity LHC (HL-LHC) is an upgrade program of the LHC with aim to provide higher peak and integrated luminosity. The scheduled upgrade scenario, refereed as Phase-II as well, is to level the instantaneous luminosity to $5 \times 10^{34} cm^{-2} s^{-1}$, or even to $7 \times 10^{34} cm^{-2} s^{-1}$ in the ultimate performance scenario. This will allow CMS and ATLAS to collect integrated luminosity of the order of 300 fb^{-1} per year and up to 3000 fb^{-1}, or up to 4000 fb^{-1} in the ultimate scenario, for the entire period of 10 years foreseen operation of HL-LHC. The machine will run at a center-of-mass energy of 14 TeV and with a bunch spacing of 25 ns.

The main challenges faced by the experiments at HL-LHC are higher radiation levels and increased pileups. The basic goal of the CMS Phase-II upgrade is to maintain the excellent performance of the detectors in terms of efficiency, resolution, and background rejection for all the physics objects used in the analysis of data. Figure 10 sketches the upgrade of the CMS subsystems.

Central to the CMS Phase-II upgrade is the complete replacement of the Silicon Tracker. The new Silicon Tracker must cope with many challenges. In order to

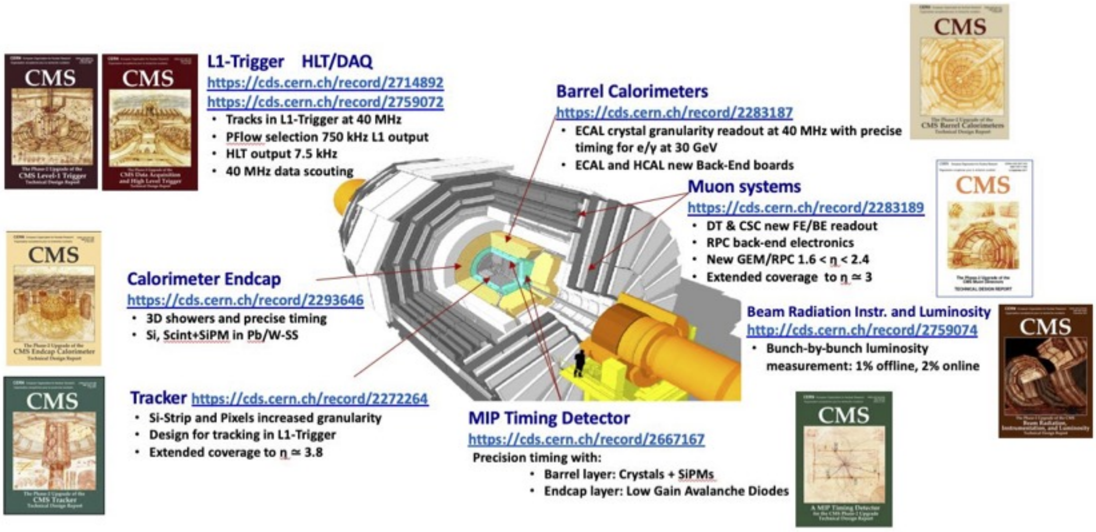

Figure 10: Sketch of the CMS detector with Phase-II upgrade plan

be radiation tolerant up to $4000 fb^{-1}$ the CMS collaboration contacted a ten years sensor $R\&D$ program that concluded with the choice of n-on-p senors to p-on- n [1] as the latter proved to exhibit higher radiation resistance. In order to handle the increased pileups, 140-200 expected compared to the current 30-40, increased granularity of the detector is needed to keep the occupancy bellow 1% and improve the resolutions at high P_t. This issue is addressed with higher segmentation of sensors and an increased latency from $3.2 ns$ to $12.5 ns$ by increasing the depth of the front end buffers. Improvement in low P_t resolution is achieved by using thinner detectors that reduce the material budget. Increased forward acceptance up to 4η is obtained with extension of the pixel detector. A novelty of the new CMS apparatus is the improvement of the trigger system by using data from the outer part of the Tracker for level one (L1) trigger.

Figure 11 shows the layout of the new CMS Tracker. It will extend from the vicinity of the beam pipe up to 1100 mm. The outer part (OT) of the detector that extends beyond 200 mm is made of two types of modules, one type consists of a pair of closed spaces microstrip sensors , the so called $2S$ modules, and the other type consists of a pair of microstrip and macropixel sensors named as PS modules in th CMS terminology. The inner part of the tracker consists of micropixel sensors.

The INPP CMS group joint the CMS Tracker in 2015. The activities of the

[1] CMS Collaboration. "Experimental study of different silicon sensor options for the upgrade of the CMS Outer Tracker". In: *JINST* (2020). DOI: 10.1088/1748-0221/15/04/P04017

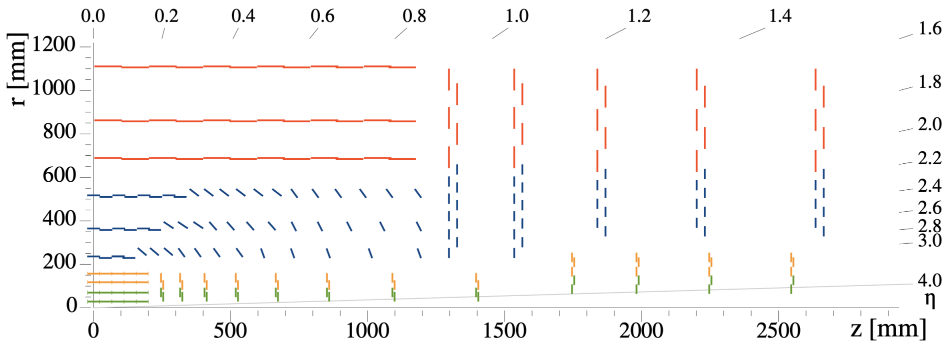

Figure 11: Layout of the CMS Phase-II silicon tracker in $r-z$ view [3]. The radial region below 200 mm is referred to as Inner Tracker and will be instrumented with pixel modules (green and orange colors). In the Outer Tracker, the radial region between 200 and 600 mm is equipped with PS modules (blue lines), while the region beyond 600 mm will be populated with 2S modules (red lines).

group were focused on the development of the Outer Tracker and especially on the silicon sensors. The group developed the necessary instrumentation and acquired the status of one among four international centers for the qualification of silicon sensor production provided by Hamamatsu Photonics in Japan. Associated with this activity is an under way program of irradiation studies with ^{60}Co-γ source. Gradually the group extended its activities to the Inner Tracker by assuming the responsibility for the development of firmware and middleware for the readout ASIC of the pixel detector.

Activities

Physics Analysis

The CMS-INPP data analysis group main goal is the deeper understanding of processes and mechanisms described by the Standard Model (SM) of particle physics and the quest for new symmetries and/or new matter in nature. To fulfill that goal the group has developed a twofold strategy: performs SM measurements and at the same time searches for specific topologies that might reveal the existence of supersymmetry or dark matter at LHC. Starting with the SM measurements, the objective is to enhance the experience of the team, gained over the past few years based on measurements in the electroweak sector of SM, by investing in studies in the field of top-quarks physics. The data from proton-proton (pp) collisions produced at the CERN LHC provide an excellent environment to investigate properties of the top quark, in the context of its production and decay, with unprecedented precision. Specifically, the measurements of the W boson helicity fractions in top quark decays, are very sensitive to the Wtb vertex structure. The comparison of the measured W helicity fractions with those estimated from the theory might reveal possible discrepancies from the SM predictions and contribute to a deeper understanding of the underlying physics processes. After the Higgs boson discovery, many theorists argue that a heavy top partner could explain the scale of the Higgs boson mass via loop cancellations. As such, an important extension of the measurements in the top-quark sector of the SM, will be a search for heavy top partners, exploring the $pp \to T^{'}T^{'} \to bbWW$ process. A new method was motivated/inspired from CMS-INPP analysis team as a new/different way to search for anything decaying like dilepton top-pairs. The CMS-INPP data analysis group also participated in the development of a methodology, called the Tag Rate Function, which allows to significantly reduce statistical uncertainties of the distributions of t¯t events with high b-tagged multiplicities utilizing the ones with lower b-tagged multiplicities. This approach has a significant impact on the systematic uncertainties of the $t^{-}tH$, $H \to b^{-}b$ measurement in the dileptonic and fully-hadronic channels. Our research program includes an extension of the above-mentioned analysis at the simulation level in order to study the increase in precision of the proposed Standard Model measurements as well as the extrapolation of the limits in searches for new physics at HL-LHC.

CMS Analysis Note: CMS AN-2021/166

Higgs Physics, G. Anagnostou, G. Daskalakis, C. K. Koraka, M. Madianos, Z. Painesis, N. Saoulidou

Short description: In this note, prospects for measuring the $t\bar{t}H, H \to b\bar{b}$ associated production are studied. The measurement is performed in the opposite sign di-lepton channel where $l\bar{l} = e^{+}e^{-}$, $\mu^{+}\mu^{-}$ and $e^{\pm}\mu^{\pm}$. The analysis is based on a novel approach that has been performed at $\sqrt{s} = 13\ TeV$ which achieves the reconstruction of the Higgs mass from its decay products while the main background contribution, which comes from $t\bar{t}$ events, is predicted in a data-driven manner, both shape and normalization-wise. Improvements in the analysis event pre-selection are presented, which are implemented with the introduction of a neural network. The results are extrapolated to the full integrated luminosity at the High-Luminosity LHC at $\sqrt{s} = 14\ TeV$ as can be seen in Fig. 12.

CMS Analysis Note: CMS AN-2020/205

Top Physics, G. Daskalakis, A.Stakia

Short description: We report a measurement of the W-boson helicity fractions from top quark decays, based on a data sample corresponding to an integrated luminosity of $137 fb^{-1}$ of proton-proton collisions at a centre-of-mass energy of $13 TeV$, collected in 2016-2018 by the CMS experiment at the LHC. The measurement uses the semileptonic decays of the tt pairs and the single top production (tW and t-channel). The results are consistent with standard model expectations, see Fig. 13.

CMS Analysis Note: CMS AN-2020/047

Higgs Physics, G.Anagnostou, G. Daskalakis,

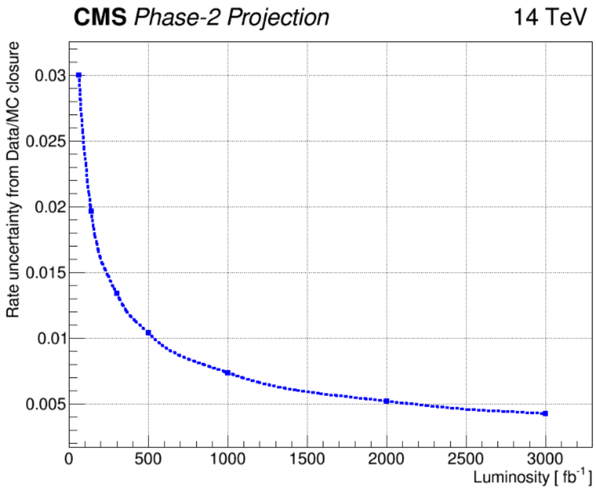

Figure 12: Projected estimated background normalization uncertainty originating from the data to simulation compatibility of the TRF closure in the CR as a function of the integrated luminosity.

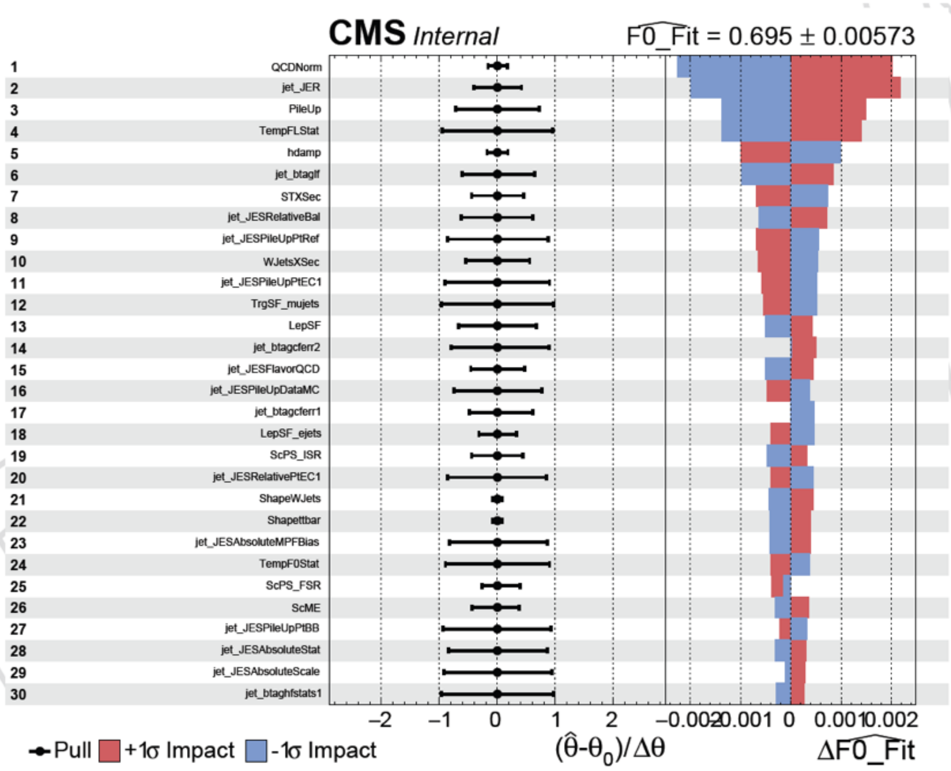

Figure 13: EXPECTED Impact plot for the F0 parameter of interest using the 2018 dataset.

Short description: In this note we describe a methodology, called the Tag Rate Function, which allows us to significantly reduce statistical uncertainties of the distributions of $t^{-}t$ events with high b-tagged multiplicities utilizing the ones with lower b-tagged multiplicities. This method is using per event weights, derived by parametrised b-tagging probabilities, in order to predict the rate and shape of several distributions in events with higher b-tag multiplicities starting from the ones with lower b-tagged multiplicities. The prediction of kinematic, topological, but also higher-level variables, like a BDT output, is examined and shown. The impact this approach has on the systematic uncertainties of the $pp \rightarrow T^{'}T^{'} \rightarrow bbWW$ measurement in the di-leptonic and fully-hadronic channels, related with the limited statistics of the simulated samples, is briefly mentioned. In addition, we present a method to approximate the MEM discriminant for events with low b-tag multiplicities, since its computation for those is very computer intensive and hence is completely absent. This variable is important for the BDT estimation, and its approximation is implemented using two complementary approached: a Look-Up-Table and a multivariate regression technique using the higher b-tagged multiplicity events for which MEM is provided, see Fig. 14.

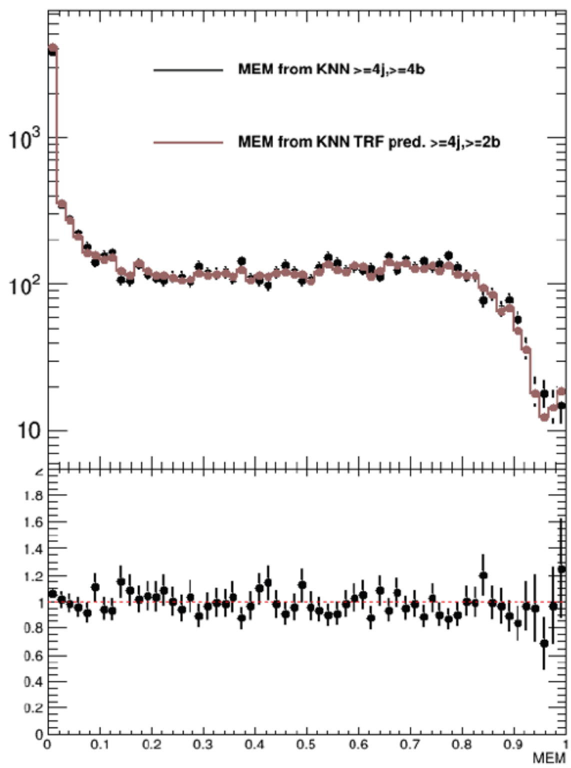

Figure 14: Closure of the TRF predicted MEM from events with at least 2 b-tagged jets with the one for events with at least 4 b-tagged jets.

Trigger Manu development

A.Stakia

Anna Stakia, as part of her service work to the CMS experiment, studied the “acceptance” of L1T seeds with respect to the related High Level Trigger paths. This consists of calculating the fraction of events passing an HLT path triggered uniquely by a particular L1 seed, compared to those events passing the same HLT path also triggered by other L1T seeds. A study of the L1T algorithms performance was conducted, estimating how often an event selected by an unprescaled L1T seed is recorded. Those studies concluded in the development of an L1T+HLT acceptance software tool, which at a first stage provided the L1T+HLT acceptance results obtained from NanoAOD input samples; the existing part of code was tested and fixed, and new parts of code were developed for this purpose, these being part of a streamlined, user-friendly workflow. At a second stage, the full set of L1T+HLT acceptance results were to be obtained starting from L1Ntuples, via modifying and upgrading the code to work in such case.

Institutional Reviews, Committees

Analysis Review Committees (ARC):

Georgios Daskalakis was the chairman of ARC for the publications:
EXO-19-017: ‘Search for new physics in lepton plus MET final state‘
EXO-21-009: ‘Search for new physics in the tau + MET final state (full Run 2)‘

Georgios Anagnostou was ARC member for the publication:
B2G-19-004: ‘Search for single production of a vector-like T quark decaying to a top quark and a Z boson in the jets plus missing transverse momentum final state at $\sqrt{s} = 13\ TeV$.

Institutional Reviews:
”WW DPS with full Run2”, CMS Collaboration, CMS Paper SMP-21-013
”Extraction and validation of a new set of CMS tunes with new color reconnection models in PYTHIA8 from underlying-event measurements”, CMS Collaboration, CMS Paper GEN-17-002
”Differential tt cross sections in the full kinematic range in lepton jets (full Run2)”, CMS Collaboration, CMS Paper TOP-20-001
”Search for a heavy resonance decaying to a top quark and a W boson at sqrt(s) = 13 TeV in the fully hadronic final state”, CMS Collaboration, CMS Paper B2G-19-003

Search in the 2-Dimensional mass space for final states with 2 invisible particles

G. Anagnostou

A generic method to search for final states with two invisible particles is presented. The method is applicable at LHC dark matter searches in terms of mass variables instead of missing energy related observables. Thus, a bump hunting is possible, allowing a stronger signal versus background discrimination. Parameters of the new theory can be extracted from the mass distributions, a valuable step towards understanding its true nature. The proof of principle is based on the existing SM top pairs in their dilepton final state. The method is applicable in many interesting searches at the LHC, including dark matter candidates or heavy top partners [4].

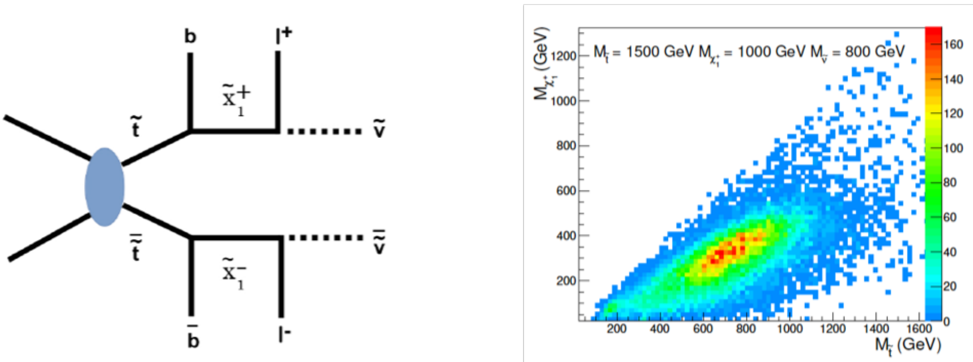

Figure 15: Left: Topologies with dark matter candidates such as stop quark pairs, Right: A pair produced stop quark topology with two invisible particles (see left) as well as reconstructed signal distributions for stop pair production with $M_{\tilde{t}} = 1500$ GeV, $M_{x_1^+} = 1000$ GeV, $M_{\tilde{\nu}} = 800$ GeV together with the expected background processes corresponding to an intergrated luminosity of 50 fb^{-1} at 13 TeV.

CMS Tracker

P.Assiouras, A.Kyriakis, I.Kazas, A.Papadopoulos, D.Loukas

During 2021 the activities of the INPP CMS group included: Process Quality Control, Development of Inner Tracker firmware and middlware and as a byproduct participation to the MuonE experiment [5]. Intensive activity on TCAD simulations is going on, mainly by Panagiotis Assiouas [6]

Process Quality Control at INPP

CMS has developed a quality assurance plan to ensure the full compliance of all sensors with the technical specifications and to monitor their production procedure and fabrication stability. Process quality control is contacted to dedicated test structures produced in the same wafer as the silicon sensors that will be installed in the CMS experiment, thus, sharing the same properties and materials.

[4] Anagnostou G. "Searching in 2-Dimensional mass space for final states with 2 invisible particles". In: *J. High Energ. Phys. 2021, 112* (2021). DOI: https://doi.org/10.1007/JHEP07(2021)112

[5] Abbiendi. "Status of the MUonE experiment," in: *PoS.* (2021). DOI: https://doi.org/10.22323/1.390.0223

[6] A. Kyriakis P. Assiouras P. Asenov and D. Loukas. "Fast calculation of capacitances in silicon sensors with 3D and 2D numerical solutions of the Laplace's equation and comparison with experimental data and TCAD simulations". In: *J. Inst. 15 P11034* (2020). DOI: https://doi.org/10.1088/1748-0221/15/11/P11034

These test structures provide access to important parameters about the fabrication quality of the sensors, including parameters that are not directly accessible on the sensors and together with the sensor quality control, consist one of the two main procedures of the quality assurance plan of the Outer Tracker silicon sensors for the Phase-2 upgrade. The procedure of the process quality control on the production phase, relies on a test structure set which provides access to all relevant process parameters. Within the set, test structures are connected to 20 contact pads that allow automated measurements to be made by using a 20-needle probe card, but also it can be operated by using individual probe needles. Test structures are separated in two subsets: the quick subset which allows the most important parameters to be measured and the extended which provides the possibility for a more detailed analysis. In this work the process quality control procedure and the related test structure set is described along with the extraction procedure of the relevant process parameters. First results from the pre-production phase are presented as well.

Test Structures

The 6" wafer layout for CMS tracker PS-s, 2S and PSp sensors as can be seen be 16 includes the sensors in the central part of the wafer and test structures in the surrounding area. These dedicated test structures are arranged around an array of 20 contact pads that are equally spaced horizontally and vertically. This array of contact pads is called "flute" and it allows automated measurements to be made, by using a 20-needle probe card and a switching matrix.

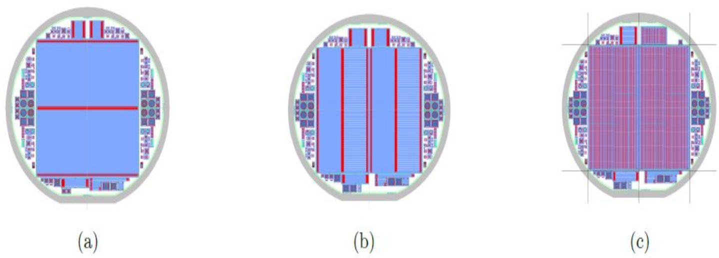

Figure 16: Wafer design of the three sensors types, 2S (a), PS-s (b) and PS-p (c). The scheme of wafer is indicative of a p-Type silicon wafer of 111 crystal oriantation

Figure 17 shows one diced part of the wafer, called "Halfmoon", in which the test structure sets are constructed. Each halfmoon contains 2 sets of 4 main flutes (labeled "PQC1–PQC4") in each side that are used in the usual procedure of the process quality control. There are also 11 additional flutes in each set that can provide the possibility for in-depth analysis if irregularities are found during a standard PQC measurement, as well as standard test structures like MOS capacitors and diodes that can be measured manually with probes. Figure 18, shows a close-up of one test structure set and its components. The main flutes are separated in:

- Quick flutes: They allow a fast evaluation of the most important parameters, consisting of:

- PQC1: It includes a quarter-sized diode (1.25×1.25 mm), from which the full depletion voltage and substrate resistivity are measured, a quarter-sized MOS capacitor (1.29×1.29 mm) for flat band voltage and fixed oxide charge concentration measurements, capacitors to evaluate the thickness of the dielectric, van der Pauw crosses [7] to measure the sheet resistances of polysilicon, n+ implant and p-stop, and a field-effect transistor to assess the inter-channel properties.
- PQC2: It provides a gate-controlled diode [8] which allows to access surface recombination velocity and interface trap density, a polysilicon resistor with the same dimensions as a standard bias resistor of the sensor strips, two line width structures of n+ and p-stop implants as an addition to the van der Pauw structures of the first flute, and a dedicated structure to measure the dielectric breakdown voltage. This flute acts as an extension to the first flute to allow a complete overview of the most relevant process parameters.

• Extended flutes: In addition with the quick flutes, the extended flutes allow a comprehensive evaluation of all relevant process parameters.

- PQC3: It provides a half-sized diode 2.5×2.5 mm, a metal meander with 12,853 squares, a clover-shaped metal van der Pauw structure, and bulk and p+ van der Pauw crosses.
- PQC4: It includes a gate-controlled diode with a wider gate than the gate-controlled diode in the second flute. Furthermore, the flute includes contact chains and cross bridge Kelvin resistance structures to determine the metal contact quality.

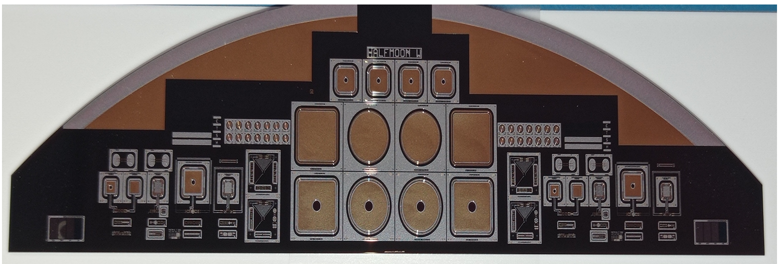

Figure 17: Photo of one halfmoon. Each halfmoon contains 2 sets of 4 main flutes. There are also additional flutes and test structures that can provide a more detailed investigation if it is needed

The PQC setup

Each PQC center has a special probe station, dedicated to test structure measurements. Although the setup in each center may vary, they share some common

[7] Dieter K. Schroder. “Semiconductor Material and Device Characterization, 3rd Edition”. In: • (2005). DOI:

[8] C Becker et al. “Gate-controlled diodes for characterization of the Si–SiO2 interface with respect to surface effects of silicon detectors”. In: *Nuclear Instruments and Methods in Physics Research Section A: Accelerators, Spectrometers, Detectors and Associated Equipment* (2000). DOI: https://doi.org/10.1016/S0168-9002(99)01177-8

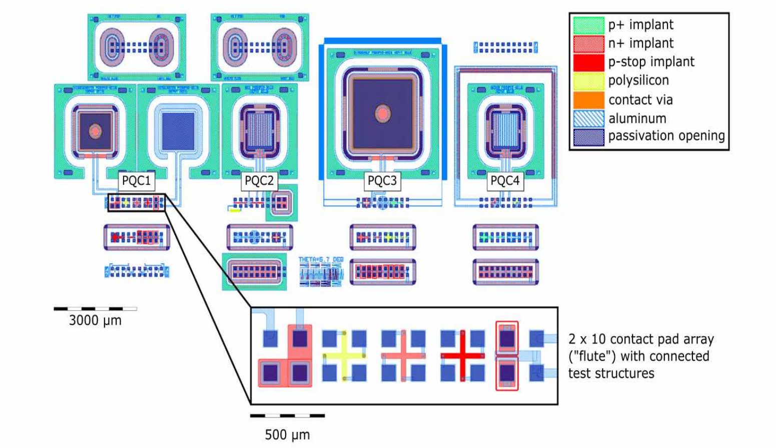

Figure 18: Schematic of the 4 different flutes that exist in each test structure set. They are separated in quick flutes allowing a fast evaluation of most important parameters and extended flutes that provide addition parameters for the quality control of the sensors. The color variation depicts the different materials and implantation with which the wafers are constructed.

features and should have some specific requirements. Each setup consists of a prober with an XYZ-stage (or XY-stage with controllable vertical position of the probe card) a jig with integral cooling system and vacuum pipes and which can provide high voltage contact to the backplane of the sensor. The whole probe station setup is inside a light-tight aluminum box enclosing the probe station which provides a dark environment and prevents electromagnetic interference. A dry air compressor is constantly filling the probe station in order to maintain the relative humidity below the 30 %. The air temperature inside the enclosure should be less than $23 \pm 5\ ^oC$ during the measurement process.

All PQC centers use Keithley 707B six-slot mainframe supporting various cards. The PQC system uses at least one 8×12 High-voltage card 7072-HV and one 8×12 "low-voltage" Semiconductor card 7072. A 20-needle probe card (figure 20) is used to contact the PQC flute test structures for performing automated measurements. It consists of a Printed Circuit Board (PCB) that provides all the connections and circuitry and a mount for the probe needles that is fixated to the PCB. The board provides 23 triax LEMO connectors, 20 of which are rooted to the probe needles via the PCB. One connects to a temperature and humidity sensor integrated in the PCB, and the remaining two connectors lead to an RC test circuit consisting of a 100 $M\Omega$ resistor and a 10-pf capacitor. An Atlas Copco air dryer lowers locally on the test structure the humidity bellow 20% RH. Figure 21 shows a photo of the measurement setup.

Example of PQC measurements: The Metal-Oxide-Semiconductor capacitor (MOS)

As an example of the PQC measurement follows the measurement and data analysis procedure for the MOS capacitors.

Metal-oxide-semiconductor capacitor is one of the most useful device in the

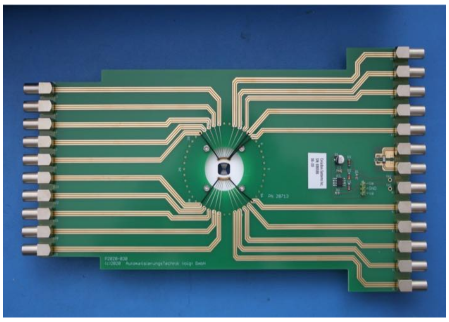

Figure 19: Probe card.

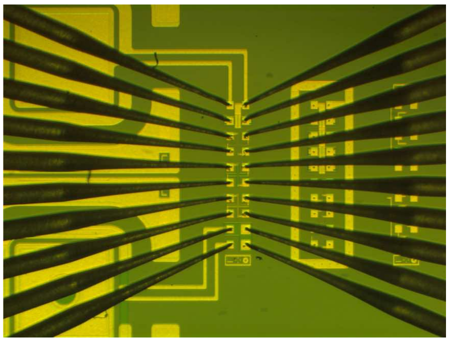

Figure 20: Probe card needls in contact with a flute.

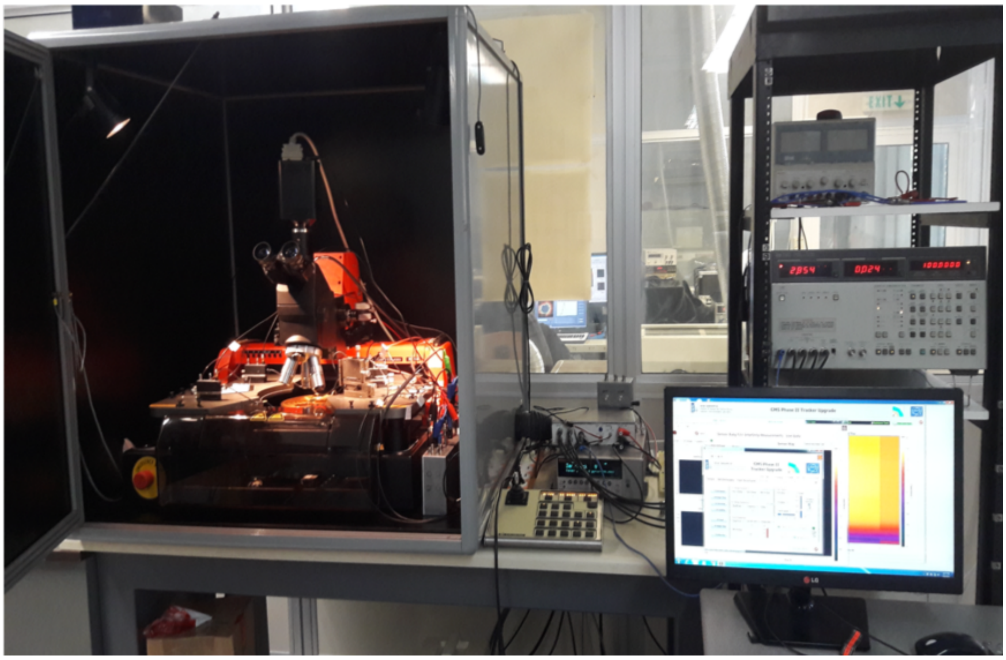

Figure 21: Photo of automatic measurement system at INPP

study of the properties of the Si-SiO_2 interface. The parameters that can be extracted with this device are the fixed oxide charge, oxide trapped charge, mobile oxide charge, interface trapped charge, the oxide capacitance and the oxide thickness. It consists of a SiO_2 layer sandwiched between a semiconductor bulk and a metal gate electrode. Figure 22 shows the design of the MOS structure of PQC1 flute.

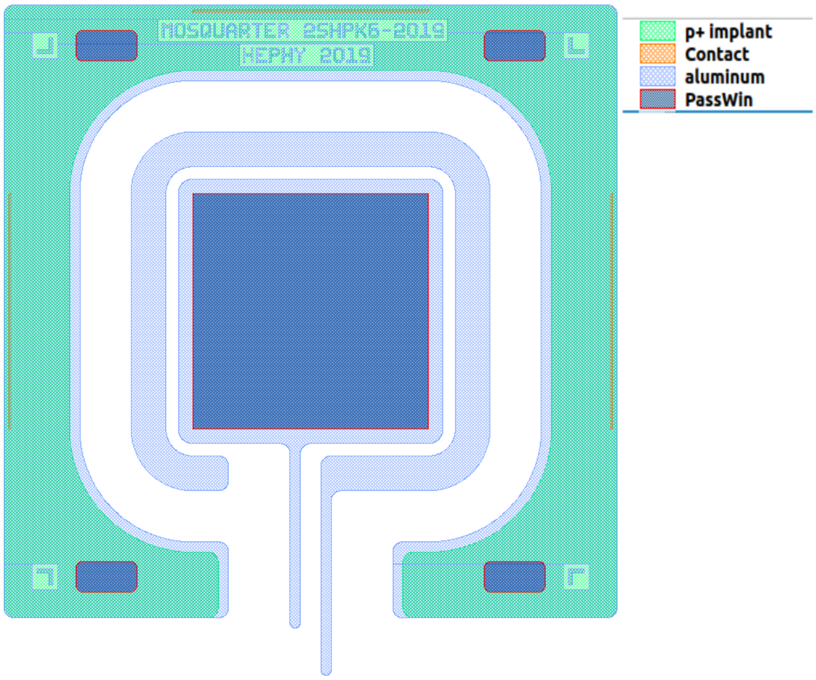

Figure 22: Design of MOS structure in PQC1 flute.

An important parameter in the study of the MOS capacitor is the flat band voltage. The flat band voltage corresponds to the voltage which when applied to the gate electrode the energy bands (Ec and Ev) of the substrate are flat at the Si/SiO_2 interface. If there is no charge present in the oxide or at the oxide-semiconductor interface, the flat band voltage (V_{fb}) simply equals the difference between the gate metal work function, ϕ_m, and the semiconductor work function, ϕ_s ($V_{fb} = \phi_m - \phi_s$), which in an ideal case equals zero ($V_{fb} = 0$). The presence of fixed (or induced by radiation) oxide charges shifts the flat band voltage and this shift of the experimental MOS curve compared to an ideal curve can be used to determine the fixed oxide charge concentration N_{ox} by using the equation 1 [9],

$$N_{ox} = \frac{C_{ox}/A(\phi_{ms} - V_{fb})}{q} \tag{1}$$

where C_{ox} is the oxide capacitance, A is the gate area of the MOS and q is the elementary charge. In the usual procedure of this measurement the bias voltage is swept from -10 to 5 V and the capacitance is measured by applying an AC pulse at 10 kHZ resulting to the characteristic curve of the MOS capacitor, figure 23.

[9] S.M. Sze and G. Gibbons. "Effect of junction curvature on breakdown voltage in semiconductors". In: *Solid-State Electronics* (1966). DOI: https://doi.org/10.1016/0038-1101(66)90033-5

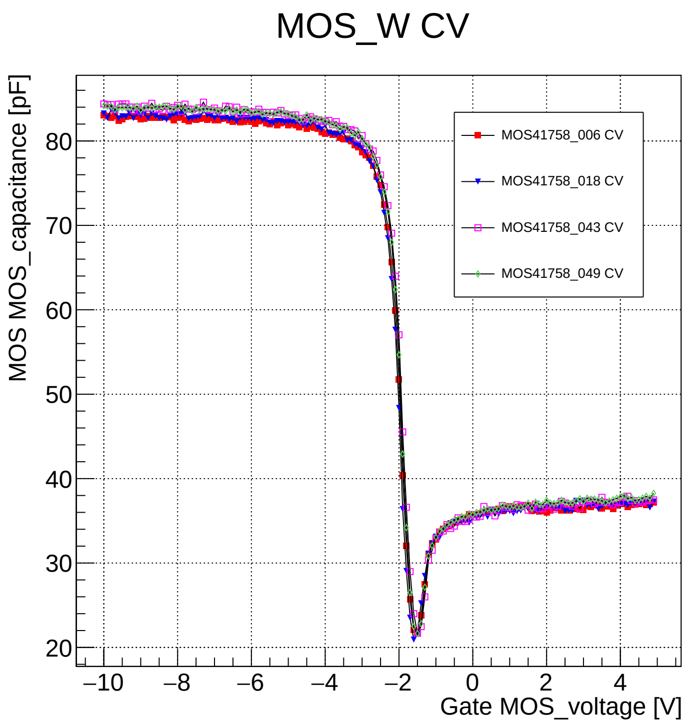

Figure 23: CV measurements performed on MOS capacitors of several wafers from an indicative production batch.

Three characteristic regions can be identified in figure 23 that corresponds to three different phase of the MOS. In left part, so called accumulation part the majority carriers populate the region beneath the oxide. In this phase the capacitance is equal to the oxide capacitance only (C_{ox}). As the gate voltage increases and becomes equal to the flat band voltage $V_g = V_{fb}$ (central part) the region beneath the oxide depletes, which corresponds to an abrupt decrease of the capacitance. The measured capacitance in depletion is given by the oxide capacitance in series with the capacitance of the depleted silicon bulk. In the inversion region (right part), when $V_g \gg V_{fb}$ minority carries accumulate beneath the oxide that stops the further extension of the depleted zone. The capacitance measured in inversion depends on the AC measurement frequency and the sweep rate of the DC gate voltage. At low frequencies (5-100 Hz) electrons are generated in the substrate which enrich the inversion layer, which can follow the variations of the gate charge caused by the AC signal. The charge of the inversion layer exceeds the charge of the depleted region. In this case the depleted area does not affect the capacitance of the device and the total capacitance is equal to that of oxide $C_{inv} = C_{ox}$. At high-frequency (> 100 Hz) the inversion charge cannot follow the AC measurement frequency. The capacitance in the high-frequency case remains constant at a minimum value given by the oxide capacitance in series with the capacitance C_d of the space-charge region at maximum depletion width $C_{inv} = C_{ox}C_d/(C_{ox} + C_d)$.

Work for the CMS Phase-II Inner Tracker

The Inner Tracker will be equipped with pixel modules. The high-luminosity operation implies extreme challenges for the design of the Inner Tracker in terms of radiation tolerance of sensors and readout electronics, as well as data volume to be stored in the front-end pipelines and sent out at high trigger rates. Thin silicon sensors (of thickness $100 - 150$ mm), segmented into pixel sizes of 25×100 μm^2 or 50×50 μm^2, are expected to exhibit the required radiation tolerance and to deliver the desired performance in terms of detector resolution, occupancy, and two-track separation. Consequently, a readout chip with a small cell size and low detection threshold is required. ATLAS and CMS were carrying out a common development in the framework of the RD53 collaboration [22] and designed a pixel chip with 2500 $\mu m2$ cell size, in 65 nm CMOS technology. With such a configuration the detector resolution is much more robust with respect to radiation damage than the present detector, where the precision relies on the ability to reconstruct the tails of the charge deposit in a 300 mm thick sensor. Figure 24 shows the first RD53 prototype, the so called RD53A chip. It has a total of 92×400 pixels arranged in three analogue blocks and common digital block. The FE_SYNC analogue block is based on a single stage design with SAR-like ToT counter using synchronous comparators. The FE_LIN block is a single stage design with current comparator and ToT counter. The FE_DIFF block is relying on a first stage with continuous reset integrator plus DC couple pre-comparator stage, figure 24 . Figure 25 outlines change of operation parameters from Phase-I CMS to Phase-II.

Our group is developing the firmware and middleware for the readout and control of the front end modules of Inner Tracker.The readout and control of the future front-end modules of the CMS Tracker, will be performed by the DAQ, Trigger and Control(DTC) System. The μDTC project was established to perform these tasks in the prototyping and production phases. Common framework for the Outer tracker (OT) and the Inner Tracker (IT) is based on FC7 board and IPBus protovol, both developed by CERN. Figure 26 shows the suite of the DAQ system and the main players. The DAQ is a versatile system capable of supporting characterization, production and integration tests of the upgraded CMS Tracker. It has been used in beam-tests, hardware characterization, serial power chain tests and in the testing campaign for RD53A.

This extensive characterization campaign of the chip, led to modifications of the chip design based on the testing results. On the next version of the chip, called RD53B, the CMS flavour of the chip (CROCv1) is equipped with the FE_LIN block as Analog Front End and among the many added features with respect to the RD53A chip, are data merging between neighboring chips, data compression to reduce the data rate by a factor of 2 and a self trigger capability. The critical IP blocks of PLL/CDR and the Shunt LDO power regulator circuits have improved greatly allowing for a reliable operation. Protection features against overvoltage and overload have been added together with an optional low power mode. To mitigate Single Event Effects (SEE) a Triple Modular Redundancy (TMR) strategy was adopted including self correction and a triplicated clock tree with skew for critical parts. The new chip was received in September 2021 and support for the new features has already been added to the DAQ. A testing campaign has

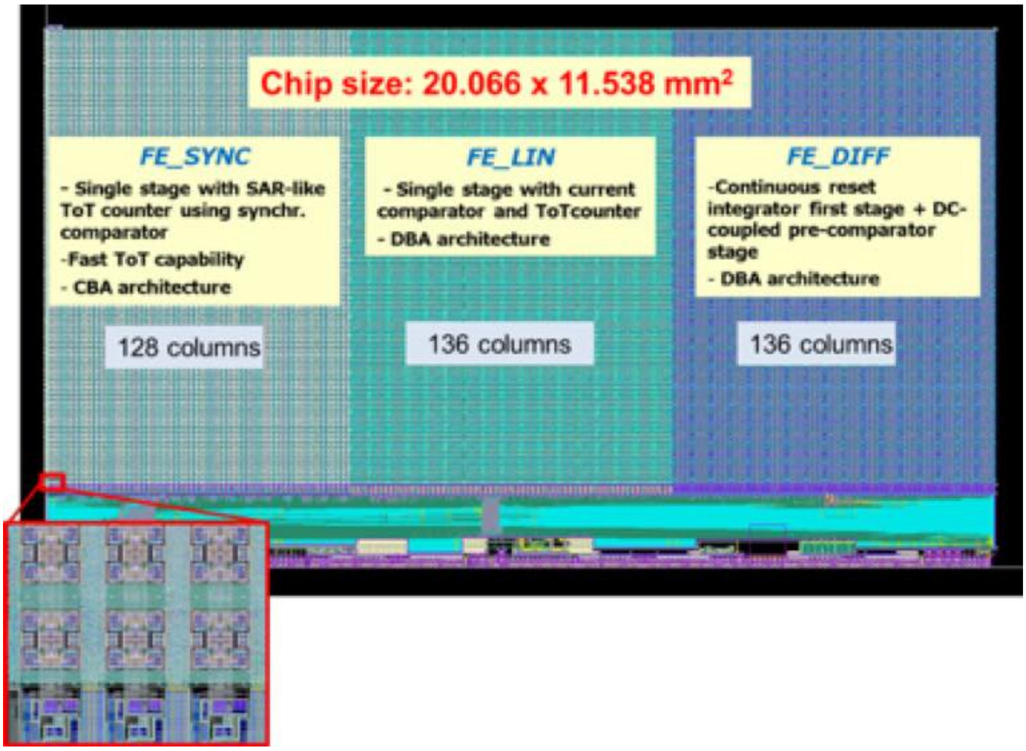

Figure 24: Layout of the RD53 ASIC

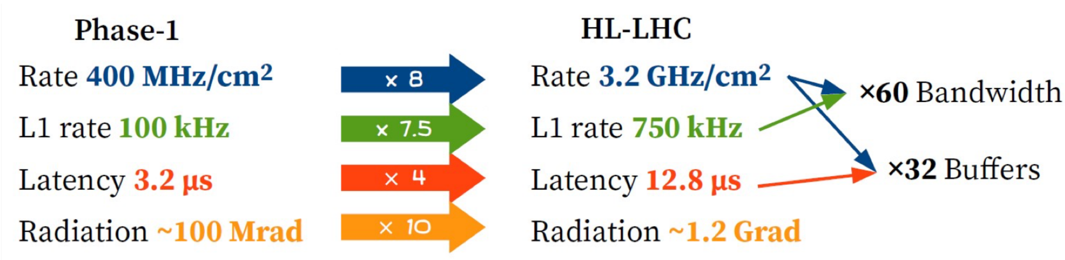

Figure 25: Change of parameters in CMS from Phase-I o Phase-II

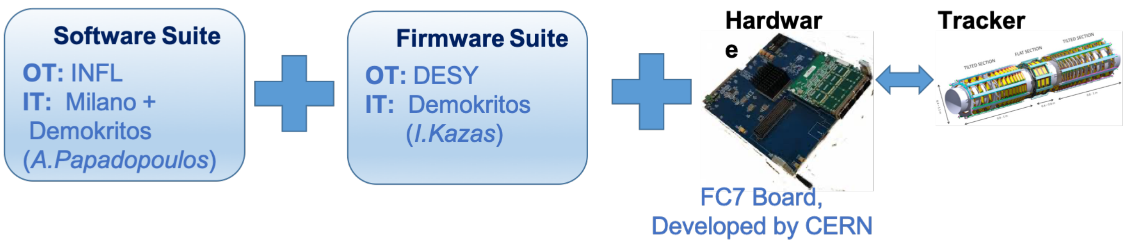

Figure 26: Block diagram of the main blocks in the CMS Phase II DAQ

been running since, in which our group is playing a major role as the coordinating group for the testing activities.

The MUonE experiment and the CMS Phase-II Tracker

The new experimental average of the recent FNAL Muon- $g-2$ measurement of the positive muon magnetic anomaly α_μ combinet with the previous measurement increases the tension between experimental and theoretical SM value to 4.2σ. It is known that hadronic contributions are responsible for almost all of the theoretical uncertainty. The leading hadronic contribution is due to hadronic vacuum polarization. However, it should be noted that a recent Lattice QCD result [10] is closer to the experimental data, in tension with the usual dispersive calculation.

MUonE [11] is an experiment aiming at an independent determination of the leading hadronic contribution to α_μ with a new method, from a precise measurement of $\Delta\alpha(t)$, the hadronic contribution to the running of the fine-structure constnant, in $\mu e \to \mu e$ elastic sacttering, by using the CERN muon beam ($E = 160\ GeV$) on a fixed target. The experiment is planned to consist of 40 tracking stations with a thin (in order to limit multiple scattering) low -Z target and 6 silicon microstrip detectors using the same $2S$ modules developed for the upgrade of the CMS aoter tracker. After the tracking station, an electromagnetic calorimeter (ECAL) and a muon filter will complete the apparatus to help with the identification and the selection (Fig. 27).

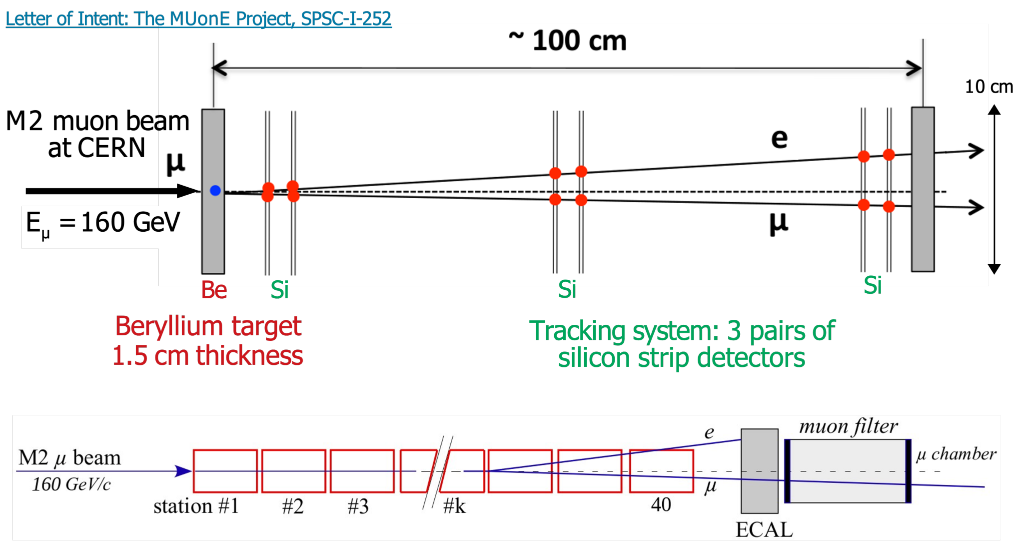

Figure 27: MUonE setup scheme where the locations of the tracking stations, ECAL, and muon chamber are indicated. (Not-to-scale.)

Our group is developing a Geant4 program in order to compare recent versions

[10] Sz. Borsanyi et al. "Leading hadronic contribution to the muon magnetic moment from lattice QCD". in: *Nature* 593 (Apr. 2021). DOI: 10.1038/s41586-021-03418-1

[11] G.Abbiendi et al. "Measuring the leading hadronic contribution to the muon g-2 via μe scattering". In: *The European Physical Journal C77, 139* (2017). DOI: https://doi.org/10.1140/epjc/s10052-017-4633-z

of Gean4, where more accurate electromagnetic processes are included, with respect to older versions. During 2021 the MUonE setup has been simulated with the recent Geant4 version containing relevant updates, mostly regarding the correct estimation of the angular distribution of the e^+e^- production from muon interactions.

Standard Geant4 tests were performed in order to determine the appropriate physics lists, models and Geant4 versions to be used in the simulation of the MUonE setup before including the reconstruction stage. The program was used for the estimation of contributions of different interaction processes to the total energy loss for the relevant materials composing the MUonE detector. The application calculates the macroscopic differential cross section $d\sigma/d\epsilon$, where the macroscopic cross section σ is related to the microscopic differential cross section σ_A by $\sigma = \sigma_A n_A/\rho_A$, where n_A is the density of atoms per unit volume and ρ_A is the material density. Tests were done for candidate target materials (beryllium and carbon) as well as for silicon, which is the main material in the tracking modules (Fig.28 top and bottom left, respectively). It was observed through simulation that the optimal physics list for MUonE should contain the Geant4 lists: FTFP-BERT, electromagnetic option 4(containing the most accurate standard and low-energy models) and the default model for muon nuclear interactions. (Option4 EM physics mainly affects the simulation of secondary particles produced by muons, and in addition is more accurate for δ-electrons and photons). The program was also used for the estimation of angular correlations. In particular, it was shown that the latest Geant4 version (from 10.7 and onward) introduce an improved simulation of the angular distribution of e^+e^- pairs. In previous versions, the e^+ and e^- were simply generated at a common outgoing direction. The recent version have an improved angular distribution, and the two exit angles show a reasonable distribution, as visible in Fig. 28 bottom right.

Funding

ESPA : Title: *"New generation of sensors and electronics for the upgrade of the CMS experiment at CERN"*. Duration ,717/03/2020 - 16/07/2021. Budget 4100.41 euro
ELIDEK: Title : *Development of the Phase-II silicon tracker of the CMS experiment at CERN* . Duration , 1/11/2019 - 31/5/2021. Budget 17200 euro (P. Assiouras)
ELIDEK : Title ¨: *Silicon Sensors R&D for the HL-LHC* . Duration 5/09/2017 - 31/03/2020. Budget 27900 euro (P.Asenov)

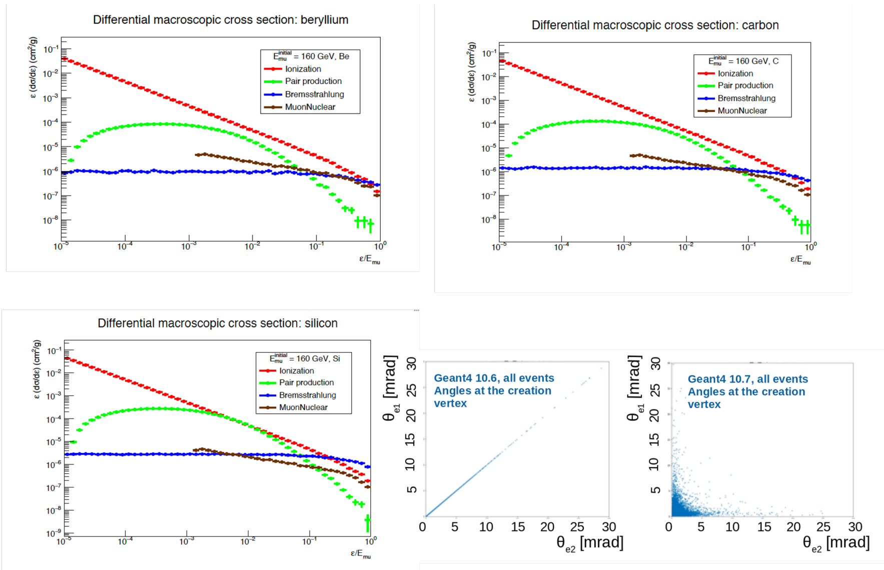

Figure 28: Geant4 (version 11.0) differential macroscopic cross section for muon interaction processes in beryllium (top left), carbon (top right) and silicon (bottom left) for production of δ-electrons, e^+e^- pairs, bremsstrahlung and nuclear interactions. Comparison of electron-positron pair angles with respect to the incoming muon in Geant4 10.6 (bottom middle) and 10.7 (bottom right).

Additional experimental activities

Researchers:	George Fanourakis
	George Stavropoulos
	Theodoros Geralis
Administration:	George Fanourakis
Employees:	Olga Zormpa
	Maria Myrto Prapa

Introduction

The European Spallation Source Neutrino Super Beam (ESSnuSB or ESSνSB, https://essnusb.eu/) project is a future accelerator-based neutrino oscillation experiment design for CP violation discoveries in the lepton sector. This facility has been proposed after measuring in 2012 a relatively large value of the neutrino mixing angle θ_{13}, opening the possibility to observe for the first time a possible CP violation in the leptonic sector which is the key ingredient to explain the lack of antimatter in the Universe. The measured value of θ_{13} also privileges the 2nd oscillation maximum for the discovery of CP violation instead of the usually used 1st oscillation maximum. The sensitivity at this 2nd oscillation maximum is about three times higher than for the 1st oscillation maximum inducing a lower influence of systematic errors. However, since the neutrino flux is reduced at the 2nd oscillation maximum, a very intense neutrino beam with the appropriate energy is required. The world's most intense pulsed spallation neutron source, the European Spallation Source (ESS), will have a proton linac of 5 MW power and 2 GeV proton kinetic energy. ESSnuSB proposes the upgrade of the ESS proton linac to 10 MW, 2.5 GeV and to use half of the protons to produce a neutrino Super Beam, leaving the ESS neutron program undisturbed. The physics performance of that neutrino Super Beam in conjunction with a megaton underground Water Cherenkov neutrino detector installed at a distance of 360–500 km from ESS is being evaluated. The ESS proton linac upgrades, the accumulator ring needed for proton pulse compression, the target station optimization and the physics potential are included in the study. The ESS neutron facility will be fully ready by 2025 at which moment the upgrades for the neutrino facility could start.

The neutrino (anti-neutrino) oscillation to be studied here is $\nu_\mu \to \nu_e$ ($\bar{\nu}_\mu \to \bar{\nu}_e$). Fig. 29 presents the unoscillated neutrino and anti-neutrino energy distributions which could be obtained by the proposed facility at an arbitrary on-axis distance of 100 km from the neutrino target.These distributions correspond to one year neutrino run (200 days). An almost pure muon neutrino (anti-neutrino) beam is produced with a main contamination of about 0.5% of electron neutrinos (anti-neutrinos). This contribution polluting the primary muon neutrino beam, could be used to measure the electron neutrino cross-section using an appropriate near detector.

Fig. 30 presents the $\nu_\mu \to \nu_e$ oscillation probability at a distance of 540 km for several values of δ_{CP} and for normal and inverted neutrino mass hierarchies. The overlapping grey distribution is the ν_e energy distribution coming from the ν_μ

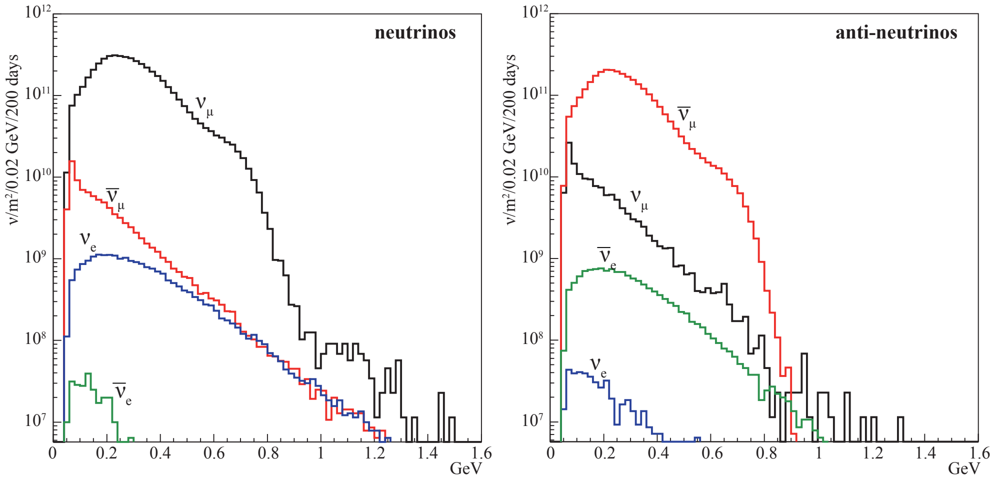

Figure 29: Energy distribution for neutrino (left) and anti-neutrino (right) beam at an arbitrary distance of 100 km from the target station, for 2.5 GeV protons.

oscillation. It is obvious that the 2nd oscillation maximum is fully covered. From this figure it is also seen that the CP violation discovery potential is not affected by the unknown neutrino mass hierarchy. It has to be mentioned that this project is exclusively devoted to CP violation discovery and not to the mass hierarchy determination which is believed to be solved by then by experiments scheduled to start taking data during the next decade.

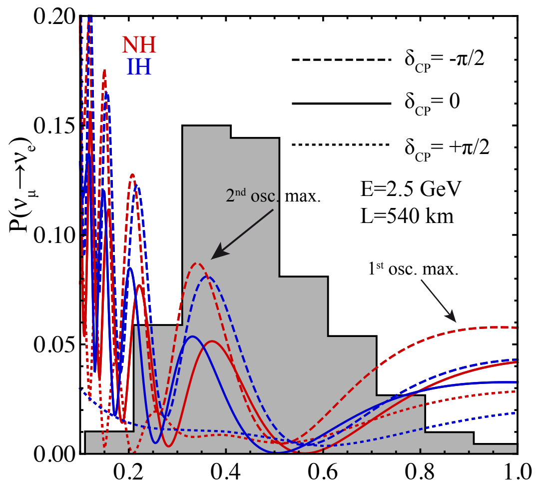

Figure 30: small $\nu_\mu \to \nu_e$ oscillation probability as a function of the neutrino energy. The red (blue) lines are for normal hierarchy (inverted). The shaded histogram is the energy distribution of ν_e produced by the ν_μ oscillation and detected by the far detector.

The physics performance strongly depends on the considered systematic uncertainties, which play less a role on the 2nd oscillation maximum thanks to the interference term in the oscillation probability dominating the solar and atmospheric terms.

After 10–years operation, it is expected that about 600 electron neutrinos and antineutrinos will be detected by the far detector. Fig. 31 slows the CP violation discovery significance versus δ_{CP}. Up to 60% of the δ_{CP} values can be covered with a significance of 5 σ. Studies are under way to increase the number of detected

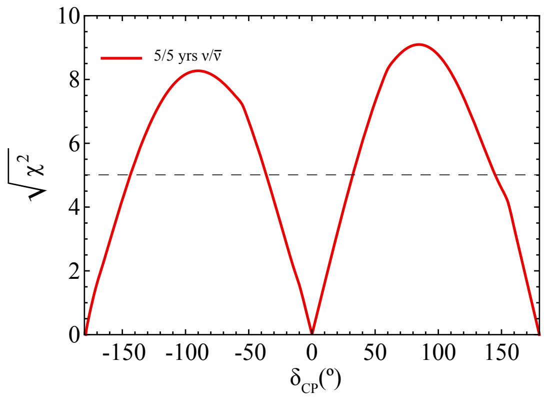

Figure 31: small The significance with which CP violation can be discovered as a function of δ_{CP}.

neutrinos by further optimising the magnetic horn shape and the far detector performance. A dedicated working group for the ESSνSB detector designs aim to reduce the systematic uncertainties in the signal/background neutrino flux to below 5%, such that the 5 σ discovery range of δ_{CP} may increase.

Activities

The ESSνSB Demokritos INPP team is part of the Detector Performance and the Physics Reach working groups. Our work has so far been mainly focused on the far detector (FD) studies.

The Detector Performance group has developed the EsbRoot environment for detector simulations and event reconstruction based on the FairRoot framework. However, for the design of water Cherenkov (WC) detectors, envisioned as a near detector (ND) as well as a far detector (FD), an additional open-source simulation package, called WCSim, is being used. WCSim is based on Geant4 and ROOT. A generalised particle source for basic diagnostic tests of the detector geometry and reconstruction algorithms has been used, as well as a Monte-Carlo neutrino event generator GENIE on the estimated neutrino flux from ESS for more realistic event simulations and detector response evaluations. Its outputs have been successfully used as inputs for EsbRoot and WCSim, and the integration of GENIE into EsbRoot is complete. A characterisation of all scattering reaction channels of the neutrinos in active detector materials is in progress. A prospect of constraining the neutrino flux from ESS with measurements of neutrino-electron reaction channels is being explored.

The FD for ESSνSB is a large water cylindrical Cherenkov detector, 78m base diameter and 78m height, based on the MEMPHYS (MEgaton Mass PHYSics) design. Studies on the expected performance of the FD were conducted via appropriately tuned EsbRoot, WCSim and fiTQun environments. Certain reconstruction and analysis strategies such as fiducial volume and timing cuts were implemented. Examples of the results of the analysis of Monte Carlo produced flat neutrino and antineutrino distributions for the geometry used in the T2K experiment are shown below:

To study the energy reconstruction capabilities of the far detector we have used a flat neutrino (antineutrino) beam distribution. The Energy distributions for the event types of interest and the neutrino beam flavors are presented in Fig. 32.

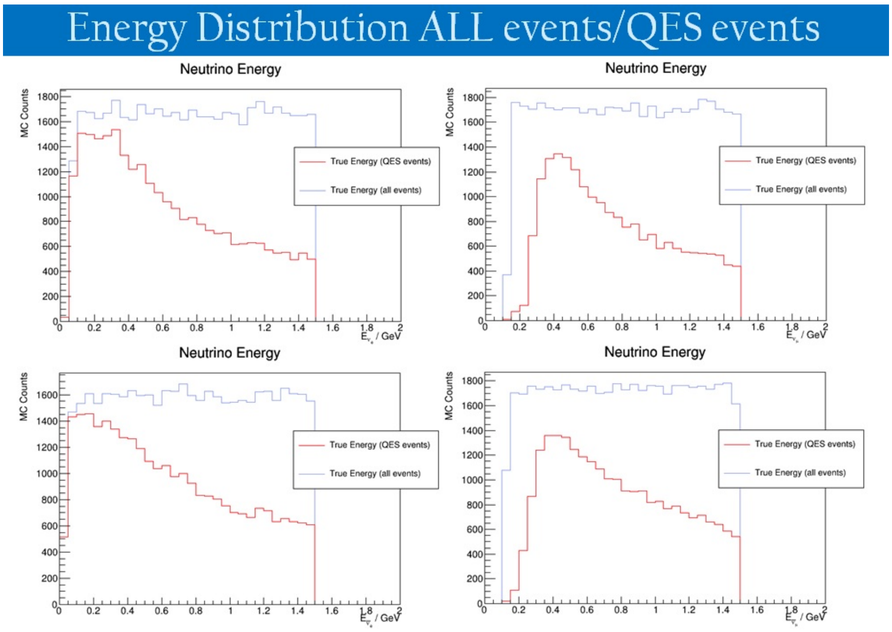

Figure 32: Energy distribution for all types and QES neutrino and antineutrino events.

The results on the migration matrices (reconstructed Energy vs true Energy), which show how well the neutrino (antineutrino) events are reconstructed, for all event and beam types are presented in Fig. 33 and for QES events in Fig. 34.

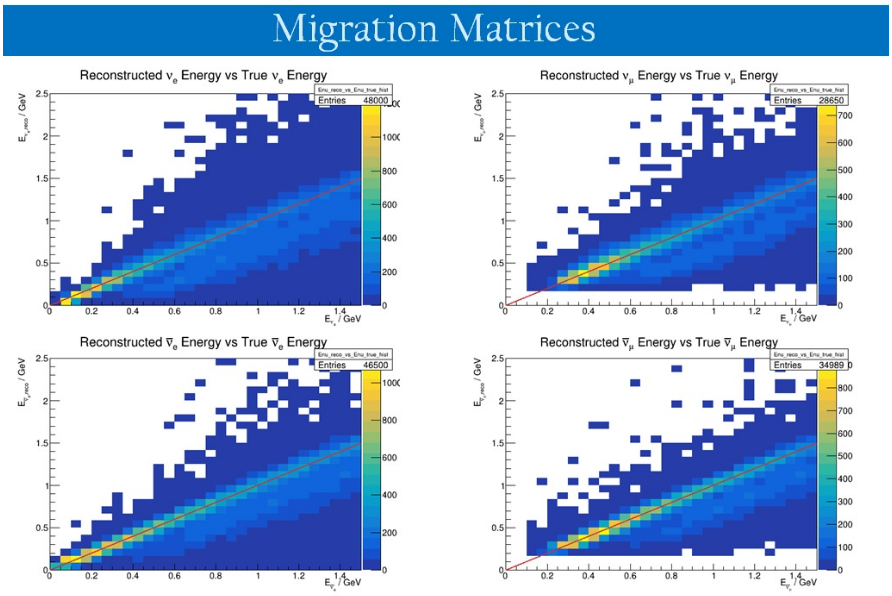

Figure 33: Reconstructed vs true energy distributions for all types of events

The analysis work for the ESSnuSB proposed detector configuration and the related parameter tuning will be in progress until early 2022.

The publications related to the ESSnuSB project work where the INPP group

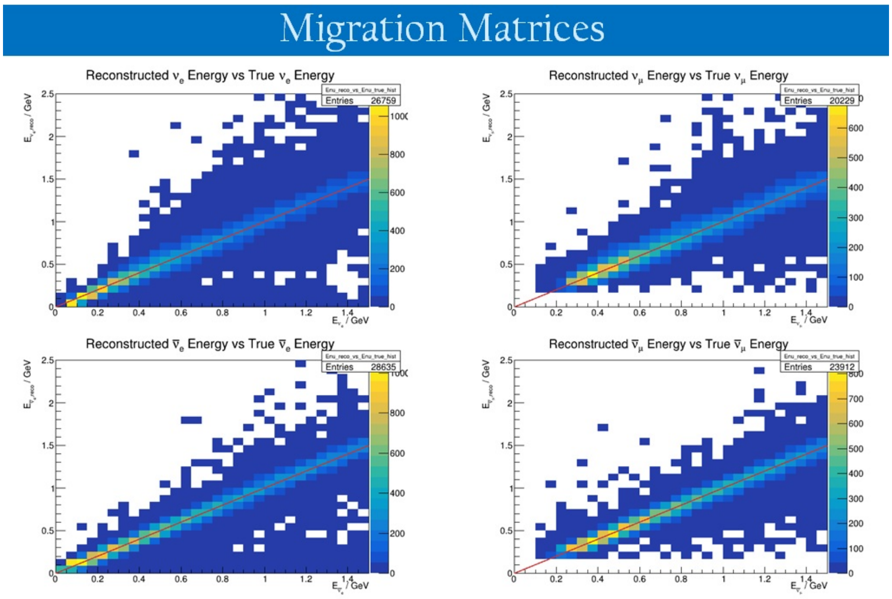

Figure 34: Reconstructed vs true energy distributions for QES events.

has contributed, during the years 2020 and 2021, include references [12], [13], [14],

Funding

This project has received funding from the European Union's Horizon 2020 research and innovation program under grant agreement No 777419. INPP group has received a total of 64,953.00 Euros for the 4 years duration of the ESSnuSB project. It has also been supported by the COST Action EuroNuNet *"Combining forces for a novel European facility for neutrino-antineutrino symmetry-violation discovery"*. This action supported travel for meetings and workshops.

Outreach

One of the members of the INPP group (GF) is part of the ESSnuSB Dissemination and Exploitation Board (DEB). DEB's tasks include the organization of participation to conferences, the editing of abstracts, talks and proceeding contributions as well as the public awareness events and materials. DEB's accomplishments include two videos about ESSnuSB, one for general public (https://youtu.be/qAnvft0nAlg) and one for scientist audience (https://https://youtu.be/PwzNzLQh-Dw).

[12] Joochun Park et al. "Status of the detector design studies for ESS*nu*SB". in: *PoS* NuFact2019 (2020), p. 041. DOI: 10.22323/1.369.0041

[13] Joakim Cederkall et al. "The ESSnuSB project". In: *PoS* EPS-HEP2019 (2020), p. 392. DOI: 10.22323/1.364.0392

[14] A. Alekou et al. "Updated physics performance of the ESSnuSB experiment: ESSnuSB collaboration". In: *Eur. Phys. J. C* 81.12 (2021), p. 1130. DOI: 10.1140/epjc/s10052-021-09845-8. arXiv: 2107.07585 [hep-ex]

Overview

The ESSnuSB project is a promising proposal for a next generation neutrino oscillation experiment tuned to the potential discovery of the CP violation in the leptonic sector. Such a discovery will solve one of the most important questions in cosmology: why there is no antimatter in the Universe? The INPP ESSnuSB group has been contributing to the work on the design and studies of the far detector since the beginning of the project. The current results exemplify the superiority of the Physics capabilities of ESSnuSB on the determination of the CP violating phase, over the currently proposed and in preparation long base line neutrino experiments.

Theoretical High Energy Physics

Researchers:	M. Axenides (Director of research)
	C. Papadopoulos (Director of research)
	G. Savvidy (Researcher emeritus)
Adjunct Scientists:	E. Floratos (Professor emeritus, NKU Athens)
Research Associates:	G. Linardopoulos
	D. Manolopoulos
	I. Mitsoulas
	G. Pastras
PhD students:	D. Canko
	D. Katsinis
	N. Syrrakos
Master students:	V. Tzotzai

Activities

High Energy Physics - Phenomenology

The research on High Energy Physics - Phenomenology aims to develop innovative methods and algorithms in order to establish an efficient framework for higher order corrections for multi-particle processes including

- amplitude reduction at the integrand level beyond one-loop,
- the evaluation of multi-loop Master Integrals and
- the application of the above-mentioned techniques to scattering processes at the LHC and beyond.

On the frontier of multi-loop calculations, the group achieved a major milestone, by completing the analytic representation of all massless planar five-point amplitudes with one off-shell leg [15]. This is a unique result world-wide. The methodology used is based upon the Simplified Differential Equations Approach (SDE) [16]. Recently, the calculation of the hexabox families has also been completed [17]. We have also studied one-loop pentagon integrals to arbitrary order in the dimensional regulator [18]. The SDE method has been also successfully applied to the canonical basis for the three-loop ladder-box with one external mass off-shell, obtaining subsequently a canonical basis for the massless three-loop ladder-box as well as its solution [19]. The application of SDE approach to problems with internal

[15] Dhimiter D. Canko, Costas G. Papadopoulos, and Nikolaos Syrrakos. "Analytic representation of all planar two-loop five-point Master Integrals with one off-shell leg". In: *JHEP* 01 (2021), p. 199. DOI: 10.1007/JHEP01(2021)199. arXiv: 2009.13917 [hep-ph]

[16] Costas G. Papadopoulos. "Simplified differential equations approach for Master Integrals". In: *JHEP* 07 (2014), p. 088. DOI: 10.1007/JHEP07(2014)088. arXiv: 1401.6057 [hep-ph]

[17] Adam Kardos et al. "Two-loop non-planar hexa-box integrals with one massive leg". In: *JHEP* 05 (2022), p. 033. DOI: 10.1007/JHEP05(2022)033. arXiv: 2201.07509 [hep-ph]

[18] Nikolaos Syrrakos. "Pentagon integrals to arbitrary order in the dimensional regulator". In: *JHEP* 06 (2021), p. 037. DOI: 10.1007/JHEP06(2021)037. arXiv: 2012.10635 [hep-ph]

[19] Dhimiter D. Canko and Nikolaos Syrrakos. "Resummation methods for Master Integrals". In: *JHEP* 02 (2021), p. 080. DOI: 10.1007/JHEP02(2021)080. arXiv: 2010.06947 [hep-ph]

masses constitutes another milestone [20]. On the frontier of two-loop scattering amplitudes, we have studied the reduction of two-loop amplitudes at the integrand level, as part of the newly developed software package HELAC-2LOOP [21]. All the above-mentioned work is essential to obtain high-precision predictions for scattering processes at the LHC, especially for the forthcoming high-luminosity Run as well as for future colliders [22].

String theory & quantum gravity

The research agenda of the group includes topics such as: (1) the bridging Quantum Field Theory (QFT) and Quantum Gravity (QGr) in the framework of the AdS/CFT duality, (2) the physics involved in the possible resolution of the black hole information paradox (3) String and M-theory. These topics constitute a very fertile ground of theoretical research on the origins of quantum gravity at the Planck scale. Quantum black holes and cosmological singularities are examples of physical systems where strong gravity effects are manifest and new concepts and principles appear to be at work such as nonlocality and strong chaotic mixing which operate in the framework of the Holographic principle and AdS/CFT correspondence. The group's published proceedings article [23] deals with M2-brane dynamics in the classical limit of the BMN matrix model. This article was the first deliverable in the group's research program "Chaotic dynamics and black holes in BMN theory" (MIS 5047794). The second deliverable of the program was the research article [24] which dealt with a cascade phenomenon in the propagation of instabilities from the leading to the next-to-leading order in perturbation theory. Other published articles of the group are [25].

[20] Nikolaos Syrrakos. "One-loop Feynman integrals for $2 \to 3$ scattering involving many scales including internal masses". In: *JHEP* 10 (2021), p. 041. DOI: 10.1007/JHEP10(2021)041. arXiv: 2107.02106 [hep-ph]

[21] G. Bevilacqua et al. "Progress on 2—loop Amplitude Reduction". In: *J. Phys. Conf. Ser.* 2105.5 (2021), p. 012010. DOI: 10.1088/1742-6596/2105/1/012010

[22] A. Blondel et al. "Standard model theory for the FCC-ee Tera-Z stage". In: *Mini Workshop on Precision EW and QCD Calculations for the FCC Studies : Methods and Techniques*. Vol. 3/2019. CERN Yellow Reports: Monographs. Geneva: CERN, Sept. 2018. DOI: 10.23731/CYRM-2019-003. arXiv: 1809.01830 [hep-ph]

[23] Minos Axenides et al. "M-theory as a dynamical system generator". In: July 2020. DOI: 10.1007/978-3-030-70795-8_6. arXiv: 2007.07028 [hep-th]

[24] M. Axenides et al. "Cascade of instabilities in the classical limit of the BMN matrix model". In: *Phys. Rev.* **D104** (2021), p. 106002. DOI: 10.1103/PhysRevD.104.106002. arXiv: 2109.01088 [hep-th]

[25] George Savvidy. "Maximally chaotic dynamical systems". In: *Annals Phys.* 421 (2020), p. 168274. DOI: 10.1016/j.aop.2020.168274; Hrachya Babujian, Rubik Poghossian, and George Savvidy. "Correlation Functions of Quantum Artin System". In: *Universe* 6.7 (2020), p. 91. DOI: 10.3390/universe6070091; Roland Kirschner and George Savvidy. "Parton Distribution Functions and Tensorgluons". In: *Universe* 6.7 (2020), p. 88. DOI: 10.3390/universe6070088; Roland Kirschner and George Savvidy. "Parton Distribution Functions and Tensor Gluons". In: (May 2020). arXiv: 2005.09700 [hep-ph]; George Savvidy. "Discovery of Chromomagnetic Gluon Condensation". In: *PoS* CORFU2019 (2020), p. 162. DOI: 10.22323/1.376.0162; George Savvidy. "Yang-Mills Classical and Quantum Mechanics and Maximally Chaotic Dynamical Systems". In: (Jan. 2020). arXiv: 2001.04902 [hep-th]; George Savvidy. "Maximally Chaotic Dynamical Systems of Anosov–Kolmogorov". In: *Phys. Part. Nucl.* 51.4 (2020), pp. 410–418. DOI: 10.1134/S1063779620040644. arXiv: 2001.01785 [hep-th]; George

Small scale structure of spacetime

The Small Scale Structure of Spacetime (SSSS) project explores the possibility of a discrete spacetime structure in strong gravity environments. It proposes a modular finite quantum mechanical model for the AdS_2 near horizon geometry for the specific class of extremal black holes. The model is holographic and exhibits desirable properties at the Planck scale such as nonlocality and chaotic mixing (fast scrambling). Recent publications of the group include a paper and a proceedings report [26].

Boundaries and defects

Boundaries and defects play central roles in quantum field theory (QFT) both as means to make contact with nature and as tools to constrain and understand QFT itself. Boundaries in QFT can be used to model impurities and also the finite extent of sample sizes, while interfaces allow for different phases of matter to interact in a controllable way. More formally, these structures shed light on the structure of QFT by providing new examples of dualities and renormalization group flows. The group's present research focuses on three areas: 1) formal and applied aspects of boundary and defect conformal field theory, from anomalies and c-theorems to topological insulators, 2) supersymmetry and duality, from exact computations of new observables to the construction of new theories, and 3) QFT in curved space and gravity, from holographic computations of entanglement entropy to ideas in quantum information theory. The latest results of the group were in the field of holographic defect CFTs and included: (1) the publication of the original research paper [27] which dealt with the solution of two very popular models of holographic dCFTs via proving closed determinant formulas for all their 1-point correlation functions, (2) the paper [28] in which the classical integrability of strings ending on a D5-brane was established, as well as (3) the proceedings submission [29] which summarized the author's oral presentation in the 2020 Corfu Summer Institute. The research on the physics of boundaries and defects was for the most part funded by the HAppEN project (see below).

Savvidy. "Extended Kolmogorov Entropy". In: (Apr. 2020). arXiv: 2004.13528 [math.DS]

[26] Minos Axenides, Emmanuel Floratos, and Stam Nicolis. "The arithmetic geometry of AdS_2 and its continuum limit". In: *SIGMA* 17 (2021), p. 004. DOI: 10.3842/SIGMA.2021.004. arXiv: 1908.06641 [hep-th]; Minos Axenides, Emmanuel Floratos, and Stam Nicolis. "The continuum limit of the modular discretization of AdS_2". In: *21st Hellenic School and Workshops on Elementary Particle Physics and Gravity*. May 2021. arXiv: 2205.03637 [hep-th]

[27] Marius De Leeuw et al. "Spin Chain Overlaps and the Twisted Yangian". In: *JHEP* 01 (2020), p. 176. DOI: 10.1007/JHEP01(2020)176. arXiv: 1912.09338 [hep-th]

[28] G. Linardopoulos and K. Zarembo. "String integrability of defect CFT and dynamical reflection matrices". In: *JHEP* **05** (2021), p. 203. DOI: 10.1007/JHEP05(2021)203. arXiv: 2102.12381 [hep-th]

[29] Georgios Linardopoulos. "Solving holographic defects". In: *PoS* CORFU2019 (2020), p. 141. DOI: 10.22323/1.376.0141. arXiv: 2005.02117 [hep-th]

Complex systems

The study of Non-linear Chaotic Dynamics and Complex Systems involves both research and teaching. It pertains to the interplay between chaotic dynamics and fundamental interactions. Noteworthy results have been obtained in the very past such as the observation of chaos in Yang Mills theories (G. K. Savvidy) as well as more recently in matrix and membrane dynamics of M-theory. Demokritos has been the hub of the national network of Complex Systems COSA-NaNet which organizes regular seminars on Nonlinear Chaotic Dynamics and Complexity along with a graduate level course on "Special topics on Complex Systems and Applications" in association with the National Technical University of Athens (see Teaching-Outreach as well as Summer schools for undergraduate University students).

HAppEN program

The aim of the research performed in the program HAPPEN is the understanding of the connection between quantum entanglement and gravity in the framework of the holographic duality. The establishment of this connection requires the study of quantum entanglement in both sides of the duality. More specifically:

- In the bulk theory, entanglement entropy is given by the area of open minimal surfaces in AdS spaces, which are anchored at the AdS boundary. In the HAPPEN program we study the integrable structure of these surfaces and try to construct non-trivial new ones.
- In the field theory side the entanglement entropy is studied. The main focus in the program HAPPEN is the study of entanglement beyond the ground state of the theory.

During 2020, the group achieved several major goals of the program.

A long program for the construction of non-trivial minimal surfaces in AdS space, based on non-linear sigma model techniques Pohlmeyer reduction and the dressing method) was concluded. The construction and the properties of these new minimal surfaces was presented in [30].

The study of these methods for the minimal surface in AdS, revealed more general properties of the non-linear sigma models in symmetric target spaces. More specifically, the application of the dressing method for an arbitrary seed was achieved and the dressed solution was interpreted as a non-linear superposition of solutions within the family of solutions with the same Pohlmeyer counterpart as the seed [31].

Although the dressed minimal surfaces are highly non-trivial, it is not possible to construct with this method the minimal surface which is defined by specific boundary data. For this purpose an alternative description of the minimal surfaces as

[30] Dimitrios Katsinis et al. "Dressed minimal surfaces in AdS_4". In: *JHEP* 11 (2020), p. 128. DOI: 10.1007/JHEP11(2020)128. arXiv: 2007.10922 [hep-th]

[31] Dimitrios Katsinis, Ioannis Mitsoulas, and Georgios Pastras. "The Dressing Method as Non Linear Superposition in Sigma Models". In: *JHEP* 03 (2021), p. 024. DOI: 10.1007/JHEP03(2021)024. arXiv: 2011.04610 [hep-th]

a geometric flow of the boundary data towards the interior of the AdS space was developed using differential geometry techniques [32]. This method cannot provide the finite terms of the holographic entanglement entropy, nevertheless it provides all divergent terms including the universal logarithmic terms in odd dimensions.

On the side of the field theory, the study of entanglement in thermal states was concluded [33]. The study reveals that the area law holds not for entanglement entropy, but for the mutual information. The results include a perturbative analytic calculation of the mutual information, as well as high and low temperature expansions.

Viewing the entangling surface as a defect (both in the bulk and in the boundary of holographic theories), the program also funded the research on Boundaries and Defects that was described in the previous section. The corresponding deliverables were [34].

The MixMax project

The primary objective of the MIXMAX project (2015-2018; H2020-MSCA-RISE-MIXMAX) was a systematic development of the state of the art new generation of Pseudo Random Number Generators based on Kolmogorov-Anosov C-K systems, which demonstrates excellent statistical properties, into a multidisciplinary usable product. This innovative class of RNG was proposed earlier by G. Savvidy in 1986 and by the members of the network and relies on the fundamental discoveries and results of Ergodic theory. It has been recently tested in many platforms and is evaluated as random number generator in the CMS simulation program. The MixMax generator is now included in: ROOT, Geant4/CLHEP as default generator (MixMax was set as default engine since release 2.4.0.0 deployed on November 2017 and in Geant4 since release 10.3), PYTHIA, GSL - GNU Scientific Library, the Extensions/Applications, CMS as default generator (CMS poster). The MIXMAX software has been used in the design of the NASA Solar Neutrino Spacecraft Detector by the group of researchers from NASA and by Wichita State University.

The Gauge Field Theory Vacuum and Cosmological Inflation

The research in cosmology and inflation theory is devoted to the derivation of the quantum energy-momentum tensor and the corresponding quantum equation

[32] Dimitrios Katsinis, Ioannis Mitsoulas, and Georgios Pastras. "Geometric flow description of minimal surfaces". In: *Phys. Rev. D* 101.8 (2020), p. 086015. DOI: 10.1103/PhysRevD.101.086015. arXiv: 1910.06680 [hep-th]

[33] Dimitrios Katsinis and Georgios Pastras. "An Inverse Mass Expansion for the Mutual Information in Free Scalar QFT at Finite Temperature". In: *JHEP* 02 (2020), p. 091. DOI: 10.1007/JHEP02(2020)091. arXiv: 1907.08508 [hep-th]

[34] Marius De Leeuw et al. "Spin Chain Overlaps and the Twisted Yangian". In: *JHEP* 01 (2020), p. 176. DOI: 10.1007/JHEP01(2020)176. arXiv: 1912.09338 [hep-th]; Georgios Linardopoulos. "Solving holographic defects". In: *PoS* CORFU2019 (2020), p. 141. DOI: 10.22323/1.376.0141. arXiv: 2005.02117 [hep-th]

of state for gauge field theory using the effective Lagrangian approach [35]. The energy-momentum tensor has a term proportional to the space-time metric and provides a finite non-diverging contribution to the effective cosmological parameter. This allows to investigate the influence of the gauge field theory vacuum polarisation on the evolution of Friedmann cosmology, inflation and primordial gravitational waves. The Type I-IV solutions of the Friedmann equations induced by the gauge field theory vacuum polarisation provide an alternative inflationary mechanism and a possibility for late-time acceleration. The Type II solution of the Friedmann equations generates the initial exponential expansion of the universe of finite duration and the Type IV solution demonstrates late-time acceleration. The solutions fulfil the necessary conditions for the amplification of primordial gravitational waves.

Funding

In Table 11 the ongoing funding of the group during 2021 is presented.

Teaching

The group offers courses in quantum field theory for graduate and undergraduate students jointly from NTUA and NCSR-Demokritos, training of graduate students for advanced degrees. Seminars and lectures in summer schools organized by Demokritos for university undergraduate students.

[35] George Savvidy. "Gauge field theory vacuum and cosmological inflation without scalar field". In: *Annals Phys.* 436 (2022), p. 168681. DOI: 10.1016/j.aop.2021.168681. arXiv: 2109.02162 [hep-th]; George Savvidy. "Gauge Field Theory Vacuum and Cosmological Inflation". In: *21st Hellenic School and Workshops on Elementary Particle Physics and Gravity.* Apr. 2022. arXiv: 2204.08933 [hep-th]

Table 11: Funding of the Theory Group

Prog. ID	Title	Host Institution	Principal Investigator	Starting date	Finishing date	Budget (€)
	CA16201: Unraveling new physics at the LHC through the precision frontier	IFIC	C. Papadopoulos	2017	2021	
	HFRI: Two-loop Amplitude Calculations Based on Integrand Reduction	NKUA	C. Papadopoulos, D Canko	2019	2022	32,400
E-12390	Operational Program Human Resources Development, Education and Lifelong Learning 2014-2020 in the context of the project 'Higher order corrections in QCD with applications to High Energy experiments at LHC'	INPP	C. Papadopoulos	2020	2022	37,000
E-12300	HFRI: Holographic APPlications of quantum ENtanglement (HAPPEN)	INPP	G. Pastras M. Axenides	2018	2021	182.598,94
E-12390	IKY: Operational Programme Human Resources Development, Education and Lifelong Learning" in the context of the project "Strengthening Human Resources Research Potential via Doctorate Research" (MIS-5000432)	INPP	M. Axenides D. Katsinis	2018	2021	30.000
E-12386	Operational Program Human Resources Development, Education and Lifelong Learning 2014-2020 in the context of the project "Chaotic dynamics and black holes in BMN theory" (MIS 5047794)	INPP	E. Floratos, M. Axenides	2020	2022	45,500

Astroparticle Physics

Astroparticle Physics

Researchers:	Dr. Christos Markou (Coordinator)
	Dr. E. Tzamariudaki
	Dr. E. Drakopoulou
Administration:	S. Bakou
PhD students:	A. Sinopoulou
	D. Tzanetatos
	D. Stavropoulos
	V. Tsourapis
Diploma students:	G. Zarpapis
	E. Katsikeros
	M. Chadolias
	E. Tragia
Employees:	G. Androulakis
	C. Bagatelas
	S. Oikonomou
Technicians:	V. Tsagkli
	A. Vougioukas

Introduction

The astroparticle physics group of the Institute of Nuclear and Particle Physics (INPP) is mainly focusing on the detection and subsequent study of neutrinos from cosmic accelerators. The study of cosmic neutrinos offers significant advantages towards answering basic questions about the origin and nature of cosmic rays. Neutrinos, being neutral, are not deflected by interstellar magnetic fields and, unlike protons, are not significantly absorbed by intervening matter. Thus, they point to their sources over all energy ranges and distance scales, and hence are uniquely valuable as cosmic messengers. In addition, the detection of astrophysical high energy neutrinos will shed light on the production mechanism of high energy gamma rays by understanding whether the sources of high energy gamma rays observed by the HESS telescope are due to electromagnetic or hadronic processes.

The INPP astroparticle physics group is a member of the KM3NeT collaboration. KM3NeT [36] is a distributed Research Infrastructure, member of the ESFRI Road Map that will consist of a network of neutrino telescopes in the Mediterranean Sea with user ports for Earth and Sea sciences. Once completed, the telescopes will have detector volumes between megaton and several cubic kilometers of clear sea water. Located in the depths of the Mediterranean Sea, KM3NeT will open a new window on our Universe and will contribute to the understanding of the properties of the elusive neutrino particles. The ARCA (*Astroparticle Research with Cosmics in the Abyss*) telescope, which is located offshore of Sicily,

[36] S Adrián-Martínez et al. “Letter of intent for KM3NeT 2.0”. In: *Journal of Physics G: Nuclear and Particle Physics* 43.8 (2016), p. 084001. ISSN: 1361-6471. DOI: 10.1088/0954-3899/43/8/084001. URL: http://dx.doi.org/10.1088/0954-3899/43/8/084001

Italy, at a maximum depth of 3450 m, is devoted to the search for neutrinos from distant astrophysical sources, such as superenovae, gamma ray bursts or colliding stars. The ORCA (*Oscillation Research with Cosmics in the Abyss*) detector which is located 40 km offshore Toulon, France, at a depth of 2450 m, aims at studying neutrino properties through the precise measurement of neutrino oscillations exploiting neutrinos generated in the Earth's atmosphere. An artistic view of the KM3NeT detectors is shown if Fig. 35.

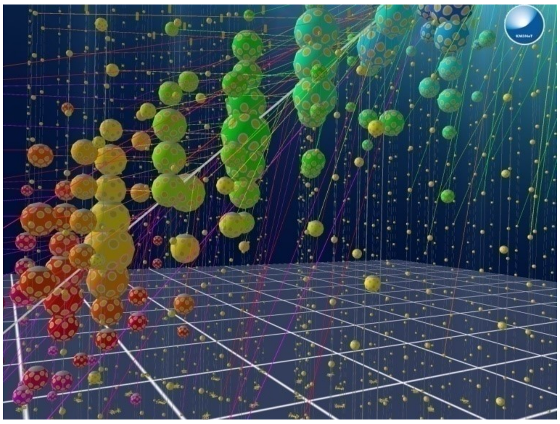

Figure 35: An artist's view of an event as it will be seen by the KM3NeT telescopes

Activities

In 2021 the group has been active in construction, testing and validation of the KM3NeT detectors and individual components, physics analyses and studies, governance and management.

KM3NeT management and governance

Dr. C. Markou acts as the Greek-site manager and is a member of the Management Team of the experiment. Dr. C. Markou is also charing the Conference committee of the experiment. Dr. C. Markou and Dr. E. Tzamariudaki are members of the KM3NeT Publication committee with Dr. E. Tzamariudaki co-chairing this committee. In addition, Dr. E. Tzamariudaki is a member of the Equality, Diversity and Inclusion committee (EDI) of KM3NeT. G. Androulakis has been the Quality Assurance / Quality Control manager of KM3NeT, member of the Management Team and the Steering Committee of the experiment.

KM3NeT contruction

Since 2016 a DOM integration, validation and testing facility has been established in the premises of INPP (Fig. 36). The DOM lab has been funded exclusively through internal funds. It was completed in record time (compared to other similar labs in KM3NeT), and has been operational in late 2016. Ever since, the lab continues with the integration of DOMs.

Figure 36: The DOM Lab at INPP

Currently the lab employs 2 FTE of skilled personnel, with additional help from other group members as the need arises. The DOM integration facility has been upgraded to speed up the DOM production. The benches used for the assembly of the DOMs have been increased, and the DOM testing setup was upgraded both in hardware and in software, to allow the integration and testing of more DOMs in prallel. During 2021, 36 DOMs (corresponding to 2 KM3NeT Detection Units) were integrated, calibrated and tested successfully.

An additional contribution to the collaboration is testing and validation effort concerning the high-pressure testing of the DOM penetrators which are used for powering the DOMs and for data transfer from the DOMs to the shore station via an electro optical cable. As the penetrators can be a single point of failure for the DOMs, acceptance testing is extremely important. These tests are curried out using a high-pressure testing chamber, capable of sustaining pressure up to 600 bars (Fig. 37). These tests are done for all KM3NeT DOM penetrators (372 penetrators during 2021).

All members of the INPP astroparticle physics group, also participate in the DOM-lab performing pressure tests, insulation tests and DOM assembly.

Physics analyses

Several group members have been active in physics analyses, focusing mainly to the analysis of the data from the first DUs of the ARCA and ORCA detectors. The group has also made a significant contribution to the MC simulation efforts for the KM3NeT/ARCA detector. Most of physics analyses were carried out either in the context of Ph.D. and M.Sc. theses or refer to interim projects. These are briefly outlined below.

“Study of the Diffuse Astrophysical Neutrino Flux with the KM3NeT/ARCA Neutrino Telescope u
Anna Sinopoulou, PhD Candidate

This analysis focuses on optimizing requirements in order to isolate well reconstructed events and in addition, on finding suitable selection criteria for suppressing the background from atmospheric muons and identifying atmospheric neutrino candidates. During 2021, Anna has been working on the data from the 6 deployed

Figure 37: Pressure testing of the penetrators

Detection Units of the KM3NeT/ARCA detector configuration. In her analysis she focused on optimizing requirements in order to isolate well reconstructed events and in addition, on finding suitable selection criteria for suppressing the background from atmospheric muons and identifying atmospheric neutrino candidates.

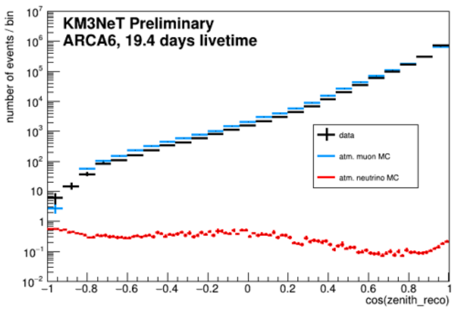

Figure 38: Distribution of the cosine of the zenith angle for all reconstructed events.

Detailed Data/MC comparisons have been performed in order to ensure a reasonable description of the variables used to select neutrino events. Requirements to reduce the background coming from K^{40} decays have been applied. MC simulation of pure noise from K^{40} decays is not necessary for KM3NeT/ARCA as the pure noise contribution can be easily suppressed. In the next figures, the likelihood of the reconstruction fit and the number of hits used by the reconstruction algorithm are shown for data (blue) and MC (red) for all reconstructed events. For low values of both the likelihood and the number of hits, a bulk of data events is observed corresponding to the K^{40} contribution and a set of anti-noise requirements has been applied ($lik > 50$, $Nhits > 20$) in order to reduce it.

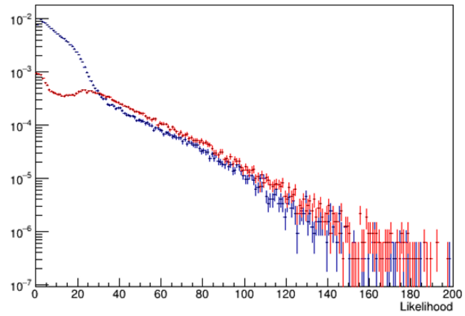

Figure 39: Distribution of the likelihood (left) and the number of hits used for the reconstruction (right) for data (blue) and MC (red) reconstructed events.

The contribution from poorly reconstructed atmospheric muon events is the main source of background for this study. As neutrinos are the only particles able to penetrate the Earth, no atmospheric muons with $\cos_{zenith} < 0$ (referred to as upgoing) are expected. The number of atmospheric muon MC simulated events reconstructed as upgoing indicates the level of the remaining atmospheric muon contamination.

The requirements applied on the reconstruction level of the data aim at suppressing the atmospheric muon background, while keeping a high efficiency for neutrino induced events. Due to the small detector volume (6 DUs) and the limited data livetime of $\tilde{1}9$ days, loose requirements have been applied. Time correlations comprise an important indicator of the quality of the event reconstruction; so a minimum number of DOMs with hits in time with the reconstructed track and a minimum percentage of noise hits were required. Requirements concerning the minimum track length of the reconstructed track and on reconstruction quality parameters have also been investigated and have been applied. All the steps of this analysis where tested in the data, atmospheric muon and atmospheric neutrino samples in order to investigate their performance and to prove their efficiency.

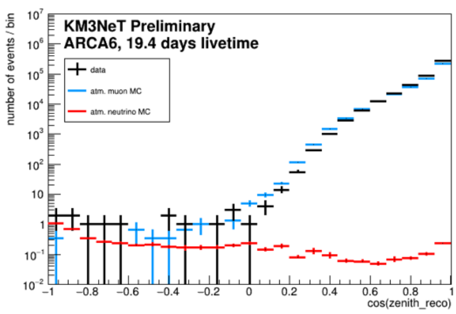

Figure 40: Distribution of the cosine of the zenith angle for events surviving the neutrino selection criteria.

After the selection criteria, an excellent angular resolution with median value 0.75° has been achieved. With the ARCA6 detector, 11.5 events per year are expected for an E^{-2} assumed astrophysical flux which is comparable to the number of events expected from the ANTARES detector. In addition, ARCA6 has significantly higher effective area than ANTARES for the high energy range (E

$> 10TeV$). Furthermore, the good data/MC agreement verifies the KM3NeT technology, the detector understanding and detector calibration illustrating the capability of the future KM3NeT detectors.

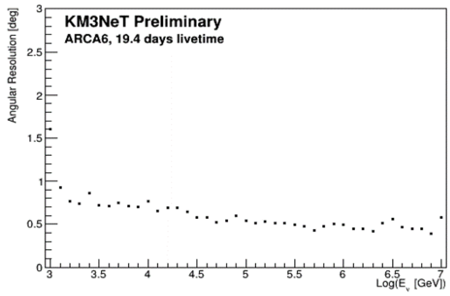

Figure 41: The median of the angular resolution for events expected to fulfill the selection criteria is 0.75°

The results have been presented in a talk at the Very Large Volume Neutrino Telescopes conference (VLVnT 2021) and in a talk at the International Cosmic Ray Conference (ICRC2021).

During this year, Anna contributed also to KM3NeT's simulation working group for the new official MC production of the full KM3NeT/ARCA detector by producing the atmospheric muon sample. She also made a thorough investigation on the can variables and input MC parameters in order to optimize the procedure in terms of number of events, energy thresholds, CPU time etc. She also performed energy studies and made an energy correction function for the deposited energy in the detector volume for the full ARCA detector. Finally, she also contributed to the official MC production for the ARCA6 detector configuration that will be used for future analyses. She has performed data quality studies in order to isolate the runs used for the data analysis for the ARCA6 detector and contributed to the Data Processing and Data Quality working group too.

"Analysis of the data collected with the 6 detection units of the under construction KM3NeT/ORCA detector"

D. Stavropoulos, PhD Candidate

The analysis focuses on data collected with the KM3NeT/ORCA detector which operated with six Detection Units (ORCA6) in the time period between January 2020 and to February 2021. With a time efficiency 92%, the time exposure of the data used in the analysis corresponds to 354.6 days. The detected event sample consists of atmospheric muons events, random noise events (coming from the K^{40} radiation in the sea water), and atmospheric neutrino events. Specific Monte Carlo (MC) productions were launched in order to simulate the atmospheric neutrinos (signal), as well as the random noise and atmospheric muons (background sources). A "cut & count" analysis was performed to reject the background events and enhance the neutrino signal. The resulting event sample consists of 1230 data events, while 1237.2 events are predicted from the atmospheric neutrino MC. Concerning the background, 16.2 atmospheric muon MC events survive the selection criteria, while all random noise MC events (coming exclusively from K^{40} decays) are rejected. As a result, 3.5 neutrino events have been detected per day, with a very small muon background contamination of 1.3%. The distributions of the cosine of the reconstructed zenith angle are shown in Fig. 42, for data and MC. The starting point (all reconstructed events) is depicted with dashed lines, while the result is depicted with solid lines. This demonstrates that a high suppression of the atmospheric muon background, that exceed the signal by 5 orders of magnitude, has been achieved and an exceptionally clean neutrino sample has been obtained.

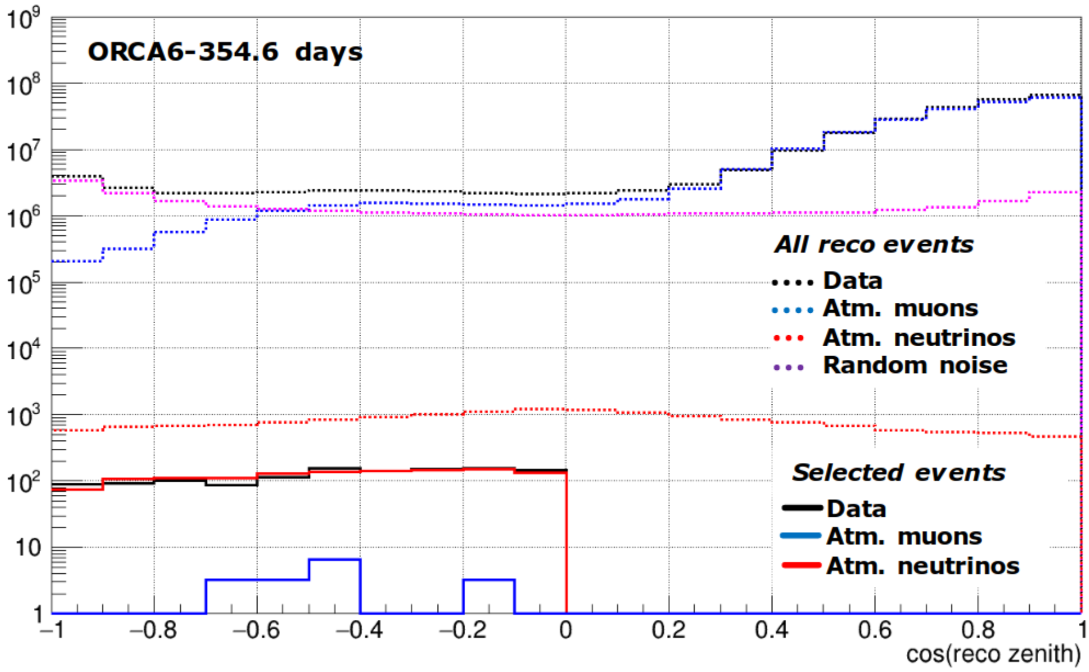

Figure 42: Distribution of the cosine of the reconstructed zenith angle for ORCA6 data and for MC simulated events, for all reconstructed events (dashed lines) and for the selected events (solid lines)

Muons originating from atmospheric neutrino interactions close to or inside the instrumented volume, while it is expected that the muon tracks for poorly reconstructed atmospheric muons are further away from the detector centre and thus only a small fraction of the induced light reaches the KM3NeT light sensors. Detailed data - MC comparisons have been performed, at different stages of the analysis, to ensure that the quantities used for the event section are adequately described by the MC simulations. Two indicative distributions are shown concerning the selected neutrino sample. The distribution of the minimum distance between the reconstructed track and the detector centre (d-closest) is shown in Fig. 43. Moreover, the distribution of the number of signal-like event hits divided by the total number of event hits is shown in Fig. 44 . A good agreement between data and MC is observed for both variables.

With the current getector geometry, ORCA is sensitive in the energy region between 10-100 GeV. The true MC energy of the atmospheric neutrino selected events is shown in Fig. 45.

This analysis was presented in the 7th International Cosmic Ray Conference - ICRC2021 (DOI: https://doi.org/10.22323/1.395.1125).

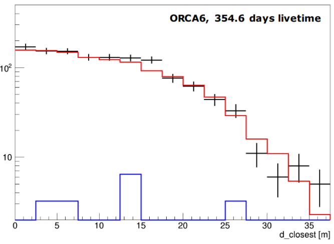

Figure 43: Distribution of the minimum distance between the reconstructed track and the detector centre. The data points are shown in black, atmospheric neutrino simulated events in red and the atmospheric muon background in blue.

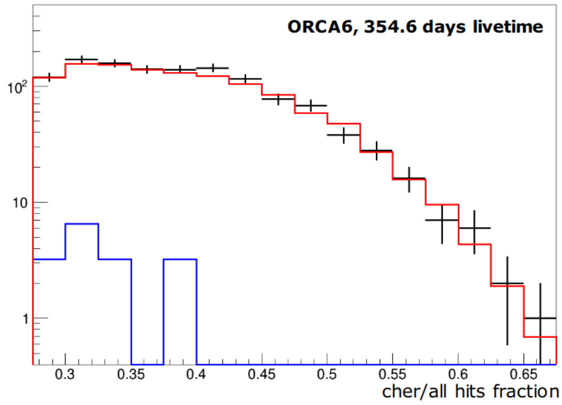

Figure 44: Distribution of the number of the number of signal-like event hits divided by the total number of event hits. The data points are shown in black, atmospheric neutrino simulated events in red and the atmospheric muon background in blue.

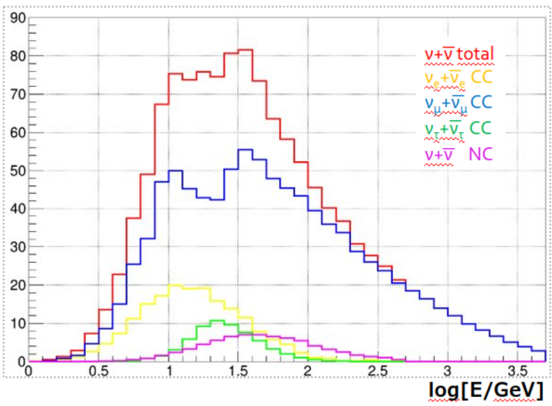

Figure 45: The true MC energy for the atmospheric neutrino MC events that survive the selection criteria.

In addition, considering the amount of data continuously recorded by the KM3NeT/ORCA detector, it becomes evident that efficient processing of the data is mandatory in order to perform analysis and extract scientific results. This need increases as the size of the detector grows. A software was developed with the aim of adding another step between that of the reconstructed files and the visualization of the data. This software preprocesses the reconstructed data and produces files with second order variables that are ready for further analysis. The software was developed for KM3NeT/ORCA, with 6 Detection Units, by Dimitris allowing all data information that is sufficient for optimising the selection cuts to be transferred to the preprocessed files.

”Data Quality checks and Studies on a full neutrino acoustic detection simulation”

V. Tsourapis, Ph.D. student. Supervisor: C. Markou

Vasilis enrolled to the PhD program in late 2020, so after the necessary preparatory months regarding the tools used by KM3NeT, he began in 2021 working on his PhD thesis. He started by making detailed Data Quality checks for the full data sample of KM3NeT/ARCA detector configuration which then operated with 6 Detection Units (ARCA6).

Running periods with stable running conditions have been selected and runs have been rejected if problems have been identified. Extensive comparisons of the data withe the MC simulations have been performed including studies of the influence of upgrades on the KM3NeT trigger and reconstruction software (Fig. 46, Fig. 47).

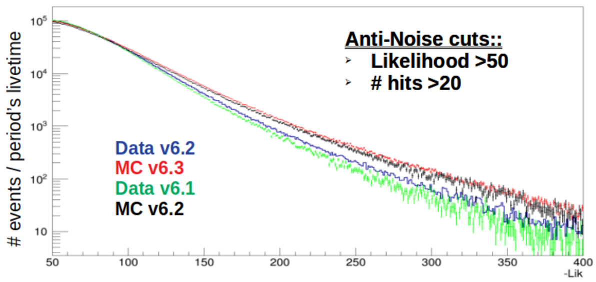

Figure 46: Likelihood of the fit in the reconstruction chain after applying cuts to reduce the contribution of noise from K^{40} decays. Study of the influence of KM3NeT software upgrades on the description of the reconstruction output variables (here for the likelihood).

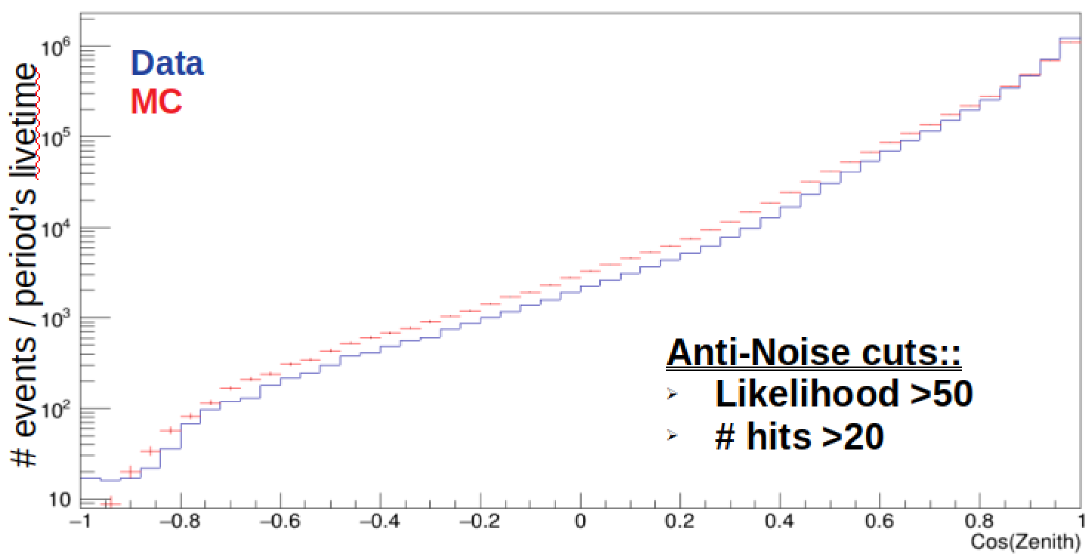

Figure 47: Distribution of the cosine of the zenith angle for events after applying cuts to reduce the contribution of noise from K^{40} decays.

All the results were presented at the online Data Processing and Data Quality working group meetings of KM3NeT.

Vasilis continued working on optimizing the existing codes used for the analysis of ARCA6 data and MC and prepared for the new upcoming ARCA8 detector configuration. In the above analyses, Vasilis tried to optimise the cuts used for the suppression of the contribution from K^{40} decays.

Alongside his work on KM3NeT/ARCA, Vasilis began working on a second project regarding Acoustic Neutrino Detection. When an Ultra High Energy neutrino interacts with sea water, a sufficient amount of energy is deposited heating the medium and producing a pressure field which, in turn, is enough to create a detectable bipolar acoustic pulse.

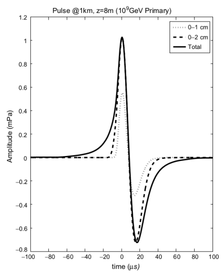

Figure 48: Bipolar acoustic pulse of a 10^9GeV neutrino at 1km as given by the ACORNE simulation, using neutrino induced showers produced by CORSIKA-IW. Almost all the contribution to the pressure field comes from whithin a radius of about 1cm from the center of the neutrino induced shower (assuming the shower has a cylindrical geometry)

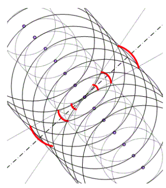

Figure 49: Constructive interference (between the Huygen's wavelets) occurs at a distance away from the original neutrino energy deposition.

Studies on this field have already been conducted by members of INPP Demokritos' APP group on the level of parameterizing the aforementioned bipolar pulse. In order to simulate the acoustic pulse, Vasilis has incorporated two software packages (CORSIKA-IW and ACORNE collaboration's work) has built a framework for the full simulation of a neutrino event and its expected detection by a grid of hydrophones (used for underwater acoustic detection).

"Analysis Framework for the measurement of the optical parameters of sea-water"

G. Zarpapis, MSc student. Supervisor: E. Tzamariudaki

Commercially available instruments are not well suited for measurements of the optical parameters of the deployment sites as the small length optical base of such instruments requires an increased accuracy of the light intensity measurement. In order to obtain a reliable measurement of the water transparency, an open geometry light measuring system, the Long Arm Marine Spectrophotometer

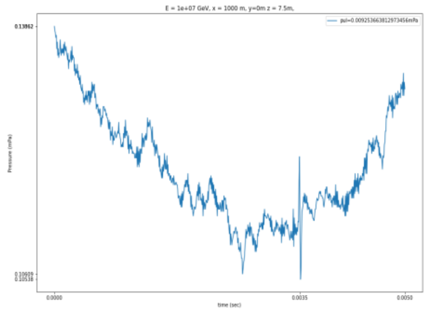

Figure 50: A bipolar pulse inserted to real sea noise using the aforementioned framework at 0.0035 sec.

(LAMS), was constructed and was used to measure the transmission length in deep sea during the sea campaigns in 2008 and 2009 ([37]). In the context of Technology transfer (WP 9 of the KM3NeT-INFRADEV project), a new version of the LAMS device has been constructed, keeping the same idea of measuring the transmission length, but simplifying the process by performing in a single deployment, simultaneous measurements at three different distances between emitter and receiver (Fig. 51) instead of three deployments needed for the original LAMS. In this way, the total measurement time can be reduced to just a few (6) hours, the time being dominated by the time required to deploy and recover the system at the intended water depth. Since the design and operation of the old version of LAMS was successful, it was decided that the changes of the redesigned system be limited to those necessary and cannot be avoided (due to the lack of components which are no longer in production for example), or to small changes that would greatly improve the efficiency of the measurement.

A software development of a framework for automising the analysis of the LAMS data was deemed necessary and was implemented by G. Zarpapis. This analysis software has also been widely used during the testing phase of the upgraded LAMS system.

The light source of the original LAMS has been used. It is contructed using eight groups of LEDs, which emit over a significant spectral region. During a measurement cycle the LEDs of a particular wavelength are turned on for 10 s, are then switched off and after 2 s the LEDs of the next wavelength are turned on. The overall measurement cycle is 108 s including a 14 s no-light gap which is inserted between the light cycles. A pattern recognition method has been devised for the automatic identification of pulses and cycles in the data. The process is split into stages, for more flexibility, allowing the programmer to intervene if something looks out of place .Dark current, light saturation, photodiode (PD) disagreement tolerance and required stability are explicitly provided as input in order to determine the "flat" surface of the pulses which is necessary for the calculation of the attenuation length. The dark reset is identified by the algorithm and is used for separating the data into cycles. The length of the different pulses within a cycle is also identied by the algorithm and the intensity of each wavelength on each cycle is calculated by taking the mean value of all the pulse values corresponding to

[37] E. G. Anassontzis et al. "Water transparency measurements in the deep Ionian Sea". In: *Astropart. Phys.* 34 (2010), pp. 187–197. DOI: 10.1016/j.astropartphys.2010.06.008

that wavelength. An example of a validated cycle with its separate pulses which is included in the analysis for the calculation of the attenuation length is shown in Fig. 51, while in Fig. 52 an example is shown of a cycle that has been identified by the algorithm and has been excluded from the analysis.

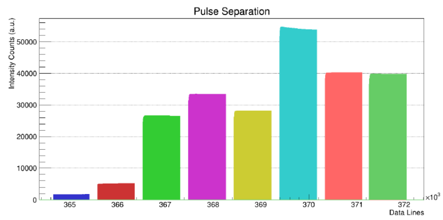

Figure 51: An example of a validated cycle. Different colours denote different wavelengths (pulses). The data presented have successfully passed all stages of the pattern recognition algorithm and are included in the analysis.

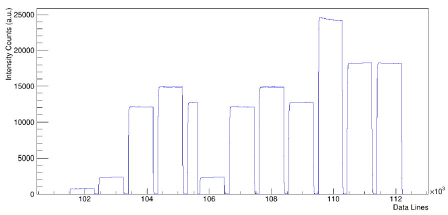

Figure 52: An example of a problematic cycle which has been identified by the algorithm and the corresponding data have been excluded from further analysis.

"Software implementation for KM3NeT/ORCA115 MC analysis"

E. Tragia – Aristotle University of Thessaloniki, interim student. Supervisor: E. Tzamariudaki

Based on the development of software machinery for adding a "preprocessing" step to the data analysis for KM3NeT/ORCA by D. Stavropoulos, Eftychia extended this framework with an implementation of this machinery to analyse events the full KM3NeT/ORCA MC simulated events. The implementation has been tested by comparing distributions of event kimenatical variables with the ones obtained without the preprocessing step.

"Study of the energy reconstruction quality of the KM3NeT/ORCA-6 detector"

M. Chadolias – Aristotle University of Thessaloniki, interim student. Supervisor: E. Tzamariudaki

During his internship, Michalis Chadolias carried out a study of the influence of the event characteristics and of the quality of the direction reconstruction on the energy reconstruction quality of neutrino candidates for KM3NeT/ORCA with 6 Detection Units.

The progress of his work is illustrated in Fig. 53, where, for some selected quantities, the difference of the shape depending on the goodness of the energy reconstruction is shown.

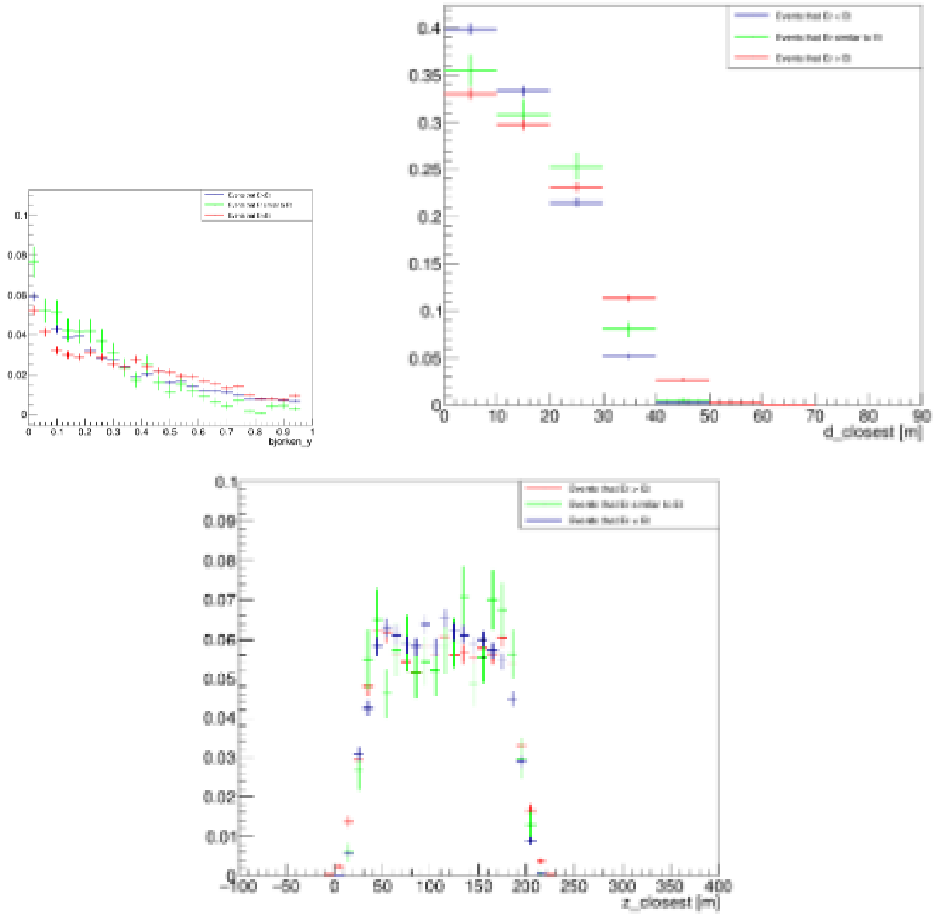

Figure 53: Correlation of the goodness of the energy reconstruction with the inelasticity (bjorken-y) of the event and with the distance of closest approach to the detector. The event variables are shown for events for which the energy is reconstructed adequately (in green), is underestimated (in blue) and is overestimated (in red).

The main goal of the analysis was to evaluate topological and event reconstruction parameters in order to investigate whether, for small detector geometries, there quality of the energy reconstruction is correlated with event characteristics.

"Approximation of the vertex position in acoustic neutrino detection"

E. Katsikeros - National Kapodistrian University of Athens, interim student. Supervisor: C. Markou

Methods for determining the position of the incoming neutrino as well as the cascade orientation have been studied assuming that a certain number of hydrophones (belonging to the observer's grid) have detected a bipolar pulse coming from a neutrino interaction. The idea is to minimize the chi-square between experimental and expected arrival times of the pulse to each hydrophone. Since, at this point, there no experimental data, a recalculation of the times was done using the hydrophones positions. In order to determine the incoming neutrino position the effective interaction volume is segmented and an optimisation of the size of the segmentation for high precision and of computational time has been attempted.

Quality Assurance and Quality Control (QA/QC) for KM3NeT

The distributed organization of KM3NeT production induces some special characteristics in the construction of the detector: there are two installation sites, integration of detection units is distributed over more than ten integration sites, qualification and acceptance testing of components is performed in several testing facilities around Europe and procurement of components is done centrally by individual institutes-budget holders. Under this framework, ensuring a uniformity in the production quality and traceability of all those components that travel continuously between European institutes are challenging tasks, requiring a robust QA/QC system.

The quality group of KM3NeT is one of the largest technical groups of KM3NeT. It is coordinated by G. Androulakis, who is interfacing between KM3NeT production and governing bodies in order to monitor and improve the quality of the detector. The scope of KM3NeT QA/QC spans all stages of commisioning of the detector, from integration, testing, installation of detection units and operation, to calibration and embedded software. In particular, the KM3NeT QA/QC group is responsible for

- KM3NeT-wide management of non-conformities;
- administration of design changes and validation thereof;
- ensuring traceability of components travelling between tens of sites and getting integrated

and contributes to

- reliability studies and identification of critical failure modes of subsystems;
- risk analysis;
- organisation of KM3NeT documentation;
- definition of the central DB structure

The QA/QC manager is responsible for reporting to oversight committees such as the KM3NeT Institute board (IB), Scientific and Technical Advisory Committee (STAC) and the Resource review Board (RRB). By the KM3NeT organogram, G. Androulakis in his capacity as QA/QC manager is de facto a member of the Project Steering Committee as well as the Management Team, thus strengthening INPP's involvement in the decision making of KM3NeT. This responsibility ended in July 2021.

”Participation to the ANNIE experiment: new advances in detector technology”

Building on previous experience of group members in neutrino physics experiments we decided to establish a collaboration with the Accelerator Neutrino Interaction Experiment (ANNIE), a 26-ton Gd-doped water Cherenkov detector installed in the Booster Neutrino Beam at Fermilab. Our group joined ANNIE in late September 2021. This collaboration will allow us to get expertise with novel photodetection techniques that will play a key role in physics experiments and applications in the next decades. The experiment has two complementary goals: (1) to study the multiplicity of final state neutrons from neutrino-nucleus interactions in water and (2) demonstrate the power of new fast-timing, position-sensitive detectors by making the first deployment of Large Area Picosecond PhotoDetectors (LAPPDs) in a physics experiment. With single photon time resolutions of roughly 50 psec and mm-level imaging capabilities, LAPPDs bring considerable new capabilities for neutrino reconstruction in Cherenkov and scintillator detectors. The LAPPDs are anticipated to be deployed in 2022 and we plan to analyse the first data using these novel PhotoDetectors and develop machine-learning algorithms for the signal selection.

Funding

Outreach

Our group participated in the 85th Thessaloniki International Fair of Thessaloniki in September 2021: Videos showing the most impressive snapshots from the deploymnet of KM3NET Detection Units were launched on large TV screeens and slide shows provided information on the physics goals of KM3NeT as well as on the technical aspects of the experiment. In addition, a Virtual Reality experience allowed visitors to “drive” to the abyssal depth of the Mediterranean sea and “observe” sea life as well as detection elements of the experiment.

The group participated to the NCSR Demokritos summer school with a presentation of KM3NeT to young students.

Overview

Nuclear Physics and Applications

Theoretical Nuclear Physics

Researchers:	Dennis Bonatsos
Research Associates:	Ioannis Assimakis
	Konstantinos Karakatsanis
	Andriana Martinou
PhD students:	Smaragda Sarantopoulou
Master students:	Spyridon Peroulis (Ph.D. since 11/2021)

Introduction

The knowledge of nuclear structure is the basis for the evolution of new technology. For instance the discovery of new metastable (long living) nuclear states can lead to new nuclear medicines. Unstable nuclei can be used in the construction of nuclear batteries, to solve the problem of energy storage and in the construction of the nuclear clock. But nuclear structure is also the basis for the discovery of new physics. The detection of dark matter relies on the calculation of the "nuclear form factors", which are derived through nuclear structure calculations. Theoretical calculations of the abundances of chemical elements in the universe can be used to approve or reject cosmological models. Such calculations rely on the firm knowledge of the nuclear structure. Physics beyond the Standard Model can emerge if the neutrino-less double beta decay is realized. The calculations for such a reaction very much depend upon the nuclear structure.

The most well-established (and actually Nobel Prized) theoretical model for the study of Nuclear Structure is the Nuclear Shell Model. Computer codes, based on the Nuclear Shell Model, have been developed by various researchers worldwide, to deliver theoretical predictions for the nuclear structure observables. But since the nucleus is a many-body system consisting by protons and neutrons, which interact through a yet unknown force, the so called "strong force", even super-computers fail to run these codes for medium mass and heavy nuclei.

Therefore the nuclear physics society is developing the Algebraic Nuclear Models, in its effort to cut back the computational work. The algebraic version of the Nuclear Shell Model, namely the Shell Model SU(3) symmetry, was introduced by J. P. Elliott in 1958 [38], but unfortunately it was meant to be applied only in light nuclei. Various attempts [39] had been made since then to extend this symmetry [40] to medium mass and heavy nuclei, in which the computational work is more

[38] J. P. Elliott. "Collective motion in the nuclear shell model. I. Classification schemes for states of mixed configurations". In: *Proceedings of the Royal Society of London. Series A. Mathematical and Physical Sciences* 245.1240 (1958), pp. 128–145. DOI: 10.1098/rspa.1958.0072

[39] József Cseh. "Some new chapters of the long history of SU(3)". In: *European Physical Journal Web of Conferences* 194 (2018). Ed. by N. Arsenyev et al., p. 05001. DOI: 10.1051/epjconf/201819405001

[40] V. K. B. Kota. *SU(3) Symmetry in Atomic Nuclei.* Springer Singapore, 2020. DOI: 10.1007/978-981-15-3603-8

demanding.

The research group of Nuclear Theory in I.N.P.P. Demokritos has developed its own theory, the proxy-SU(3) symmetry, which actually extends the Shell Model SU(3) symmetry to medium mass and heavy nuclei. The model was introduced in 2017 in Ref. [41] and gave immediately parameter free calculations for the nuclear shape in Ref. [42], which led to two important results. First, they resolved the long-standing puzzle of the dominance of prolate over oblate shapes in the ground state bands of even-even nuclei [43]. Second, they predicted in a parameter-free way the place on the nuclear chart at which a shape transition from prolate to oblate nuclei is observed [44].

A major step forward has been taken in 2020 [45], with the connection of the proxy-SU(3) symmetry to the shell model, using the Shell Model SU(3) symmetry as a bridge. It has been proved that the replacement of the intruder orbitals in a major shell of the shell model (which are pushed down from the upper shell by the spin-orbit interaction) by the deserting orbitals (which are pushed by the spin-orbit interaction to the shell below) is not an arbitrary approximation, but it has deep mathematical roots, being equivalent to a unitary transformation.

Potentially in the future, the proxy-SU(3) symmetry can be used for the calculation of literally every nuclear observable. For instance the life-times of long living nuclear states (metastable or isotopic states), which are important for nuclear medicines and nuclear batteries, can be predicted. Realistic calculations can also be performed about: a) the nuclear spectrum and b) the nuclear binding energies, which are vital for the knowledge of nuclear stability, for the energy amount which is stored in a nucleus and for the nuclear astrophysical processes. Those mentioned above are only few of the vast future applications of the proxy-SU(3) symmetry.

Activities

Despite the fact that the year 2021 was the year of the pandemic and of worldwide lock-downs, it was a very productive year for the Nuclear Theory group in the I.N.P.P. The group published 5 articles in peer review journals during 2021 and opened up the proxy-SU(3) symmetry to national and international collaborators.

The most pathbreaking work of the group in 2021 regards a novel dual-shell

[41] Dennis Bonatsos et al. “Proxy-SU(3) symmetry in heavy deformed nuclei”. In: *Physical Review C* 95.6 (2017). DOI: 10.1103/physrevc.95.064325

[42] Dennis Bonatsos et al. “Analytic predictions for nuclear shapes, prolate dominance, and the prolate-oblate shape transition in the proxy-SU(3) model”. In: *Physical Review C* 95.6 (2017). DOI: 10.1103/physrevc.95.064326

[43] Dennis Bonatsos. “Prolate over oblate dominance in deformed nuclei as a consequence of the SU(3) symmetry and the Pauli principle”. In: *European Physical Journal A* 53.7 (2017), p. 148. DOI: 10.1140/epja/i2017-12346-x

[44] Dennis Bonatsos et al. “Analytic predictions for nuclear shapes, prolate dominance, and the prolate-oblate shape transition in the proxy-SU(3) model”. In: *Physical Review C* 95.6 (2017). DOI: 10.1103/physrevc.95.064326

[45] Andriana Martinou et al. “Proxy SU(3) symmetry in the Shell Model basis”. In: *European Physical Journal A* 56.9 (2020), p. 239. DOI: 10.1140/epja/s10050-020-00239-0

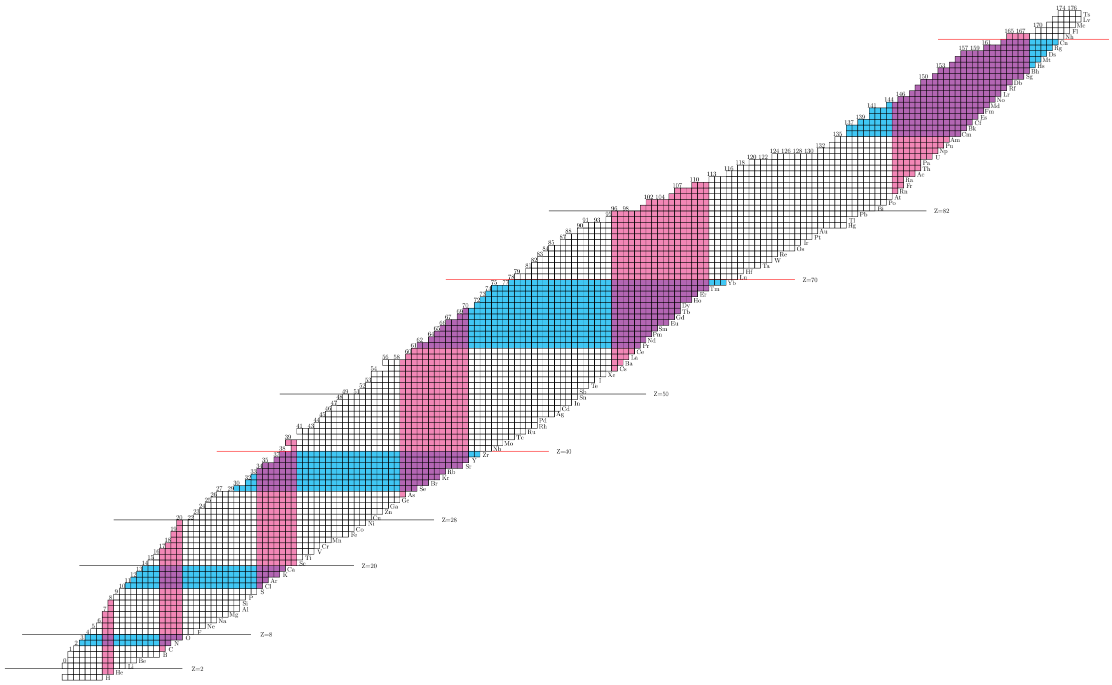

Figure 54: This map indicates, which nuclei have to be examined both theoretically and experimentally for manifesting shape coexistence according to the proposed mechanism. The colored regions possess proton or neutron number between $7-8$, $17-20$, $34-40$, $59-70$, $96-112$, $145-168$. The horizontal stripes correspond to the proton induced shape coexistence, while the vertical stripes correspond to the neutron induced shape coexistence.

mechanism for the phenomenon of shape coexistence in nuclei within the Elliott SU(3) and the proxy-SU(3) symmetry, applicable to all mass regions [46]. The Nuclear Theory Group proposed, that shape coexistence is activated by large quadrupole-quadrupole interaction and involves the interchange among the spin-orbit (SO) like shells within nucleon numbers 6-14, 14-28, 28-50, 50-82, 82-126, 126-184, which are being described by the proxy-SU(3) symmetry, and the harmonic oscillator (HO) shells within nucleon numbers 2-8, 8-20, 20-40, 40-70, 70-112, 112-168 of the Shell Model SU(3) symmetry. The outcome is, that shape coexistence may occur only in certain islands on the nuclear map, as seen in Fig. 54, in contrast to the common belief [47] of the international community, that it can occur everywhere over the nuclear chart. The dual-shell mechanism predicts without any free parameters, that nuclei with proton number (Z) or neutron number (N) between 7-8, 17-20, 34-40, 59-70, 96-112, 146-168 are possible candidates for shape coexistence. In the light nuclei the nucleons flip from the HO shell to

[46] Andriana Martinou et al. "The islands of shape coexistence within the Elliott and the proxy-SU(3) Models". In: *European Physical Journal A* 57 (2021), p. 84. DOI: 10.1140/epja/s10050-021-00396-w

[47] Kris Heyde and J. L. Wood. "Shape coexistence in atomic nuclei". In: *Rev. Mod. Phys.* 83.4 (2011), pp. 1467–1521. DOI: 10.1103/revmodphys.83.1467

the neighboring SO-like shell, which means, that particle excitations occur. For this mass region, the predicted islands of shape coexistence, coincide with the islands of inversion appearing in the earlier literature. But in medium mass and heavy nuclei, in which the nucleons inhabit the SO-like shells, shape coexistence is accompanied by a merging of the SO-like shell with the open HO shell.

An equally pathbreaking work of the group in 2021 was the study [48] of the consequences of the attractive, short-range nucleon-nucleon (NN) interaction on the wave functions of the Elliott SU(3) and the proxy-SU(3) symmetry are discussed. The NN interaction favors the most symmetric spatial SU(3) irreducible representation, which corresponds to the maximal spatial overlap among the fermions. The percentage of the symmetric components out of the total in an SU(3) wave function is introduced, through which it is found, that no SU(3) irrep is more symmetric than the highest weight irrep for a certain number of valence particles in a three dimensional, isotropic, harmonic oscillator shell. The conclusion is that the appropriate SU(3) irrep for the description of the ground state of even-even nuclei is the highest weight (hw) irrep, and not the irrep possessing the highest eigenvalue of the second order Casimir operator C_2 of SU(3), as believed by the international community so far. Although the hw irrep and the highest C_2 irrep are identical up to midshell, they become radically different beyond this point. The consideration of the highest weight irreps in nuclei and in alkali metal clusters, leads to the prediction of a prolate to oblate shape transition beyond the proton or neutron mid-shell region, supported by experimental results in both physical systems, thus indicating the universality of our result.

Having in mind the calculation of energy spectra in the proxy-SU(3) framework, the systematics of experimental energy differences between the levels of the ground state band and the γ_1 band in even-even deformed nuclei have been studied [49] as a function of the angular momentum L, demonstrating a decrease of the energy differences with increasing L, in contrast to what is seen in vibrational, γ-unstable, and triaxial nuclei. This observation is corroborated by numerical results and analytical expressions in the framework of several special solutions of the Bohr Hamiltonian.

Dealing with collaborators from Iran in the last few years with the Nilsson model as a test ground for proxy-SU(3), we have been attracted [50] by a paradox appearing in the well-known Nilsson diagrams, depicting the dependence of the nuclear single-particle energy levels on quadrupole deformation. Indeed a spin paradox appears as the deformation sets in, leading from spherical shapes to prolate deformed shapes with cylindrical symmetry. Bunches of levels corresponding to a spherical shell model orbital, sharing the same orbital angular momentum and the same total angular momentum, appear to correspond to Nilsson energy levels,

[48] Andriana Martinou et al. “Why nuclear forces favor the highest weight irreducible representations of the fermionic SU(3) symmetry”. In: *European Physical Journal A* (2021). DOI: 10.1140/epja/s10050-021-00395-x

[49] Dennis Bonatsos et al. “Energy differences of ground state and γ1 bands as a hallmark of collective behavior”. In: *Nuclear Physics A* 1009 (2021), p. 122158. DOI: 10.1016/j.nuclphysa.2021.122158

[50] Hadi Sobhani, Hassan Hassanabadi, and Dennis Bonatsos. “Resolution of the spin paradox in the Nilsson model”. In: *The European Physical Journal Plus* 136.4 (2021), p. 398. DOI: 10.1140/epjp/s13360-021-01300-7

labeled by asymptotic quantum numbers in cylindrical coordinates, some of which have spin up, while some others have spin down. Furthermore, for some orbitals the correspondence between spherical shell model quantum numbers and Nilsson asymptotic quantum numbers is not the same for protons and for neutrons. Introducing a new rule of correspondence between the two sets of quantum numbers, we show that the spin paradox is resolved and full agreement between the proton and neutron Nilsson diagrams is established. The form of the Nilsson diagrams as a function of the quadrupole deformation remains unchanged, the only difference between the new diagrams and the traditional ones being the mutual exchange of the Nilsson labels for certain pairs of single-particle energy levels.

Also with collaborators from Iran, an analytical description of the parity doublet structure appearing in odd-A nuclei has been found [51]. The controlled single particle (CSP) concept, introduced earlier by the same group, has been used in order to construct an analytical model. In a parity doublet structure, bands consisting of states with alternating positive and negative parity appear. Calculated results are compared to the experimental data of ^{151}Pm, with good agreement found.

Table 12: Grants used by the Nuclear Theory group of the I.N.P.P. Demokritos in 2021.

Prog. ID	Title	Host Institution	Principal Investigator	Starting date	Finishing date	Budget (€)
5033021	Magic numbers of exotic nuclei	I.N.P.P. Demokritos	A. Martinou	01/01/2020	31/12/2021	26,400.00
5047793	Nucleon separation energies	I.N.P.P. Demokritos	D. Bonatsos	27/04/2020	26/08/2021	41,541.50
KP-06-N48/1	Evolution of nuclear structure, shapes and symmetries in the standard and extreme regions of nuclear masses and energy	INRNE-BAS	N. Minkov	26/11/2020	26/11/2023	86,920.00

Funding

In 2021 the Nuclear Theory research group has taken advantage of the two grants awarded in 2020. Both proposals had been written by Andriana Martinou.

The first has been awarded by the State Scholarships Foundation (I.K.Y.) to Andriana Martinou for Post Doctoral research. It has a duration of 24 months, a total budget of 26,400.00€, and MIS number 5033021. The research aims to investigate the "Magic Numbers of Exotic Nuclei" and especially the connection of the phenomenon of shape coexistence in nuclei to the nuclear magic numbers.

The second grant has been awarded through the Operational Program "Human Resources Development, Education and Lifelong Learning 2014-2020" in the context of the project "Nucleon Separation Energies" with MIS number 5047793.

[51] Hadi Sobhani et al. "An analytical description of the parity-doublet structure in an odd-A nucleus". In: *Nuclear Physics A* 1013 (2021), p. 122224. DOI: 10.1016/j.nuclphysa.2021.122224

The program supported the Principal Investigator (Dennis Bonatsos), a Post Doctoral Researcher (Konstantinos Karakatsanis) and a Ph.D. candidate (Smaragda Sarantopoulou). The total budget is 41.451,50€ and the duration is 15 months.

A third grant with MIS number KP-06-PN48/3 has been awarded by the National Science Fund of Bulgaria to N. Minkov in the I.N.R.N.E. in Sofia, Bulgaria. Three members (D. Bonatsos, A. Martinou and S. Sarantopoulou) of the Nuclear Theory group of the I.N.P.P. in Demokritos have participated in the proposal. The research aims to investigate the " Evolution of nuclear structure, shapes and symmetries in the standard and extreme regions of nuclear masses and energy". The three members of the Nuclear Theory group in the I.N.P.P. use the fund to cover travel expenses and fees for conferences.

Outreach

The M.Sc. thesis of S. Peroulis has been completed at NTUA in 11/2021 [52]. Peroulis in his Master's thesis calculated within the proxy-SU(3) symmetry the electric quadrupole transition probabilities (B(E2)s) among various nuclear states of heavy and deformed nuclei. His calculations are the first step towards the construction of an online tool (in alignment with the open-science practices), which shall give to the users the predictions of the proxy-SU(3) for various nuclear observables. Peroulis will continue this work in his Ph.D. thesis in the Nuclear Theory Group.

Despite the restrictions imposed by the pandemic, the group participated in the organization and the scientific program of the following conferences:
1. International Workshop on Shapes and Dynamics of Atomic Nuclei: Contemporary Aspects (SDANCA-21), Sofia, Bulgaria, 9/2021. Bonatsos served as a member of the International Program Committee. Talks have been given by Bonatsos [53] and Martinou [54], as well as by our experimental collaborators at the U. of Athens (Mertzimekis [55], Zyriliou [56], Vasileiou [57]).
2. 6th Hellenic Institute of Nuclear Physics Workshop on New Aspects and Perspectives in Nuclear Physics (HINPw6), Athens, 5/2021. Bonatsos served as a member of the Organizing Committee. Talks have been given by Bonatsos [58],

[52] Spyridon Peroulis. *Electric quadrupole transitions in Algebraic Nuclear Models.* 2021. DOI: 10.26240/HEAL.NTUA.21869

[53] D. Bonatsos et al. "Unified Picture of Nucleon Pairs Playing Leading Roles in Nuclear Collectivity." In: *Bulgarian Journal of Physics* 48.5-6 (2021), p. 441

[54] Andriana Martinou. "The L-projection of the shell model SU(3) wave functions". In: *Bulgarian Journal of Physics* 48 (2021), p. 557

[55] T.J. Mertzimekis et al. "Experimental investigations of nuclear structure around A=180". In: *Bulgarian Journal of Physics* 48 (2021), p. 625

[56] A. Zyriliou et al. "Reviewing nuclear structure properties of even-even Yb isotopes". In: *Bulgarian Journal of Physics* 48 (2021), p. 608

[57] P. Vasileiou et al. "Experimental investigation of the nuclear structure in the neutron-rich 180Hf". In: *Bulgarian Journal of Physics* 48 (2021), p. 618

[58] D. Bonatsos et al. "Connecting the proxy-SU(3) symmetry to the shell model". In: *The European Physical Journal Web of Conferences* 252 (2021), p. 02004. DOI: 10.1051/epjconf/202125202004

Martinou [59], and Sarantopoulou [60].
3. 29th Annual Symposium of the Hellenic Nuclear Physics Society, Athens, 9/2021. Martinou served as a member of the Organizing Committee. Talks have been given by Bonatsos [61] and Martinou [62], as well as by our experimental collaborators at the U. of Athens (Zyriliou [63], Vasileiou [64]).
In addition, group members participated on-line to the XXIInd Colloque GANIL, Autrans-Méaudre en Vercors, France, 9/2021.

During 2021 the research group of the Nuclear Theory in the I.N.P.P had been working remotely with the following network of international collaborators:
a) **Klaus Blaum**[1], **R. Burcu Cakirli**[2], **Richard F. Casten**[3]
[1] *Max Planck Institute for Nuclear Physics, Heidelberg, Germany,*
[2] *Istanbul University, Turkey,*
[3] *Yale University, USA*
Proxy–SU(3) has been discovered in collaboration with the above-mentioned experimentalists, who were the first to notice the importance of the 0[110] Nilsson pairs of orbitals in creating nuclear deformation.

b) **Jozsef Cseh**[4]
[4] *Institute for Nuclear Research, Debrecen, Hungary*
Collaboration on the connection of proxy-SU(3) to the shell model through the Elliott model.

c) **Jerry P. Draayer**[5], **Feng Pan**[6], **Ziwei Feng**[6], **Sai Cui**[6]
[5] *Louisiana State University, USA,*
[6] *Liaoning Normal University, Dalian, P.R. China*
Collaboration on microscopic fermionic nuclear models taking advantage of symmetries.

d) **Hassan Hassanabadi**[7], **Hadi Sobhani**[7]
[7] *Shahrood University of Technology, Iran*
Collaboration on the connection of proxy-SU(3) to the shell model through the Nilsson model.

[59] Andriana Martinou. “A mechanism for shape coexistence”. In: *The European Physical Journal Web of Conferences* 252 (2021). Ed. by A. Pakou et al., p. 02005. DOI: 10.1051/epjconf/202125202005

[60] Andriana Martinou et al. “Highest weight irreducible representations favored by nuclear forces within SU(3)-symmetric fermionic systems”. In: *The European Physical Journal Web of Conferences* 252 (2021). Ed. by A. Pakou et al., p. 02006. DOI: 10.1051/epjconf/202125202006

[61] D. Bonatsos et al. “Shell model foundations of the proxy-SU(3) symmetry: Nucleon pairs creating nuclear deformation”. In: *HNPS Advances in Nuclear Physics.* 2021

[62] Andriana Martinou. “The microscopic origin of the Interacting Boson Model”. In: *Proceedings of the 29th Annual Symposium of the Hellenic Nuclear Physics Society.* HNPS Advances in Nuclear Physics. 2021

[63] A. Zyriliou et al. “Nuclear structure investigations in Yb isotopes”. In: *Proceedings of the 29th Annual Symposium of the Hellenic Nuclear Physics Society.* HNPS Advances in Nuclear Physics. 2021

[64] P. Vasileiou et al. “Experimental study of the nuclear structure of 180Hf: Preliminary results”. In: *Proceedings of the 29th Annual Symposium of the Hellenic Nuclear Physics Society.* HNPS Advances in Nuclear Physics. 2021

e) **Nikolay Minkov**[8]
[8] *INRNE, Bulgarian Academy of Sciences, Sofia, Bulgaria*
Close collaboration on all group theoretical and numerical aspects of the development of the proxy-SU(3) model from its very beginning, as part of a long term collaboration going on for 30 years.

f) **T. J. Mertzimekis**[9], **K. Zyriliou**[9], **P. Vasileiou**[9], **S. Pelonis**[9], **V. Lagaki**[9], **G. Siltzovalis**[9], **M. Efstathiou**[9], **A. Chalil**[10], **P. Koseoglou**[11]
[9] *Physics Department, National Kapodistrian University of Athens, Athens, Greece*
[10] *Institute of Research into the Fundamental Laws of the Universe, CEA, Saclay, France,*
[11] *Technische Universität Darmstadt, Darmstadt, Germany*
Collaboration in experimental proposals approved at the Horia Hulubei National Institute for R & D in Physics and Nuclear Engineering, Bucharest, Romania. The experiments aim to measure the spectrum and the lifetimes of the ^{178}Yb and ^{180}Hf isotopes. The theory group at the I.N.P.P. in Demokritos participated in the proposal and will deliver theoretical predictions about the lifetimes and the electric transition probabilities among the the nuclear states.

Overview

The Nuclear Theory group in the I.N.P.P. Demokritos has developed its own theory, the proxy-SU(3) symmetry. Thus, a unique in the world expertise on this model has been created in the Institute. The M.Sc. and Ph.D. students and the postdoctoral fellows of the Nuclear Theory group have a valuable know-how on the Shell Model SU(3) and the proxy-SU(3) symmetry.

The group has expanded its network of collaborators despite the transportation difficulties due to the pandemic. Nuclear theorists from the East to the West are by now familiar with the proxy-SU(3) symmetry. Collaborations with colleagues from P.R. China, Iran, Bulgaria, Hungary, U.S.A., Turkey, Germany and Greece resulted to 5 peer-review publications and 12 conference papers, and may result to many more in the future.

The support from two funding agencies was decisive and valuable for the evolution of the group. The group received 67.941,50€ to cover the scholarships of two Post Doctoral fellows and one Ph.D. student. Without this support the above achievements would not have been possible.

By now the proxy-SU(3) symmetry is a model, which is of interest only to those working on the basic research in Nuclear Structure Theory. But this model has the future potential to be linked to various new a) technologies, such as nuclear medicines, nuclear batteries and nuclear clock, b) physics beyond the Standard Model, through calculations concerning the neutrino-nucleus reactions, c) Nuclear Physics, by unifying the nuclear models, or by further investigating the phenomenon of shape coexistence in nuclei, d) cosmological models, since one may use the proxy-SU(3) symmetry to calculate the nucleon capture cross sections, the nuclear level densities and the nuclear binding energies, all of them being valuable in nuclear astrophysics and in cosmology.

Experimental Nuclear Physics

Researchers:	Sotirios. V. Harissopoulos
	Anastasios Lagoyannis
	Michail Axiotis
Research Associates:	Zoi Kotsina
	Eleni Vagena
	Prodromos Chatzispyroglou
PhD students:	Aggelos Laoutaris
	Ioannis Madesis
	Stefanos Nanos
	Kostas Preketes-Sigalas
	Stefanos Papagiannis
	Pavlos Tsavalas
Master students:	Maria Peoviti
	Stefanos Nanos
	Evangelia Taimpiri
	Anastasia Ziagkova
	Anastasia Kotsovolou
Diploma students:	Christos Andrikopoulos

Introduction

The scientific program in Experimental Nuclear Physics & Ion-Beam Applications is implemented at the in-house Tandem Accelerator Laboratory (TAL). Our research team focuses its efforts on two main directions: nuclear astrophysics and Ion Beam Analysis (IBA) techniques. Moreover, it maintains a close collaboration with the Universities of Ioannina around a research program on atomic physics with accelerators. Finally, during 2021, the group continued its collaboration with other Greek institutions for the implementation of the European Space Agency's (ESA) G4G program.

Apart from its main research activities, the group continues to support the external users at the accelerator both during the preparation and the running of their experiments.

Activities

In the following sections the scientific output of the group during 2021 is briefly presented.

Nuclear Astrophysics

In brief, the Nuclear Astrophysics activities of the group focus on the study of nuclear capture reactions relevant to the understanding of a nucleosynthetic mechanism occurring in certain explosive stellar environments, such as supernovae. This mechanism, termed p-process, is responsible for the synthesis of certain 35 neutron-deficient nuclei heavier than iron that lie "north-west" of the stability valley, between ^{74}Se and ^{196}Hg. These nuclides are known as the p-nuclei and have, so far, been observed only in the solar system. Aiming at the understanding of p-process, the major research objective of the Nuclear Astrophysics program of INPP is the establishment of a proper cross-section database. For this purpose, systematic cross-section measurements of proton and α-particle capture reactions in medium-mass nuclei, from Cu to Cs, are performed. During 2021,our group has measured the cross sections of proton capture reactions on Sr isotopes and also published an ongoing study on the systematics of the semimicroscopic proton-nucleus optical potential at low energies In the framework of fundamental research, multiparticle emission may play a role in nuclear astrophysics. More specifically, the (n,2n) channel may dominate the (n,γ) channel at relatively high temperatures. This could play a crucial role in the nucleosynthesis of neutron-rich isotopes and, hence, in the r-process nucleosynthesis. Therefore, the assumption that the multiparticle emission is negligible at astrophysics-relevant energies needs to be tested. For this reason, the cross-section measurements of the (n,2n) reaction channel are important.Towards this end, UoI and NTUA, in collaboration with our group, has measured and published the cross-sections of the reaction. A systematic study of neutron-induced nuclear reactions for a particular mass region utilizing in parallel the technological and simulation advances constitutes a valuable tool both for nuclear technology and fundamental research. The present work concerns the measurement of the (n,2n) reaction channel for the medium-to heavy-mass region. Through the present work the $^{156}Dy(n,2n)$ reaction has been measured at energies above 17 MeV. According to our knowledge, the experimental data for this reaction in the literature are limited in a narrow energy range between 13.5 and 15 MeV. The experimental data were compared to statistical calculations of the TALYS code and the impact of different models was investigated.

IBA

The group continued its studies, in collaboration with INRASTES, on fusion related materials. The objectives of the work were the investigation of W lamellae samples from Tile 5 regarding a) the quantification and depth profile of carbon, b) sample morphology and elemental analysis. For the carbon quantification, NRA measurements employing a 2H beam were carried out using the $^{12}C(^{2}H,p)^{13}C$ reaction. The NRA measurements were carried out using a 1.35 MeV deuteron beam. The produced particles were detected at an angle of 170 degrees with respect to the beam axis employing a silicon surface barrier detector of 1000 um thickness covering a solid angle of 1.5 msr. The chamber was kept under vacuum (10^{-7} mbar). Two of the samples were analysed using a deuterium micro-beam because of the small width of their surface (1 mm). The W(d, d)W peak was used for the charge determination and the $^{12}C(^{2}H,p)^{13}C$ peak using the cross section as calculated by SigmaCalc for the carbon content. The analysis was performed using the simNRA software. Apart from the carbon peak, the peaks of the beryllium and the oxygen were also detected on some samples, but the statistics are too low to allow proper quantification.

G4G

The activities of the group in the context of the G4G ESA's project mainly involve the porting of the GRAS Geant4 based code to multi-threading and the newest version of Geant4. In this framework the group has almost completed the task of implementing multi-threading capabilities to the code. The code will be handed to ESA and will be released, most probably, during next year or early 2022.

Funding

Table 13: Funding of the Nuclear Physics Experimental group of the I.N.P.P. Demokritos in 2021.

Prog. ID	Title	Host Institution	Principal Investigator	Starting date	Finishing date	Budget (€)
11551	Fusion – Radiation studies	I.N.P.P.	A. Lagoyannis	1/12/2008	31/03/2023	30,000.00
11893	LIBRA	I.N.P.P.	S. Harissopulos	1/9/2014	31/8/2023	200,000.00
11985	ENSAR 2 – H2020	I.N.P.P.	S. Harissopulos	1/3/2016	30/4/2021	60,000.00
12239	CALIBRA	I.N.P.P.	S. Harissopulos	1/1/2017	30/9/2022	3,422,000.00
12335	GEANT4-based particle simulation facility for future science mission support	I.N.P.P.	A. Lagoyannis	1/4/2019	30/4/2022	120.935,00
12356	Access to Ion and Neutron Beams at NCSR "Demokritos"	I.N.P.P.	A. Lagoyannis	13/6/2019	12/6/2024	15.000,00

Outreach

PhD Thesis

1. **E. Georgali:** "Study of neutron induced reactions in rare earth Isotopes"; Axiotis, Lagoyannis (member of Advisory and Examination committee), UOI, 2021
2. **I. Madesis:** "Investigation of electron capture in swift C4+ (1s2s 3S) collisions with gas targets using a Zero degree Auger projectile spectroscopy apparatus built with the L45 beam line at the Demokritos 5.5MV tandem accelerator"; Harissopulos (member of Examination committee), UOC, 2021

PhD Thesis - Ongoing

1. **S. Chasapoglou:** Lagoyannis, NTUA
2. **A. Laoutaris:** Lagoyannis, UoC
3. **S. Nanos:** Axiotis, UoI
4. **K. Preketes - Sigalas:** Lagoyannis, NTUA
5. **P. Tsavalas:** Lagoyannis, NTUA
6. **A. Zyriliou:** Lagoyannis, NKUA

MSc Thesis

1. **M. Peoviti:** "HPGe detectors characterization and feasibility study for cross section measurements of neutron induced reactions on mid-weight nuclei at INPP NCSR Demokritos"; Axiotis, UOI, 2021

MSc Thesis - Ongoing

1. **A. Ziagkova:** Axiotis, NTUA
2. **E. Taimpiri:** Axiotis, Lagoyannis, NTUA

X-ray Spectrometry

Researchers:	Dr. Andreas-Germanos Karydas
Research Associates:	Maria Kaparou
PhD students:	Kalliopi Tsampa
	Nikoletta-Kanella Kladouri
Master students:	Eva Eleftheriou
	Dimitra Tsakou
	Elena Kwnstantakopoulou
	Theofanis Tsakiris
	Michail Chrysovalantis Papadakis

Introduction

The research interests of the x-ray spectrometry group (INPP-XRS), include three basic directions:

1. the use of synchrotron radiation for basic and applied research. The basic research activities refer to the measurement of fundamental x-ray and atomic parameters related to the interaction of X-rays with matter and atom de-excitation processes, whereas applications involve the characterization of advanced nanostructured and Cultural Heritage materials
2. the development of laboratory or/and portable x-ray fluorescence methodologies and applications in the fields of cultural heritage and environmental monitoring, including the design, realization and characterization of new spectrometers.
3. the development of cultural heritage and environment- related applications using x-rays induced through the inner shell atoms ionization by energetic proton beams with micrometer or millimeter size (micro-PIXE and external beam PIXE)

During 2021, the INPP-XRS intensified its research program related to the aforementioned multi-thematic areas, succeeded in generating substantial results and scientific contributions. International collaborations include colleagues from the Istituto di Scienze per il Patrimonio Culturale, Consiglio Nazionale delle Ricerche (ISPC-CNR), the Nuclear Engineering and Techniques Group, Center for Nuclear Sciences and Technologies Dept. of Nuclear Sciences and Engineering Instituto Superior Técnico, Universidade de Lisboa, Portugal, the LIBPhys-UNL -Laboratório de Instrumentação, Engenharia Biomédica e Física da Radiação, Department of Physics, NOVA School of Science and Technology, Portugal, Elettra Sincrotrone Trieste in Italy and Physics Department of Panjab University, India. With respect to National Collaborations the INPP-XRS group leader has been assigned as member of the PhD committee of three PhD students, namely of Dimitrios Mitsos (PhD thesis on Corrosion of Cultural Heritage monuments and Environmental factors. Study on Attica and Central Peloponnese monuments), University of Peloponnese, Theofanis Gerodimos (PhD thesis on Hyperspectral imaging and data analysis techniques in X-ray emission spectroscopy), University of Ioannina and of Stelios Kesidis (PhD thesis on Scientific examination of the palette of Greek painters from the 19th to beginning of the 20th cent.), University of Peloponnese

The internal collaborations – within N.C.S.R. "Demokritos" – were further enhanced with Dr Eleni Makarona (Energy Harvesting and Autonomous Sensors Group, Institute of Nanoscience and Nanotechnology (INN)) whereas the fruitful long-standing collaboration with the Environmental Radioactivity Laboratory (ERL) of the Institute of Nuclear and Radiological Sciences and Technology, Energy and Safety (INRASTES) was continued.

Activities

Synchrotron Measurement of Fundamental X-ray Parameters

The motivation for this activity originates from the fact that the fostering of XRF applications in various disciplines, presenting high relevance with technological, societal, cultural and policy making needs, calls for further advances, not only with respect to improved equipment performance and capabilities, but also to our basic knowledge regarding X-ray fundamental processes with matter. Concerning the latter, despite the existence of many compilations of X-ray fundamental Parameters (FPs) exhibiting internal consistency, as a result of specific atomic model calculations or of careful evaluations using both theoretical and experimental available data, there is in fact a lack of systematic and consistent FP experimental data associated with low relative uncertainties ($\leq$ 5/During 2021 two important contributions were published regarding the measurement of FPs for few key elements (Sn, Sb, W, Re), including fluorescence yields, Coster-Kronig transitions and X-ray production cross sections. More specifically, those measurements have provided experimental evidence for the energy cut-off or onset of certain decay channels for Sn and Re respectively, after L-shell ionization, that alter systematics of certain FPs over atomic number dependence. The FP measurements were carried out using the selective photoionization method with tunable synchrotron radiation of highly spectral quality delivered at the XRF beamline of Elettra Sincrotrone Trieste by appropriate double crystal monochromators and high order suppressor optics. The activity at Elettra Sincrotrone Trieste continued in 2021 and two experiments were conducted with the participation of Andreas Karydas under the proposal #20200190 entitled: A Preliminary Study of Grazing Angle X-ray Fluorescence (GI-XRF) and X-ray Reflectometry (XRR) as Enabling Characterization Tools of Patterned Hierarchical Nanoarchitectures, July 2021, with PI Eleni Makarona, and of the proposal #20210466 entitled: Measurements of different M-shell physical parameters for high atomic number elements Bi (Z=83) and Th (Z=90), December 2021 with PI, Prof S. Puri

Cultural Heritage (CH)

During 2021, the external Ion Beam Analysis end-station developed in the framework of the National Infrastructure project CALIBRA with PIS Dr Sotirios Harissopulos and Dr. A. Lagoyannis, was completed and commissioning experiments were carried out within November-December 2021 delivering a Technical Report as one of the deliverables of the CH work package (WP8). The main features of the external IBA end-station are described in the published work by S. Harissopulos, et al., “The Tandem Accelerator Laboratory of NCSR ”Demokritos”: Current status and perspectives”, The European Physical Journal Plus 136(6) (2021) Within 2021 the results of a long-lasting project regarding the pXRF characterization of wall-painting pigments from the Palace of Nestor were published in collaboration with Dr. Hariclia Brecoulaki, from the Institute of Historical Research, Department of Greek and Roman Antiquity, National Research Foundation, as chapter entitled: “Re-presenting in colours at the “Palace of Nestor”: Original Polychromy and painting materials”, in the book Representations, Material and Immaterial Modes of Communication in the Bronze Age Aegean, Edited by John Bennet, Oxbow Books, (2021) pp. 53-106. In the framework of the PhD thesis of Ms Nikoleta-Kanella Kladouri, first results obtained from micro-XRF measurements performed at the XRF laboratory of INPP were published in JAS Reports 7 (2021) 102975 in a paper entitled: “Bronze votive pins from the sanctuary of Athena Alea at Tegea, Arcadia, Greece, 9th-7thc. BCE: A microscopic and compositional study using portable micro X-ray fluorescence spectrometry (micro-XRF)” by N. K. Kladouri, A.G. Karydas, V. Orfanou, V. Kantarelou, N. Zacharias. Finally, analytical results from the MSc thesis of Ms Nikoleta Tasiouli, partly conducted at the XRF laboratory of INPP, were published in collaboration with colleagues from the University of West Attica, Department of Conservation of Antiquities and Works of Art (N. Tasiouli, S. Boyatzis, A. Karatzani, A. G. Karydas, “Study and Conservation of a 19th Century Printed Silk Scarf from the Collection of the National Historical Museum of Greece”, Archaeology 9(1) (2021) 56-67). Finally, in collaboration with colleagues from the Laboratory for Ion Beam Interactions, Division of Experimental Physics, Rudjer Boskovic Institute in Zagreb, Croatia, it has been demonstrated the usefulness of multivariate techniques for quantitative analysis of two-dimensional (2D) spectral images obtained by proton beam ionization (PIXE mode) and combined proton beam and photoionization with X-ray tube (PIXE+XRF mode). Two different multivariate analysis approaches were used: (i) Principal Component Analysis (PCA) for dimensionality reduction followed by k-means clustering for the identification of different sample regions, (ii) t-Distributed Stochastic Neighbour Embedding technique (t-SNE) (I. Božičević Mihalić, et al., “Multivariate analysis of PIXE+XRF and PIXE spectral images”, Journal of Analytical Atomic Spectrometry 36(3) (2021) pp. 654-657)

Environmental monitoring

The XRF laboratory participated in an intercomparison exercise to evaluate the measurement uncertainty and instruments performance using multi-element dust standard reference samples deposited on PTFE filters. This study was triggered by the fact that the quantification of the elemental concentration of ambient particulate matter is a challenging task because the observed elemental loadings are not well above the detection limit for most analytical techniques. Although non-destructive nuclear techniques are widely used for the chemical characterization of ambient aerosol, only one multi-element standard reference filter material that mimics ambient aerosol composition has become recently available in the market. Thus, to ensure accuracy, reliability and comparability of instruments performance, multiple reference materials with different elemental mass loadings are necessary. The filter samples, produced by means of dust dispersion, were tested in terms of homogeneity, reproducibility and long-term stability (≈80 month). Eight laboratories participated in the exercise. The results showed that most of the reported on the certificate of analysis elements were efficiently detected in the sample loadings prepared as representative for atmospheric samples by the Expert Laboratory. The average absolute relative difference between the reported and the reference values ranged between 0.1% (Ti) and 33.7% (Cr) (CRM-2584). The work published by M. Gini et al., "Inter-laboratory comparison of ED-XRF/PIXE analytical techniques in the elemental analysis of filter-deposited multi-elemental certified reference materials representative of ambient particulate matter", Science of the Total Environment, 780 (2021) 146449)

Materials Science

In this area and in collaboration with Dr. E. Makarona from the Institute of Nanoscience and Nanotechnology, the XRF laboratory of INPP contributed to investigating the uniform dispersion of copper oxide (CuO) nanofillers within the poly(methyl methacrylate (PMMA) matrix and to assist in the selection of the optimum preparation conditions. Polymer nanocomposites have emerged as a new powerful class of materials because of their versatility, adaptability and wide applicability to a variety of fields. The work conducted by G. Geka et al., aimed to develop a facile and cost-effective method to realize CuO/PMMA polymer nanocomposites that could be used as resist materials for e-beam lithography (EBL) with the intention of being integrated into nanodevices (G. Geka, et al., "CuO/PMMA Polymer Nanocomposites as Novel Resist Materials for E-Beam Lithography", Nanomaterials 11 (2021) 762)

XRS at XRF Laboratory

During 2020 a significant part of the XRS group research work has been directed to further exploiting and developing the imaging capabilities of the so-called macroscopic XRF analysis, when applied to archaeological materials (one publication and one MSc thesis awarded), but also to utilizing the laboratory experience and available spectrometers in new investigations of materials with strong archaeological interest (two publications). Moreover, the interest and involvement in environmental monitoring studies is reflected in two other publications, whereas the established in 2020 close collaboration with the Institute of Nanoscience and Nanotechnology (INN) and Eleni Makarona (Energy Harvesting and Autonomous Sensors Group) resulted in our first common publication supported by measurements performed in the XRF laboratory.

Analytical Services

The XRF laboratory provided analytical services within three (3) contracts as follows:

1. With the McDonald Institute at the Cambridge University, UK, within the framework of PLOMAT project: "Plotting the material flows of common-

place Late Bronze Age Seals in Western Eurasia Portable X-ray fluorescence (pXRF) for the characterization of ancient seals made of vitreous materials (faience, frit, glass)" with principal investigator Dr. Christina Tsouparopoulou, Senior Research Associate & Marie Skłodowska-Curie Fellow at the McDonald Institute for Archaeological Research. The services were carried out in collaboration with Department of Department of Materials Science & Engineering, University of Ioannina (Prof. Dimitrios Anagnostopoulos and Ph.D candidate Anastasios Asvestas)

2. With the University of Copenhagen within the framework of the research program: 'The Rhodes Centennial Project', conducted in collaboration of the Ephorate of Antiquities of the Dodecanese and the University of Copenhagen. The services included the analysis of one hundred and twenty-two (122) coins of which one hundred and eleven (111) are copper and eleven (11) silver coins originating from the Ancient city and necropolis of Rhodes and the preparation of an archaeometrical report
3. With the Creative Systems Engineering, private vendor in Greece, to evaluate the analytical capabilities of a pXRF spectrometer in industrial oriented applications. The services and consulting were carried out in collaboration with Department of Department of Materials Science & Engineering, University of Ioannina (Prof. Dimitrios Anagnostopoulos and Ph.D candidate Anastasios Asvestas)

Presentations at Conferences/Meetings/Symposia contributions

1. Oral presentation by A.G Karydas at the annual meeting of the Italian Synchrotron Radiation Society (SILS), "Depth profiling of deep implanted ions in silicon by Grazing Incidence X-ray Fluorescence (GI-XRF) spectrometry", June 2021
2. Authorship in Poster Presentation at PIXE 2021, "XAHRM-Lab, an X-ray Advanced HiREDS Research and Metrology Laboratory"
3. Co-Authorship in Poster presentation at PTB-Seminar, VUV and EUV Metrology EUV2021, "TXRF/GIRXF high precision laboratory setup with high flux monochromatic source", 19 - 20 October 2021
4. HNPS Symposium, October 2021, "Macroscopic X-ray fluorescence characterization of Platinum Group Mineral inclusions in archaeological gold", Kalliopi Tsampa, Claudia Caliri, Francesco Paolo Romano, Jack Davis, Sharon R. Stocker, Andreas Germanos Karydas", Oral presentation by Kalliopi Tsampa
5. HNPS Symposium October 2021, "Advanced XRF Tools and Methodologies for the Revisualization of Vanished Ancient Polychrome", E. Eleftheriou, C. Caliri, P. Romano, K. Tsampa, S. Sotiropoulou and A. G. Karydas, Poster presentation by Evaggelia Eleftheriou

Invited talks-Seminars (by Andreas Karydas)

1. X-ray Fluorescence: a technique unravelling the secrets behind ancient and modern advanced materials, alongside exploring ancient alien life traces, Aris-

totle University of Thessaloniki, May 2021

2. X-ray Fluorescence at the service of Archaeology and Conservation Science: Experiences, modern approaches and future perspectives, Workshop on Analytical Techniques in Cultural Heritage in the framework of ARISTEAS (Advancing Research Infrastructure & Scientific Techniques in Archaeological Science) project by the University of Peloponnese, October 2021
3. Best practices for safely operating HH-XRF analyzer, The Cyprus Institute, October 2021

Participation at Elettra Sincrotrone Trieste Beamtimes:

1. Beamtime proposal #20200190, A Preliminary Study of Grazing Angle X-ray Fluorescence (GI-XRF) and X-ray Reflectometry (XRR) as Enabling Characterization Tools of Patterned Hierarchical Nanoarchitectures, July 2021
2. Beamtime proposal #20210466, Measurements of different M-shell physical parameters for high atomic number elements Bi (Z=83) and Th (Z=90), December 2021

DOM

Researchers:	Dr. Christos Markou (Coordinator)
	Dr. E. Tzamariudaki
	Dr. E. Drakopoulou
Administration:	S. Bakou
PhD students:	A. Sinopoulou
	D. Tzanetatos
	D. Stavropoulos
	V. Tsourapis
Diploma students:	G. Zarpapis
	E. Katsikeros
	M. Chadolias
	E. Tragia
Employees:	G. Androulakis
	C. Bagatelas
	S. Oikonomou
Technicians:	V. Tsagkli
	A. Vougioukas

Introduction

The astroparticle physics group of the Institute of Nuclear and Particle Physics (INPP) is mainly focusing on the detection and subsequent study of neutrinos from cosmic accelerators. The study of cosmic neutrinos offers significant advantages towards answering basic questions about the origin and nature of cosmic rays. Neutrinos, being neutral, are not deflected by interstellar magnetic fields and, unlike protons, are not significantly absorbed by intervening matter. Thus, they point to their sources over all energy ranges and distance scales, and hence are uniquely valuable as cosmic messengers. In addition, the detection of astrophysical high energy neutrinos will shed light on the production mechanism of high energy gamma rays by understanding whether the sources of high energy gamma rays observed by the HESS telescope are due to electromagnetic or hadronic processes.

The INPP astroparticle physics group is a member of the KM3NeT collaboration. KM3NeT [65] is a distributed Research Infrastructure, member of the ESFRI Road Map that will consist of a network of neutrino telescopes in the Mediterranean Sea with user ports for Earth and Sea sciences. Once completed, the telescopes will have detector volumes between megaton and several cubic kilometers of clear sea water. Located in the depths of the Mediterranean Sea, KM3NeT will open a new window on our Universe and will contribute to the understanding of the properties of the elusive neutrino particles. The ARCA (*Astroparticle*

[65] S Adrián-Martínez et al. "Letter of intent for KM3NeT 2.0". In: *Journal of Physics G: Nuclear and Particle Physics* 43.8 (2016), p. 084001. ISSN: 1361-6471. DOI: 10.1088/0954-3899/43/8/084001. URL: http://dx.doi.org/10.1088/0954-3899/43/8/084001

Research with Cosmics in the Abyss) telescope, which is located offshore of Sicily, Italy, at a maximum depth of 3450 m, is devoted to the search for neutrinos from distant astrophysical sources, such as superenovae, gamma ray bursts or colliding stars. The ORCA (*Oscillation Research with Cosmics in the Abyss*) detector which is located 40 km offshore Toulon, France, at a depth of 2450 m, aims at studying neutrino properties through the precise measurement of neutrino oscillations exploiting neutrinos generated in the Earth's atmosphere. An artistic view of the KM3NeT detectors is shown if Fig. 55.

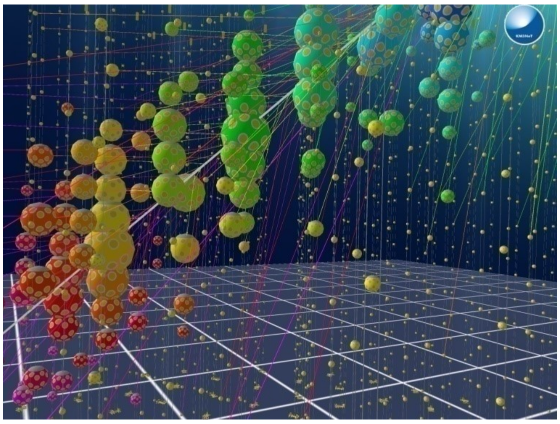

Figure 55: An artist's view of an event as it will be seen by the KM3NeT telescopes

Activities

In 2021 the group has been active in construction, testing and validation of the KM3NeT detectors and individual components, physics analyses and studies, governance and management.

KM3NeT contruction

Since 2016 a DOM integration, validation and testing facility has been established in the premises of INPP (Fig. 56). The DOM lab has been funded exclusively through internal funds. It was completed in record time (compared to other similar labs in KM3NeT), and has been operational in late 2016. Ever since, the lab continues with the integration of DOMs.

Currently the lab employs 2 FTE of skilled personnel, with additional help from other group members as the need arises. In 2020 the DOMs of ORCA-DU1 which have been recovered due to an electrical problem and have been sent to the INPP DOM Lab, have been thouroughly tested and were successfully refurbished.

An additional contribution to the collaboration are testing and validation efforts concerning the high-pressure testing of the DOM penetrators which are used for powering the DOMs and for data transfer from the DOMs to the shore station via an electro optical cable. As the penetrators can be a single point of failure for the DOMs, acceptance testing is extremely important. These tests are curried out

Figure 56: The DOM Lab at INPP

using a high-pressure testing chamber, capable of sustaining pressure up to 600 bars (Fig. 57). These tests are done for a large fraction of the KM3NeT DOM penetrators (120 penetrators during 2020), as the only other similar facility is in NIKHEF, Amsterdam.

Figure 57: Pressure testing of the penetrators

The group has also undertaken the calibration of the DOM compasses which are mounted on the central logic boards (CLBs). These tests are done for the KM3NeT collaboration only in the premises of INPP. More than 100 compasses were calibrated in INPP during 2020.

In order to improve and standardize the calibration procedure, a fully automated gimbal was designed and put in operation at the INPP in N.C.S.R. "Demokritos" (project of the interim student Ph. Katsimalis). All parts are

3D printable or standard commercial components (Fig. 58). The rotations along all 3 axes are performed automatically via Arduino controlled stepper motors with pre-defined angular speed and breaks between successive rotations, eliminating the human error factor in the final calibration quality.

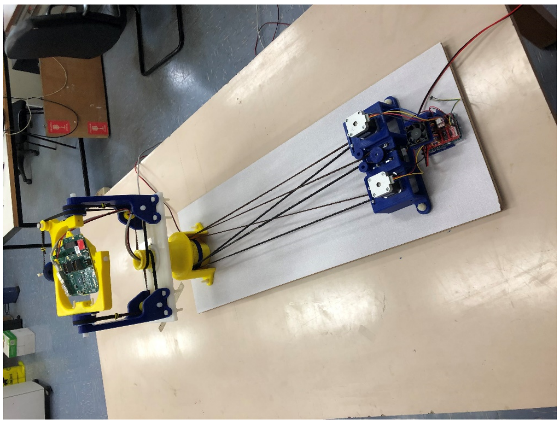

Figure 58: The fully automated gimbal designed in INPP

Activities in the Kalamata branch

The group activities in SW Peloponnese have been expanded via a collaboration between Université Côte d'Azur, CNRS, Febus-optics, HCMR and our group has been established aiming at the distributed sensing of earthquakes and ocean-solid Earth interactions using two orthogonal fiber optic seafloor cables, offshore Methoni in Greece. To investigate the potential of this novel technique for monitoring underwater seismic activity, there have been two campaigns to date, with data recorded from the two optic seafloor cables and compared with the activity recorded by seismic stations that have been installed for this purpose.

Researchers:	Sotirios. V. Harissopoulos
	Anastasios Lagoyannis
	Michail Axiotis
Research Associates:	Zoi Kotsina
	Eleni Vagena
	Prodromos Chatzispyroglou
PhD students:	Aggelos Laoutaris
	Ioannis Madesis
	Stefanos Nanos
	Kostas Preketes-Sigalas
	Stefanos Papagiannis
	Pavlos Tsavalas
Master students:	Maria Peoviti
	Stefanos Nanos
	Evangelia Taimpiri
	Anastasia Ziagkova
	Anastasia Kotsovolou
Diploma students:	Christos Andrikopoulos

Introduction

The Tandem Accelerator Laboratory (TAL) is a unique Research Infrastructure in Greece. Its total surface Laboratory is app. 2000 sq. meters, half of which are covered by the Tandem accelerator hall and two "target rooms" where the experimental setups are installed. The remaining area is covered by a machine workshop, a target preparation room, an XRF laboratory, the control room, work spaces and offices. In 2016, the Tandem laboratory has been included in the National Roadmap for Research infrastructures with the aim to be fully upgraded and establish the CALIBRA Research Infrastructure. CALIBRA stands for "Cluster of Accelerator Laboratories for Ion Beam Research and Applications" and is one of the 20 infrastructures of the current National Roadmap. CALIBRA is currently been implemented through the CALIBRA project, funded with 3.42 million Euros by the currently running strategic plan for growth in Greece, called "Partnership Agreement (PA) for the Development Framework 2014-2020" . In CALIBRA Phase-1, i.e., by the end of September 2022, the existing 5.5 MV Tandem will be completely upgraded with new components including a Pelletron charging chain, new ion sources, new injection beamline, new voltage stabilizers, new foil and gas strippers, beam profile monitors, and a fully computer-controlled operation system. In addition, a 2.5 MV Tandetron for Accelerator Mass Spectrometry, donated by the University of Oxford will be installed. Also, a donated 17 MeV PET Cyclotron, already transferred from Netherlands, will be used to establish a PET radioisotope production laboratory (subject of implementation of CALIBRA's Phase-2). TAL is an open access facility offering yearly at least 2000 hours of beamtime to internal and external users. Roughly 60% of the beamtime refers to ion-beam applications and irradiation services, with the rest being devoted to basic research in nuclear physics and atomic physics with accelerated ions. Good part of the experiments in basic research focus on the study of neutron-induced reactions. The laboratory and the setups presented below are described in detail in the paper by S. Harissopulos et al., Eur. Phys. J. Plus 136, 617 (2021).

The TANDEM Accelerator Laboratory

Currently, the following two accelerators are in operation.

- 5.5 MV T11/25 Tandem Van de Graaf accelerator: It was manufactured by the High Voltage Engineering Corporation (HVEC) and delivered its first beams in 1973. Between 2009 and 2012, the accelerator was significantly refurbished through a project funded by the European Commission (FP7/REGPOT Grant LIBRA, budget ?1.5 million Euros). The accelerator provides currently proton and deuteron beams as well as ions of various elements, from Carbon to Copper. By end of 2022 and thanks to the CALIBRA project presented below, the Tandem accelerator will be completely upgraded
- PAPAP accelerator: PAPAP stands for "Petit Accellerateur pour l'Astrophysique". It is a 250-keV single-stage accelerator capable of delivering proton and deuteron beams of hundreds of micro-Amps. It was built and initially installed at CSNSM, Orsay, France, with the purpose of investigating nuclear reactions related to solar neutrino problem. When this program was terminated, it was donated to INPP. PAPAP is also equipped with a state-of-the-art scattering chamber for material analysis, with sample cooling option down to liquid nitrogen temperatures.

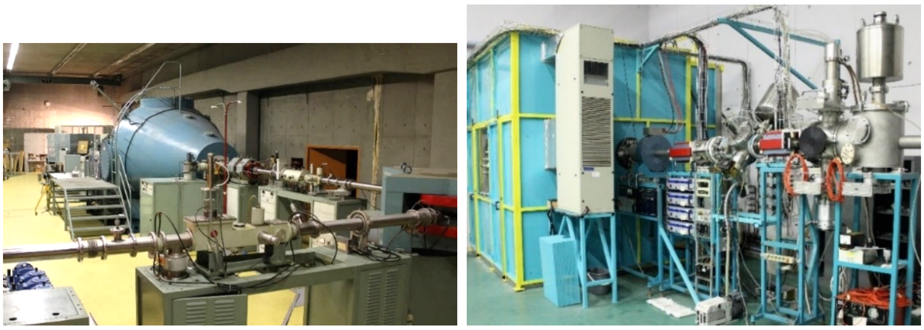

Figure 59: The T11/25 Tandem accelerator (left) and the single-stage PAPAP accelerator (right).

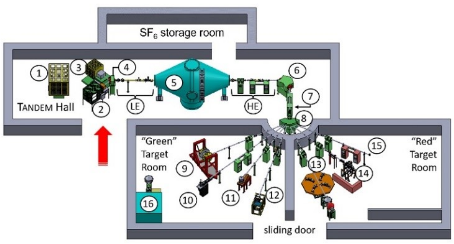

Figure 60: Schematic layout of the Tandem-hall and the two target rooms of the laboratory.

The main accelerator components and setups are described in the table below

Table 14: Accelerator components and beamlines indicated with circled numbers in the above figure

Circled number	Desription
1	Ion source electronics Faraday cage
2,3	Duoplasmatron and Sputter sources
4	30-deg. injector magnet
5	Tank; VdG Generator (terminal)
6	90-deg. Analyzing Magnet
7	Poststripper
8	Switching magnet (8 ports)
9	60-deg. Beamline (R60): GASPAR 4π BGO-Calorimeter
10	45-deg. Beamline (R45): nuclear microprobe
11	32.5-deg. Beamline (R32.5): RBS/Channeling chamber and external micro-PIXE setup
12	15-deg. Beamline (R15): NaI calorimeter (14 in. x 14 in.) and HPGe detector array; nuclear astrophysics and depth profiling
13	25-deg. Beamline (L25): Universal scattering chamber for NRA and ion irradiations
14	45-deg. Beamline (L45): Zero-degree Auger Projectile Spectrometer (ZAPS) for ion-atom collision studies
15	60-deg. (L60) multi-purpose beamline: irradiations with neutrons produced via the d+D or d+T reactions, or material irradiations with ions
16	PAPAP accelerator

Experimental Setups

TAL is currently equipped with following major experimental setups and other nuclear instruments:

Nuclear Microprobe: It is a standard micro-beam system purchased by Oxford Microbeams Ltd for the determination of the elemental composition of material surfaces. The different beam defining and focusing elements are shown in the figure on the left. The chamber has 22 ports at several angles, where detectors and auxiliary equipment can be attached. It is equipped with a load lock chamber, a microscope just above the chamber entrance and a CCD camera.

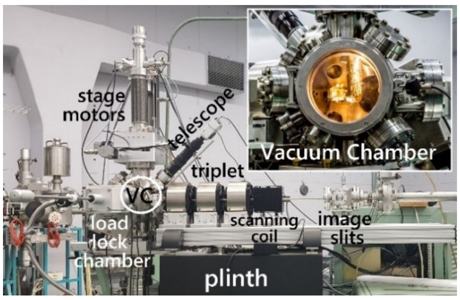

Figure 61: The nuclear microprobe

NEOPTOLEMOS Calorimeter: It is a cylindrically-shaped large volume (14 in.x 14 in.) NaI(Tl) detector with a borehole of 32 mm diameter along its axis. It is used to apply the 4π γ-summing technique in nuclear astrophysics studies of capture reactions, where the cross sections of interest are very small making the use of high-efficient HPGe detectors, even with Anti-Compton shields, impractical. NEOPTOLEMOS has an absolute efficiency better than 50% for a two-fold γ-cascade. It can also be used for depth-profiling measurements. The 4π-summing technique is described in the review paper by: Sotirios V. Harissopulos, Eur. Phys. J. Plus 133, 332 (2018).

GASPAR BGO Ball: Loaned by LNL, the Laboratori Nazionali di Legnaro, Padova, Italy, GASPAR stands for "GASP for Astrophysics Research", with "GASP" standing for GAmma Spectrometer previously operating at LNL (see in: the GASP website: http://gasp.lnl.infn.it/). GASPAR is a calorimeter composed of 80 BGO crystals covering 80% of the solid angle. It is to be used for the study of reactions relevant to nuclear astrophysics. Its advantage over NEOPTOLEMOS is its ability, not only to sum transitions forming a 4γ-cascade, but also to provide the cascade's multiplicity, which defines the detector's summing efficiency. This way, Monte-Carlo efficiency simulations can be by-passed. GASPAR has recently been equipped with new digital electronics for signal processing using funds from the CALIBRA project (see below).

Figure 62: The NEOPTOLEMOS Summing Spectrometer (left) and the GASPAR BGO Ball (right)

External ion beam analysis end-station: It integrates the analytical capabilities of the PIXE, RBS and PIGE ion beam analysis techniques in one experimental set-up, so that to attain a complete elemental and near surface structural characterization of samples in an almost non-destructive way and without any limitation concerning their size or conductive state. The set-up experimental was developed to be used with protons as well as with heavier ions. Probe dimensions down to ?1 mm2 can be analyzed. It uses simultaneously five spectrometers; two for the implementation of PIXE by utilizing newly acquired Silicon Drift detectors (SDDs) with 30mm2 and 150 mm2 active areas supported by digital pulse processors, one for RBS/NRA, one for PIGE, whereas an additional miniature SDD X-ray detector is also employed for dose monitoring purposes. The exit ion-beam nozzle through appropriate collimation confines the ion beam size (?1mm at the analysis point), whereas the selected exit window (100 nm Si3N4 thin film) and the short distance (?5mm), in which the charged particles travel across the air path, minimize the ion beam energy loss and the straggling effect. Up to date, the setup has been employed in analytical diagnostic studies of a few representative paintings of contemporary Greek painters in order to identify and document pigments, materials and techniques and prevent trade of fakes. In addition, ancient glass beads were also examined with respect to their sodium concentration and their in-depth homogeneity.

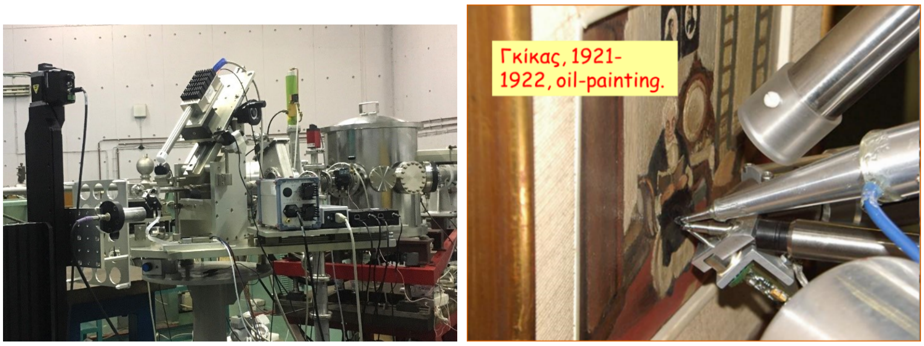

Figure 63: Picture of the newly developed External Ion Beam end-station (left) and during the analysis (right) of the contemporary Greek painter Gkikas, in collab. with Benaki Museum and Thetis Authentics LtD.

RBS/Channeling setup: RBS and Channeling measurements are performed with the chamber shown in panel a) of the figure below. It is made of stainless steel and is cylindrically-shaped with a 20-inch diameter. It contains a sample positioning manipulator, which is shown in panel b). A laser (L) mounted outside the chamber is used for the placement of the detectors at the desired scattering angles and for beam alignment. Samples are loaded through a sample loading door (SLD). A glass view port (VP) allows for visual monitoring of the chamber's interior, the sample's translations and rotations and the beam spot's location and shape.

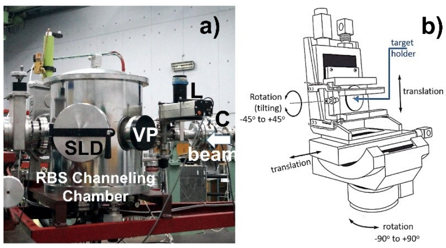

Figure 64: Left: The RBS/Channeling chamber installed at the R32.5 beamline. The ion beam is coming from the right as indicated by the white arrow. Right: the sample manipulator and its possible translations and rotations

ZAPS setup: ZAPS stands for Zero-degree Auger Projectile Spectroscopy. It was installed by the Atomic Physics Groups from the Universities of Crete and Ioannina, Greece, to perform high resolution studies of Auger electrons emitted from projectile ions excited in ion-atom collisions. The workhorse of the ZAPS setup is the single stage hemispherical deflector analyzer (HDA) combined with a two-dimensional Position Sensitive Detector (PSD) and a four-element injection lens.

The IR2 material irradiation setup: It was developed by the Fusion Technology Group of NCSR "Demokritos" for Ion iRradiations of materials with in-situ

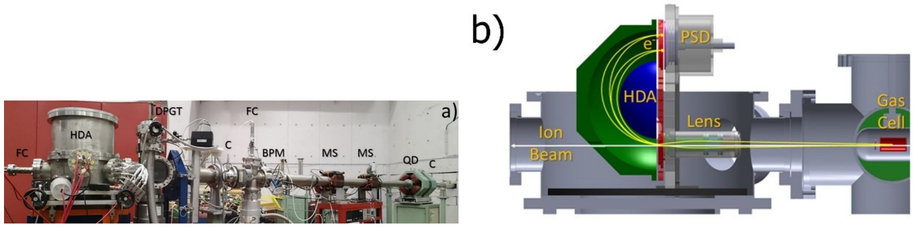

Figure 65: The ZAPS beamline (top): QD, Quadrupole Doublet; MS, Magnetic Steerer; BPM, Beam Profile Monitor; FC, Faraday Cup; C, Collimators; DPGT, Differentially Pumped Gas Target. ZAPS is housed in the last chamber of the beamline. Bottom: The projectile ions traverse the gas cell. The Auger electrons (yellow trajectories) exit the gas cell (where the ions are excited to auto-ionizing states by the collision in the gas target) along the ion direction (0?), enter the lens and are dispersed by the HAD. They are focused onto the PSD where their positions are recorded leading to a 2-D image.

electrical Resistivity measurements. It is used to study radiation damage and recovery in alloys and other fusion relevant materials at well controlled ion fluxes and temperature, from the cryogenic range (?10 K) up to 700 K by means of a dedicated cryo-cooler.

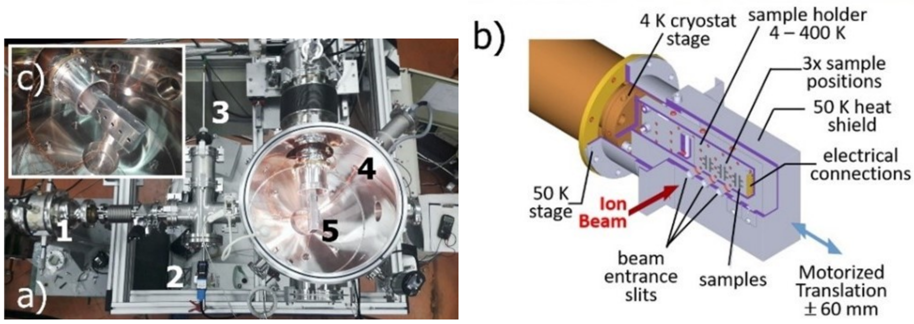

Figure 66: The IR2 material irradiation setup. Panel (a) shows: Ta slits (1), CCD camera (2), Faraday cup (3), vacuum chamber (4) and target holder position (5). Panel (b) depicts the individual parts of the target holder that is shown in panel (c).

Other setups and scientific instruments: Among the experimental devices used the most are the multi-purpose large-volume scattering chamber used for Nuclear Reaction Analysis (NRA), for charged-particle activations as well as for particle-spectroscopy, in general, and the deuterium-filled gas cell for the production of quasi-monochromatic neutrons with the d+D and d+T reactions. They are described in detail in the paper by S. Harissopulos et al., Eur. Phys. J. Plus 136, 617 (2021); https://doi.org/10.1140/epjp/s13360-021-01596-5 and references given therein. In addition to these instruments, an array of 16 3He-gas-filled neutron counters is available for the study of neutron-emitting reactions. All three experimental devices are shown below. An array of 3 HPGe detectors with 80% relative efficiency equipped with BGO crystals for Compton background suppression is also available at the Tandem laboratory.

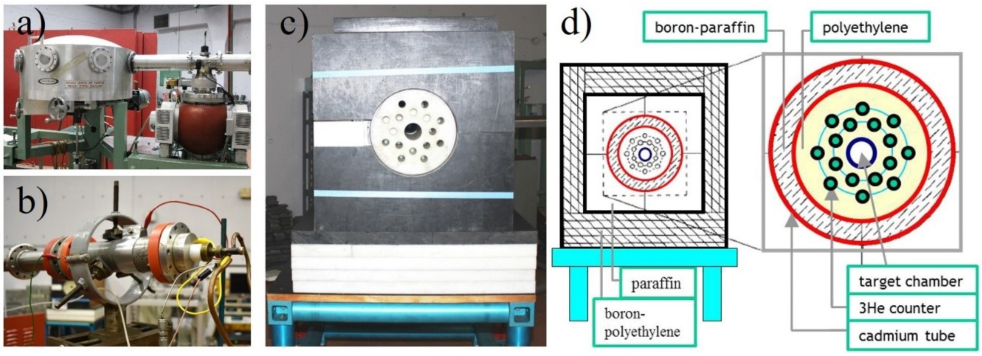

Figure 67: Panel (a): The multi-purpose scattering chamber installed at the L25 beamline. Panel (b): gas cell used for the production of neutrons. It is installed at the L60 beamline and is the main tool for the study of neutron-induced reactions, primarily (n, 2n). Panel (c): Array of 16 3He-gas-filled neutron counters. Panel (d) displays the different components of the array. The array can be mounted per demand at the L60 beamline

Apparatus for particle induced quasi-monochromatic X-ray Beams (PIXE-XRF): The experimental apparatus consists of an x-ray spectrometry end station of moderate energy resolution operating with proton-induced quasi-monochromatic x-ray beams. It was designed, installed and implemented at the 5.5MV Tandem Accelerator of the INPP with the support of several funded projects (PEP Attikis Framework, Project ATT-29, 2006 - 2008, DEMO-RESEARCH, 2007-2008 and of an IAEA Coordinated Research Project, No. 13833, 2006-2009). The apparatus is described in detail by Sokaras et al. (https://doi.org/10.1063/1.4768735) and its utilization in atomic fundamental studies by Sokaras et al. (10.1103/PhysRevA.81.012703, 10.1103/PhysRevA.83.052511).

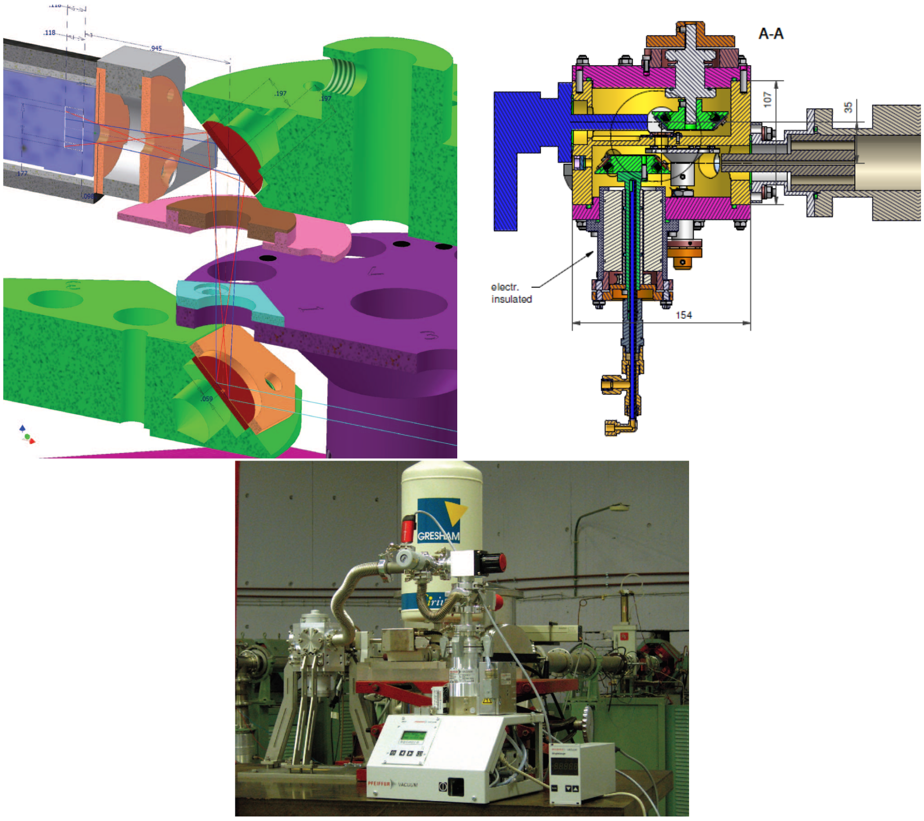

Figure 68: Transverse cross section of the PIXE-XRF scattering chamber Schematic drawing of the PIXE-XRF scattering chamber allowing using multiple electrically isolated and water-cooled primary targets The PIXE-XRF apparatus installed at the TANDEM accelerator beamline

AILAB

Researchers:	A.Kyriakis D.Loukas
Practical work students:	O. Likouresis, C.Malakis, P. Oustric, O. Zampetaki
Engineers:	I. Kazas (ELE)

Introduction

The main activities of the artificial inteligence for radiation detection lab (AILAB) are related to development of technologies for radiation detection, identification and localization.

The lab project can be summarized as follows:

- Design detector networks for radiation detection and source localization,
- Develop both analytical and AI algorithms for radioactive source localization,
- Develop AI algorithms for radioactive source type identification,
- Design radiation detectors based on Scintillators - SiPMs for radioactive source localization,
- Study of new materials for radiation detection,

- Develop moving detector schemes for radioactive source localization and identification in ground, air and sea

During 2021 the INPP AILAB lab was envolved it tree main tasks that will be explained in the next sessons.

Radioactive Source Localization from single sensor and collimator

In general localization of radioactive sources or hotspots is a major issue for radiological safety of operators in nuclear facilities and in National Security. For this purpose, portable Gamma-Ray Imaging (GRI) systems allow remote localization of radioactive sources from greater distances than conventional rate meters, leading to significant reductions of the dose received by operators.

One of the fist methodologies for the localization of a radioactive source was the use of a mechanical collimator around the γ-ray sensor. Thus a raster scanning is used with a single detector of one pixel that is moving around. This is relatively inexpensive but the whole process is rather slow. This type of imaging systems are based on a shielded collimated detector. It has a limited field of view of a few degries and an image is produced by raster scanning the sensor head and recreating the gamma image by overlapping the results of each measurement.

Our lab applied an idea to increase the localization accuracy of such a device is to move the detector inside the mechanical collimator. In figure 69(left) this device is hosted in a semi-autonomous rover. The machanical collimator can be made from lead of at least 1cm in thickness whilst the sensor can move inside this with a piston like mechanism (figure 69(Right). The measurements performed using a laboratory low activity ^{152}Eu radioactive source can be seen in figure 70.

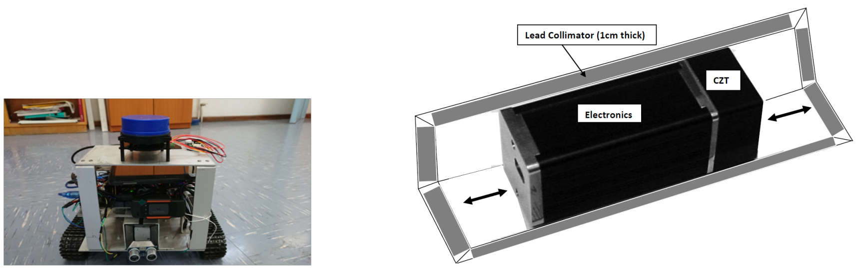

Figure 69: Left: Rover with the solid state sensor ($CdZnTe$) and the lead colimmator Right: Schematic of the piston system that moves the sensor inside the collimator.

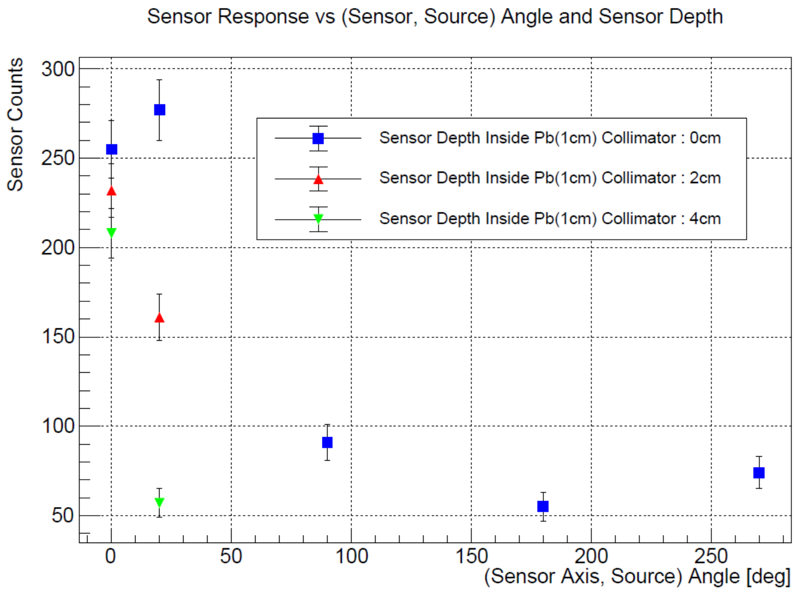

Figure 70: Shematic of the CMS detector with Phase-II upgrade plan

Radioactive Source Localization using a network of CZT sensors

A second approach for the localization of radioactive sources and applied by ou lab is a small form factor ($0.5cm^3$) CdZnTe sensor network consisted of a number of five sensors in a planar cruciform topology (figure 71) capable to localize a stationary radiation source in 3D.

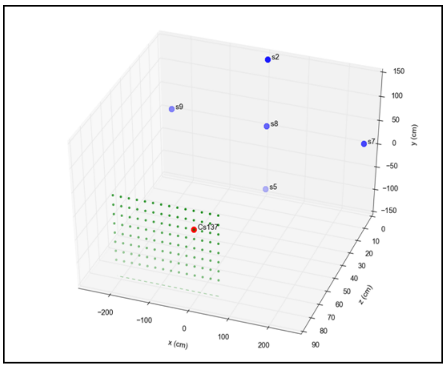

Figure 71: Shematic of the five sensors in a planar cruciform topology network

The localization was performed with fusion algorithms based on MVA techniques. The algorithms make use of Multy Layer Persepton Neural Networks and Boosted Desission Trees. The training of the MVA methods has been done using an enriched set of experimental data (defined as the response of the sensors in different 3D radiation source positions) collected with the sensor network and exploiting the symmetry of its topology. The initial small set of experimental data points was increased to a few thousand points by utilizing both the symmetry of the network topology and the fact that the response of the sensors is proportional to $Ae^{-\mu R}/R^2$, where A represents the source activity and the sensor efficiency and R is the distance in 3D between each sensor and the radiation source and the factor e-μR corresponds to the absorption term. Using the above data driven method thousands of data points have been generated and subsequently used for the training of the MVA algorithms. The benefit of this approach is that without any significant computational cost the effects of both the radiation absorption and scattering can be taken into account, which in other circumstances would require a detailed description of the surrounding materials in order to produce reliable simulated data of the experimental setup.

This data driven method used to increase the initially small sample of experimental data and the MVA techniques were applied to localize bare and slightly shielded radioactive sources. For the slightly shielded source we used a lead shield of 1 cm width around the bare ^{137}Cs source. A set of weight factors were produced in each case separately, during the training of the MVA methods. The following source localization results produced with a set of experimental data not used in the training of the MVA methods. Figure 72 shows the horizontal (top), vertical (middle) and depth (bottom) resolution defined as the RMS of the accuracy (estimated — true coordinate) distribution as a function of the exposure time in seconds. Left (Right) column shows the bare (slightly shielded) source results for a ^{137}Cs source ($180\mu Ci$) at various parallel plains ($Z = 40cm, 80cm, 120cm$) to the sensor plain for both the MLP and the BDTG methods. A bare source localization resolution of the order of less than 15 cm has been archived in both horizontal and vertical directions after at least of 40 sec of exposure time, whilst the corresponding depth resolution is of the order of less than 20 cm. The resolution is slightly improved with exposure time. Also the two MVA methods give very similar results. In addition a slightly shielded source can be also localized in 3D with corresponding resolutions of less than 20 cm in both horizontal and vertical directions and 30 cm in depth after at least of 40 sec of exposure time within a monitored volume of 5 m $\times$ 2.8 m $\times$ 2 m. We should also mention that the mean value of the accuracy distribution is affected by a small bias which varies up to 15 cm the maximum especially at large values of the depth coordinate. This can be caused by the small number of recorded counts in this region.

Radioactive Source Localization using a single sensor in 360^o

During 2021 our lab performed an extended simulation campaign for the new Anger type γ-ray device using the ANTS2 software. Various sources spanning from ^{241}Am to ^{60}Co were positioned around the detector in 36 different azimuthal angle positions, with a separation space of 10^o between them. In Figure 73 an indicative graph of a simulated NaI cylindrical scintillator, the SiPM layer and the source moving around the axis of the scintillator(Y axis) anti-clockwise is shown.

The response to the light emitted by the NaI scintillator crystal will be collected

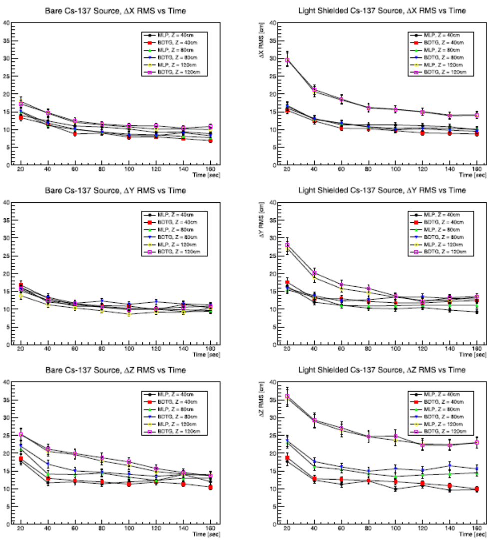

Figure 72: Horizontal (top), vertical (middle) and depth (bottom) resolution defined as the RMS of the accuracy (estimated — true coordinate) distribution as function of the exposure time in seconds. Left (right) column shows the bare (slightly shielded) source results for a ^{137}Cs source ($180\mu Ci$) at various parallel plains ($Z = 40cm80cm120cm$) to the sensor plain and for both MLP and BDTG methods

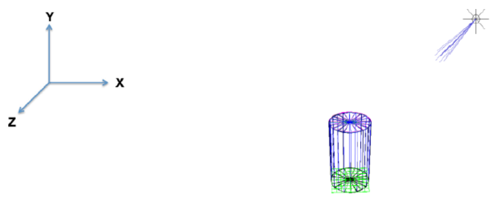

Figure 73: Schemmatic of the simulated Scintillator (Blue-Black line), the SiPM layer (Green line) and the source using the ANTS2 software

by the SiPM array, stored and subsequently analyzed. In Figure 74(Left) an indicative simulated response of the SiPMs is shown for a ^{57}Co source that emits at an azimuthal angle of 160 degrees (conventionally source azimuthal angle of 0o is considered a source emitting from the right). Similarly in Figure 74(Right) an indicative simulated response of the SiPMs is shown for a 137Cs source that emits at an azimuthal angle of 270 deg.

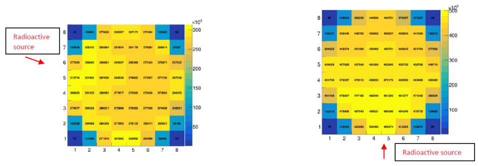

Figure 74: Left: SiPM indicative response for a ^{57}Co source emitting at emitting at 160^o(red arrow). Right: SiPM indicative response for a ^{137}Cs source emitting at emitting at 270^o(red arrow)

As a first approach a simple algorithm that can be used to estimate the source azimuthal direction by using the SiPM response is the following. The centre of gravity (CoG) of each event (response of SiPMs to a γ-ray from the source) can be constructed defined as the weighted sum of each SiPM local position multiplied by the deposited number of counts, divided by the sum of the recorded counts from all SiPMs. Then a directional vector can be produced by taking as the vector starting point the centre of the SiPM array and as the vector ending point the above mentioned CoG point. In addition the vectorial sum of the directional vectors can be constructed from all the available events. The azimuthal angle of this final vector can be used as an estimator of the source azimuthal angle. The advantage of this approach is that background events show an equally distributed response in the SiPM array and thus cancel out each other from the CoG calculation. More advanced MVA regression techniques could also be used for improved azimuthal resolution.

In Figure 75 the difference between the azimuthal angle estimated by the above described algorithm and the true source azimuthal angle can be seen for ^{57}Co, ^{137}Cs and ^{60}Co sources. Thus the estimated source azimuthal angle resolution is of the order of 1^o in case of low energy sources like the 122keV ^{57}Co source and can be of the order of 9^o for much higher energy sources like the 1172keV, 1332keV ^{60}Co source showing an almost linear behavior.

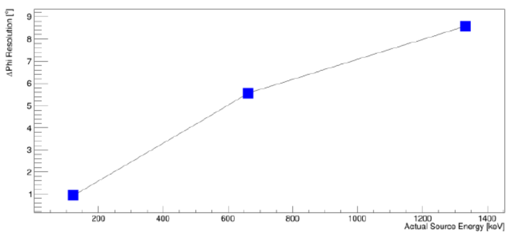

Figure 75: Difference between the azimuthal angle estimated by the above described algorithm and the true source azimuthal angle as a function of the source energy for an indicative simulated device.

Education and Outreach Activities

Among the activities of the Institute of Nuclear and Particle Physics education is of great importance. In this context, the INPP offers opportunities to both university students and high school and primary school aged children. The main educational activities can be summarized below:

Graduate and PostGraduate Educational activities

INPP in collaboration with the National Technical University of Athens (NTUA) organize a program of postgraduate studies which leads to a MSc or a PhD degree. The researchers of the Institute along with professors of NTUA jointly teach classes in this program. Furthermore, researchers of the Institute supervise and guide graduate students for the completion of their degree. During 2020 the following PhD and MSc degrees have been awarded:

- Dimitrakopoulos Nikolaos, MSc, A. Lagoyannis
- Eleutheriou Eva, MSc, A. Karydas
- Nanos Stefanos, MSc, M. Axiotis
- Peroulis Spyridon, MSc, D. Bonatsos
- Trantou Foteini Faidra, MSc, T. Geralis
- Tsakou Dimitra, MSc, A. Karydas
- Vasiliou Polytimos, MSc, A. Lagoyannis
- Asenov Patrick, PhD, D. Loukas
- Khaliel Ahmed, PhD, M. Axiotis
- Ntemou Eleni, PhD, A. Lagoyannis
- Paspalaki Garyfallia, PhD, A. Kyriakis
- Sobhani Hadi, PhD, D. Bonatsos

The following PhD/MSc efforts are ongoing:

- Peoviti Maria, MSc, M. Axiotis
- Assiouras Panagiotis, PhD, D. Loukas
- Asvestas Anastasios, PhD, A. Karydas
- Canko Dhimiter, PhD, K. Papadopoulos
- Chasapoglou Sotirios, PhD, A. Lagoyannis
- Georgali Eustathia, PhD, A. Lagoyannis & M. Axiotis
- Kladouri Nikoletta-Kanella, PhD, A. Karydas
- Laoutaris Aggelos, PhD, A. Lagoyannis
- Madesis Ioannis, PhD, S. Charisopoulos
- Nanos Stefanos, PhD, M. Axiotis
- Panagopoulou Tatiana, PhD, A. Karydas
- Papagiannis Stefanos, PhD, A. Karydas
- Prapa Maria-Myrto, PhD, T. Geralis
- Preketes - Sigalas Konstantinos, PhD, A. Lagoyannis
- Sarantopoulou Smaragda, PhD, D. Bonatsos
- Sinopoulou Anna, PhD, E. Tzamariudaki
- Stakia Anna, PhD, G. Daskalakis

- Stavropoulos Dimitrios, PhD, E. Tzamariudaki
- Syrrakos Nikolaos, PhD, K. Papadopoulos
- Tsampa Kalliopi, PhD, A. Karydas
- Tsavalas Pavlos, PhD, A. Lagoyannis
- Tsourapis Vasileios, PhD, C. Markou
- Tzanetatos Dimitrios, PhD, C. Markou
- Zorba Olga, PhD, T. Geralis
- Zyriliou Ekaterini, PhD, A. Lagoyannis

INPP, through agreements with Universities in Greece, supervise and guide undergraduate students during their Diploma thesis as well as their practical training. Students are trained by participating to the research projects of the Institute in order to acquire a training certificate (about 1-3 months training) or a diploma thesis needed for their graduation (about 6 months training). During 2020 nine (17) undergraduate students were trained from the INPP researchers.

- Biniskos Andreas, Diploma thesis, M. Axiotis
- Blanas Vasilis, Diploma thesis, T. Geralis
- Dizis Aggelos, Diploma thesis, D. Loukas
- Tsantiri Artemis, Diploma thesis, A. Lagoyannis
- Agoritsis Georgios, Practical Training, G. Anagnostou
- Androutsou Eleni, Practical Training, G. Stavropoulos
- Iatridis Georgios, Practical Training, C. Markou
- Giannakopoulos Dimitrios, Practical Training, G. Stavropoulos
- Kalpakidou Eudoksia, Practical Training, G. Daskalakis
- Katsimalis Philippos, Practical Training, C. Markou
- Ligda Artemis, Practical Training, E. Tzamariudaki
- Moniaki Melina, Practical Training, E. Tzamariudaki
- Mpari Zoi, Practical Training, A. Karydas
- Papaphillipou Dimitris, Practical Training, D. Loukas
- Peza Aleksandra, Practical Training, C. Markou
- Remoundou Theodora, Practical Training, G. Stavropoulos
- Tsolis Nikolaos, Diploma thesis, C. Papadopoulos
- Velezioti Marilia, Practical Training, G. Anagnostou
- Zarpapis Georgios, Practical Training, E. Tzamariudaki

Cadet Researchers

"Cadet Researchers: A life experience" is an educational activity held in NCSR DEMOKRITOS with the initiative of the Institute of Nuclear and Particle Physics. 2020 marked the 5th consecutive year "Cadet Researchers" was organized, although this time in a different manner due to COVID-19 related restrictions. "Cadet Researchers" comprises of a written physics competition among students of B' Lykeiou from schools in the Attica region. The top 8 students are invited to the INPP laboratories for a full week to participate in experiments ranging from scattering experiments in the TANDEM accelerator, to studies of novel particle physics detectors, to astroparticle physics detector investigations. In addition, a series of seminars on modern physics topics is planned during this week. In 2020, the lockdown measures did not allow the physical presene of the students in either the written competition or the laboratory experiments. Instead, an expanded series of seminars were organized over the internet in which more than 100 students from Lyceums participated. We expect and hope that in 2021 this activity will be held in the normal way, with physical presence of the students. Details can be found on https://www.dokimoierevtnites.gr

Particle Physics Masterclasses

The Institute of Nuclear and Particle Physics of NCSR Demokritos, organizes every year the Particle Physics Masterclasses for high school students. The international particle physics masterclasses are workshops organized by the International Particle Physics Outreach Group (IPPOG, http://ippog.org/). The Masterclasses take place in more than 50 countries and more than 200 universities and research institutes all over the world. In Greece, the participants are the universities of Athens, Thessaloniki, Crete, the National Technical University (NTUA), as well as NCSR Demokritos. During the day, high school students have the opportunity to work together with researchers in high energy physics and analyze particle physics data from the Large Hadron Collider (LHC). Initially, the students attend presentations for particle physics theory, accelerators, detectors and cosmology. Then, in the second part of the masterclass, the students are trained to analyze events from CMS experiment and "discover" by themselves the Higgs Boson. Finally, a teleconference takes place with other high schools around the world participating in the masterclass at the same day. During the conference, the students present and discuss their results and familiarize themselves with the international/multicultural tradition of research in fundamental physics. In 2020, INPP organized a virtual masterclass (due to Pandemic) at NCSR Demokritos.

www.physicsmasterclasses.org
https://physicsmasterclasses.org/index.php?cat=country&page=gr_athen3
www.facebook.com/InternationalParticlePhysicsMasterclasses
https://twitter.com/physicsIMC

NCSR Demokritos Summer School

INPP scientists have been members of the organizing committees and have participated as lecturers in Summer Schools for University graduate students and young scientists. The Summer School organized each year by NCSR Demokritos is a two-week course and aims to keep them up-to-date with the latest research developments at the Center and internationally. Speeches are given by Institute members and guest speakers, while participants visit the Institute's laboratory facilities. INPP speakers are ranked at the top positions based on students' evaluation.

Complex Systems and Applications (C.O.S.A.)

Our theory group research activity on Classical and Quantum Chaotic Dynamics is strengthened with the COSA Initiative. It was kicked off in 2006 by an act of the Council of institute Directors of NCSR Demokritos at the scientific recommendation of researchers from the center. Its purpose was to set up an interdisciplinary network of Greek researchers, with NCSR Demokritos as its cross-fertilizing hub. Its aim is to promote the study of the emerging new field of complexity research. It requires the synergy of a variety of concepts, methods and techniques from a variety of fields such as information Science, Nonlinear Sciences-deterministic chaos, nonequilibrium statistical mechanics and Fractal geometry. It equally touches through its insights a wide range of the human scientific endeavor ranging from particle and nuclear physics, cosmology and astrophysics, nanotechnology and mesoscopic physics as well as biology, economics and social sciences.

COSA's activities are educational and outreach through

- a semester course offered for credit in collaboration with the National Technical University of Athens on "Special Topics on Complex Systems"
- Cosa seminars on "Nonlinear Science and Complexity"

High Energy Physics - ATLAS

[Aab+21] Morad Aaboud et al. "Measurement of the relative B_c^{pm}/B^{pm} production cross section with the ATLAS detector at $sqrts = 8$ TeV". In: *Phys. Rev. D* 104.1 (2021), p. 012010. DOI: 10.1103/PhysRevD.104.012010. arXiv: 1912.02672 [hep-ex].

[Aad+21a] Georges Aad et al. "A search for the decays of stopped long-lived particles at $sqrtmathrms = 13$ TeV with the ATLAS detector". In: *JHEP* 07 (2021), p. 173. DOI: 10.1007/JHEP07(2021)173. arXiv: 2104.03050 [hep-ex].

[Aad+21b] Georges Aad et al. "A search for the dimuon decay of the Standard Model Higgs boson with the ATLAS detector". In: *Phys. Lett. B* 812 (2021), p. 135980. DOI: 10.1016/j.physletb.2020.135980. arXiv: 2007.07830 [hep-ex].

[Aad+21c] Georges Aad et al. "Configuration and performance of the ATLAS b-jet triggers in Run 2". In: *Eur. Phys. J. C* 81.12 (2021), p. 1087. DOI: 10.1140/epjc/s10052-021-09775-5. arXiv: 2106.03584 [hep-ex].

[Aad+21d] Georges Aad et al. "Determination of the parton distribution functions of the proton from ATLAS measurements of differential W'^{b1} and Z boson production in association with jets". In: *JHEP* 07 (2021), p. 223. DOI: 10.1007/JHEP07(2021)223. arXiv: 2101.05095 [hep-ex].

[Aad+21e] Georges Aad et al. "Differential cross-section measurements for the electroweak production of dijets in association with a Z boson in protontextendashproton collisions at ATLAS". In: *Eur. Phys. J. C* 81.2 (2021), p. 163. DOI: 10.1140/epjc/s10052-020-08734-w. arXiv: 2006.15458 [hep-ex].

[Aad+21f] Georges Aad et al. "Evidence for Higgs boson decays to a low-mass dilepton system and a photon in pp collisions at s=13 TeV with the ATLAS detector". In: *Phys. Lett. B* 819 (2021), p. 136412. DOI: 10.1016/j.physletb.2021.136412. arXiv: 2103.10322 [hep-ex].

[Aad+21g] Georges Aad et al. "Exclusive dimuon production in ultraperipheral Pb+Pb collisions at $sqrts_{mathrmNN} = 5.02$ TeV with ATLAS". In: *Phys. Rev. C* 104 (2021), p. 024906. DOI: 10.1103/PhysRevC.104.024906. arXiv: 2011.12211 [nucl-ex].

[Aad+21h] Georges Aad et al. "Jet energy scale and resolution measured in protontextendashproton collisions at $sqrts = 13$ TeV with the ATLAS detector". In: *Eur. Phys. J. C* 81.8 (2021), p. 689. DOI: 10.1140/epjc/s10052-021-09402-3. arXiv: 2007.02645 [hep-ex].

[Aad+21i] Georges Aad et al. “Longitudinal Flow Decorrelations in Xe+Xe Collisions at $sqrts_{mathrmNN}$ = 5.44 TeV with the ATLAS Detector”. In: *Phys. Rev. Lett.* 126.12 (2021), p. 122301. DOI: 10.1103/PhysRevLett.126.122301. arXiv: 2001.04201 [nucl-ex].

[Aad+21j] Georges Aad et al. “Measurement of b-quark fragmentation properties in jets using the decay $B^{pm}toJ/psiK^{pm}$ in pp collisions at $sqrts$ = 13 TeV with the ATLAS detector”. In: *JHEP* 12 (2021), p. 131. DOI: 10.1007/JHEP12(2021)131. arXiv: 2108.11650 [hep-ex].

[Aad+21k] Georges Aad et al. “Measurement of hadronic event shapes in high-p_T multijet final states at $sqrts$ = 13 TeV with the ATLAS detector”. In: *JHEP* 01 (2021). [Erratum: JHEP 12, 053 (2021)], p. 188. DOI: 10.1007/JHEP01(2021)188. arXiv: 2007.12600 [hep-ex].

[Aad+21l] Georges Aad et al. “Measurement of light-by-light scattering and search for axion-like particles with 2.2 nb^{-1} of Pb+Pb data with the ATLAS detector”. In: *JHEP* 03 (2021). [Erratum: JHEP 11, 050 (2021)], p. 243. DOI: 10.1007/JHEP11(2021)050. arXiv: 2008.05355 [hep-ex].

[Aad+21m] Georges Aad et al. “Measurement of single top-quark production in association with a W boson in the single-lepton channel at $sqrts = 8, textTeV$ with the ATLAS detector”. In: *Eur. Phys. J. C* 81.8 (2021), p. 720. DOI: 10.1140/epjc/s10052-021-09371-7. arXiv: 2007.01554 [hep-ex].

[Aad+21o] Georges Aad et al. “Measurement of the CP-violating phase phi_s in $B^0_stoJ/psiphi$ decays in ATLAS at 13 TeV”. In: *Eur. Phys. J. C* 81.4 (2021), p. 342. DOI: 10.1140/epjc/s10052-021-09011-0. arXiv: 2001.07115 [hep-ex].

[Aad+21p] Georges Aad et al. “Measurement of the associated production of a Higgs boson decaying into b-quarks with a vector boson at high transverse momentum in pp collisions at $sqrts$ = 13 TeV with the ATLAS detector”. In: *Phys. Lett. B* 816 (2021), p. 136204. DOI: 10.1016/j.physletb.2021.136204. arXiv: 2008.02508 [hep-ex].

[Aad+21q] Georges Aad et al. “Measurement of the jet mass in high transverse momentum $Z(rightarrowboverlineb)gamma$ production at $sqrts$ = 13 TeV using the ATLAS detector”. In: *Phys. Lett. B* 812 (2021), p. 135991. DOI: 10.1016/j.physletb.2020.135991. arXiv: 1907.07093 [hep-ex].

[Aad+21r] Georges Aad et al. “Measurement of the production cross section of pairs of isolated photons in pp collisions at 13 TeV with the ATLAS detector”. In: *JHEP* 11 (2021), p. 169. DOI: 10.1007/JHEP11(2021)169. arXiv: 2107.09330 [hep-ex].

[Aad+21s] Georges Aad et al. “Measurement of the $toverlinettoverlinet$ production cross section in pp collisions at $sqrts$ = 13 TeV with the ATLAS detector”. In: *JHEP* 11 (2021), p. 118. DOI: 10.1007/JHEP11(2021)118. arXiv: 2106.11683 [hep-ex].

[Aad+21t] Georges Aad et al. “Measurements of $W^+W^- + ge1$ jet production cross-sections in pp collisions at $sqrts = 13$ TeV with the ATLAS detector”. In: *JHEP* 06 (2021), p. 003. DOI: 10.1007/JHEP06(2021)003. arXiv: 2103.10319 [hep-ex].

[Aad+21u] Georges Aad et al. “Measurements of WH and ZH production in the $Hrightarrowbbarb$ decay channel in pp collisions at 13 TeV with the ATLAS detector”. In: *Eur. Phys. J. C* 81.2 (2021), p. 178. DOI: 10.1140/epjc/s10052-020-08677-2. arXiv: 2007.02873 [hep-ex].

[Aad+21v] Georges Aad et al. “Measurements of differential cross-sections in four-lepton events in 13 TeV proton-proton collisions with the ATLAS detector”. In: *JHEP* 07 (2021), p. 005. DOI: 10.1007/JHEP07(2021)005. arXiv: 2103.01918 [hep-ex].

[Aad+21w] Georges Aad et al. “Measurements of Higgs bosons decaying to bottom quarks from vector boson fusion production with the ATLAS experiment at $sqrts = 13, textTeV$”. In: *Eur. Phys. J. C* 81.6 (2021), p. 537. DOI: 10.1140/epjc/s10052-021-09192-8. arXiv: 2011.08280 [hep-ex].

[Aad+21x] Georges Aad et al. “Measurements of sensor radiation damage in the ATLAS inner detector using leakage currents”. In: *JINST* 16 (2021), P08025. DOI: 10.1088/1748-0221/16/08/P08025. arXiv: 2106.09287 [hep-ex].

[Aad+21y] Georges Aad et al. “Measurements of the inclusive and differential production cross sections of a top-quarktextendashantiquark pair in association with a Z boson at $sqrts = 13$ TeV with the ATLAS detector”. In: *Eur. Phys. J. C* 81.8 (2021), p. 737. DOI: 10.1140/epjc/s10052-021-09439-4. arXiv: 2103.12603 [hep-ex].

[Aad+21z] Georges Aad et al. “Measurements of top-quark pair single- and double-differential cross-sections in the all-hadronic channel in pp collisions at $sqrts = 13\, textrmTeV$ using the ATLAS detector”. In: *JHEP* 01 (2021), p. 033. DOI: 10.1007/JHEP01(2021)033. arXiv: 2006.09274 [hep-ex].

[Aad+21aa] Georges Aad et al. “Medium-Induced Modification of Z-Tagged Charged Particle Yields in $Pb+Pb$ Collisions at 5.02 TeV with the ATLAS Detector”. In: *Phys. Rev. Lett.* 126.7 (2021), p. 072301. DOI: 10.1103/PhysRevLett.126.072301. arXiv: 2008.09811 [nucl-ex].

[Aad+21ab] Georges Aad et al. “Muon reconstruction and identification efficiency in ATLAS using the full Run 2 pp collision data set at $sqrts = 13$ TeV”. In: *Eur. Phys. J. C* 81.7 (2021), p. 578. DOI: 10.1140/epjc/s10052-021-09233-2. arXiv: 2012.00578 [hep-ex].

[Aad+21ac] Georges Aad et al. “Observation of photon-induced W^+W^- production in pp collisions at $sqrts = 13$ TeV using the ATLAS detector”. In: *Phys. Lett. B* 816 (2021), p. 136190. DOI: 10.1016/j.physletb.2021.136190. arXiv: 2010.04019 [hep-ex].

[Aad+21ad] Georges Aad et al. "Optimisation of large-radius jet reconstruction for the ATLAS detector in 13 TeV protontextendashproton collisions". In: *Eur. Phys. J. C* 81.4 (2021), p. 334. DOI: 10.1140/epjc/s10052-021-09054-3. arXiv: 2009.04986 [hep-ex].

[Aad+21ae] Georges Aad et al. "Performance of the ATLAS RPC detector and Level-1 muon barrel trigger at $sqrts = 13$ TeV". In: *JINST* 16.07 (2021), P07029. DOI: 10.1088/1748-0221/16/07/P07029. arXiv: 2103.01029 [physics.ins-det].

[Aad+21af] Georges Aad et al. "Search for a heavy Higgs boson decaying into a Z boson and another heavy Higgs boson in the $ellellbb$ and $ellellWW$ final states in pp collisions at $sqrts = 13 textTeV$ with the ATLAS detector". In: *Eur. Phys. J. C* 81.5 (2021), p. 396. DOI: 10.1140/epjc/s10052-021-09117-5. arXiv: 2011.05639 [hep-ex].

[Aad+21ag] Georges Aad et al. "Search for bottom-squark pair production in pp collision events at $sqrts = 13$ TeV with hadronically decaying tau-leptons, b-jets and missing transverse momentum using the ATLAS detector". In: *Phys. Rev. D* 104.3 (2021), p. 032014. DOI: 10.1103/PhysRevD.104.032014. arXiv: 2103.08189 [hep-ex].

[Aad+21ah] Georges Aad et al. "Search for charged Higgs bosons decaying into a top quark and a bottom quark at $sqrtmathrms = 13$ TeV with the ATLAS detector". In: *JHEP* 06 (2021), p. 145. DOI: 10.1007/JHEP06(2021)145. arXiv: 2102.10076 [hep-ex].

[Aad+21ai] Georges Aad et al. "Search for charged-lepton-flavour violation in Z-boson decays with the ATLAS detector". In: *Nature Phys.* 17.7 (2021), pp. 819–825. DOI: 10.1038/s41567-021-01225-z. arXiv: 2010.02566 [hep-ex].

[Aad+21aj] Georges Aad et al. "Search for charginos and neutralinos in final states with two boosted hadronically decaying bosons and missing transverse momentum in pp collisions at $sqrts = 13$,,TeV with the ATLAS detector". In: *Phys. Rev. D* 104.11 (2021), p. 112010. DOI: 10.1103/PhysRevD.104.112010. arXiv: 2108.07586 [hep-ex].

[Aad+21ak] Georges Aad et al. "Search for charginotextendashneutralino pair production in final states with three leptons and missing transverse momentum in $sqrts = 13$ TeV pp collisions with the ATLAS detector". In: *Eur. Phys. J. C* 81.12 (2021), p. 1118. DOI: 10.1140/epjc/s10052-021-09749-7. arXiv: 2106.01676 [hep-ex].

[Aad+21al] Georges Aad et al. "Search for dark matter in association with an energetic photon in pp collisions at $sqrts = 13$ TeV with the ATLAS detector". In: *JHEP* 02 (2021), p. 226. DOI: 10.1007/JHEP02(2021)226. arXiv: 2011.05259 [hep-ex].

[Aad+21am] Georges Aad et al. "Search for dark matter in events with missing transverse momentum and a Higgs boson decaying into two photons in pp collisions at $sqrts = 13$ TeV with the ATLAS detector". In: *JHEP* 10 (2021), p. 013. DOI: 10.1007/JHEP10(2021)013. arXiv: 2104.13240 [hep-ex].

[Aad+21an] Georges Aad et al. “Search for Dark Matter Produced in Association with a Dark Higgs Boson Decaying into W^pmW^mp or ZZ in Fully Hadronic Final States from $sqrts = 13$ TeV pp Collisions Recorded with the ATLAS Detector”. In: *Phys. Rev. Lett.* 126.12 (2021), p. 121802. DOI: 10.1103/PhysRevLett.126.121802. arXiv: 2010.06548 [hep-ex].

[Aad+21ao] Georges Aad et al. “Search for dark matter produced in association with a single top quark in $sqrts = 13$ TeV pp collisions with the ATLAS detector”. In: *Eur. Phys. J. C* 81 (2021), p. 860. DOI: 10.1140/epjc/s10052-021-09566-y. arXiv: 2011.09308 [hep-ex].

[Aad+21ap] Georges Aad et al. “Search for dark matter produced in association with a Standard Model Higgs boson decaying into b-quarks using the full Run 2 dataset from the ATLAS detector”. In: *JHEP* 11 (2021), p. 209. DOI: 10.1007/JHEP11(2021)209. arXiv: 2108.13391 [hep-ex].

[Aad+21aq] Georges Aad et al. “Search for Displaced Leptons in $sqrts = 13$ TeV pp Collisions with the ATLAS Detector”. In: *Phys. Rev. Lett.* 127.5 (2021), p. 051802. DOI: 10.1103/PhysRevLett.127.051802. arXiv: 2011.07812 [hep-ex].

[Aad+21ar] Georges Aad et al. “Search for doubly and singly charged Higgs bosons decaying into vector bosons in multi-lepton final states with the ATLAS detector using proton-proton collisions at $sqrtmathrms = 13$ TeV”. In: *JHEP* 06 (2021), p. 146. DOI: 10.1007/JHEP06(2021)146. arXiv: 2101.11961 [hep-ex].

[Aad+21as] Georges Aad et al. “Search for exotic decays of the Higgs boson into long-lived particles in pp collisions at $sqrts = 13$ TeV using displaced vertices in the ATLAS inner detector”. In: *JHEP* 11 (2021), p. 229. DOI: 10.1007/JHEP11(2021)229. arXiv: 2107.06092 [hep-ex].

[Aad+21at] Georges Aad et al. “Search for heavy resonances decaying into a pair of Z bosons in the $ell^+ell^-ell'^+ell'^-$ and $ell^+ell^-nubarnu$ final states using 139 $mathrmfb^{-1}$ of protontextendashproton collisions at $sqrts = 13$,TeV with the ATLAS detector”. In: *Eur. Phys. J. C* 81.4 (2021), p. 332. DOI: 10.1140/epjc/s10052-021-09013-y. arXiv: 2009.14791 [hep-ex].

[Aad+21au] Georges Aad et al. “Search for Higgs boson production in association with a high-energy photon via vector-boson fusion with decay into bottom quark pairs at $sqrts$=13 TeV with the ATLAS detector”. In: *JHEP* 03 (2021), p. 268. DOI: 10.1007/JHEP03(2021)268. arXiv: 2010.13651 [hep-ex].

[Aad+21av] Georges Aad et al. “Search for new phenomena in pp collisions in final states with tau leptons, b-jets, and missing transverse momentum with the ATLAS detector”. In: *Phys. Rev. D* 104.11 (2021), p. 112005. DOI: 10.1103/PhysRevD.104.112005. arXiv: 2108.07665 [hep-ex].

[Aad+21aw] Georges Aad et al. “Search for new phenomena in events with an energetic jet and missing transverse momentum in *pp* collisions at *sqrts* =13 TeV with the ATLAS detector”. In: *Phys. Rev. D* 103.11 (2021), p. 112006. DOI: 10.1103/PhysRevD.103.112006. arXiv: 2102.10874 [hep-ex].

[Aad+21ax] Georges Aad et al. “Search for new phenomena in events with two opposite-charge leptons, jets and missing transverse momentum in pp collisions at *sqrtmathrms* = 13 TeV with the ATLAS detector”. In: *JHEP* 04 (2021), p. 165. DOI: 10.1007/JHEP04(2021)165. arXiv: 2102.01444 [hep-ex].

[Aad+21ay] Georges Aad et al. “Search for new phenomena in final states with b-jets and missing transverse momentum in *sqrts* = 13 TeV *pp* collisions with the ATLAS detector”. In: *JHEP* 05 (2021), p. 093. DOI: 10.1007/JHEP05(2021)093. arXiv: 2101.12527 [hep-ex].

[Aad+21az] Georges Aad et al. “Search for New Phenomena in Final States with Two Leptons and One or No b-Tagged Jets at *sqrts* = 13 TeV Using the ATLAS Detector”. In: *Phys. Rev. Lett.* 127.14 (2021), p. 141801. DOI: 10.1103/PhysRevLett.127.141801. arXiv: 2105.13847 [hep-ex].

[Aad+21ba] Georges Aad et al. “Search for new phenomena with top quark pairs in final states with one lepton, jets, and missing transverse momentum in *pp* collisions at *sqrts* = 13 TeV with the ATLAS detector”. In: *JHEP* 04 (2021), p. 174. DOI: 10.1007/JHEP04(2021)174. arXiv: 2012.03799 [hep-ex].

[Aad+21bb] Georges Aad et al. “Search for pair production of scalar leptoquarks decaying into first- or second-generation leptons and top quarks in protontextendashproton collisions at *sqrts* = 13 TeV with the ATLAS detector”. In: *Eur. Phys. J. C* 81.4 (2021), p. 313. DOI: 10.1140/epjc/s10052-021-09009-8. arXiv: 2010.02098 [hep-ex].

[Aad+21bc] Georges Aad et al. “Search for pair production of third-generation scalar leptoquarks decaying into a top quark and a *tau*-lepton in *pp* collisions at *sqrts* = 13 TeV with the ATLAS detector”. In: *JHEP* 06 (2021), p. 179. DOI: 10.1007/JHEP06(2021)179. arXiv: 2101.11582 [hep-ex].

[Aad+21bd] Georges Aad et al. “Search for phenomena beyond the Standard Model in events with large b-jet multiplicity using the ATLAS detector at the LHC”. In: *Eur. Phys. J. C* 81.1 (2021). [Erratum: Eur.Phys.J.C 81, 249 (2021)], p. 11. DOI: 10.1140/epjc/s10052-020-08730-0. arXiv: 2010.01015 [hep-ex].

[Aad+21be] Georges Aad et al. “Search for R-parity-violating supersymmetry in a final state containing leptons and many jets with the ATLAS experiment using *sqrts* = $13TeV$ protontextendashproton collision data”. In: *Eur. Phys. J. C* 81.11 (2021), p. 1023. DOI: 10.1140/epjc/s10052-021-09761-x. arXiv: 2106.09609 [hep-ex].

[Aad+21bf] Georges Aad et al. “Search for resonances decaying into photon pairs in 139 fb^{-1} of pp collisions at *sqrts*=13 TeV with the ATLAS detector”. In: *Phys. Lett. B* 822 (2021), p. 136651. DOI: 10.1016/j.physletb.2021.136651. arXiv: 2102.13405 [hep-ex].

[Aad+21bg] Georges Aad et al. “Search for squarks and gluinos in final states with jets and missing transverse momentum using 139 fb^{-1} of *sqrts* =13 TeV pp collision data with the ATLAS detector”. In: *JHEP* 02 (2021), p. 143. DOI: 10.1007/JHEP02(2021)143. arXiv: 2010.14293 [hep-ex].

[Aad+21bh] Georges Aad et al. “Search for squarks and gluinos in final states with one isolated lepton, jets, and missing transverse momentum at $sqrts = 13$ with the ATLAS detector”. In: *Eur. Phys. J. C* 81.7 (2021). [Erratum: Eur.Phys.J.C 81, 956 (2021)], p. 600. DOI: 10.1140/epjc/s10052-021-09748-8. arXiv: 2101.01629 [hep-ex].

[Aad+21bi] Georges Aad et al. “Search for supersymmetry in events with four or more charged leptons in 139 fb^{uc0u87221} of $sqrts = 13$ TeV pp collisions with the ATLAS detector”. In: *JHEP* 07 (2021), p. 167. DOI: 10.1007/JHEP07(2021)167. arXiv: 2103.11684 [hep-ex].

[Aad+21bj] Georges Aad et al. “Search for trilepton resonances from chargino and neutralino pair production in $sqrts = 13$ TeV pp collisions with the ATLAS detector”. In: *Phys. Rev. D* 103.11 (2021), p. 112003. DOI: 10.1103/PhysRevD.103.112003. arXiv: 2011.10543 [hep-ex].

[Aad+21bk] Georges Aad et al. “Search for type-III seesaw heavy leptons in dilepton final states in pp collisions at $sqrts = 13$ TeV with the ATLAS detector”. In: *Eur. Phys. J. C* 81.3 (2021), p. 218. DOI: 10.1140/epjc/s10052-021-08929-9. arXiv: 2008.07949 [hep-ex].

[Aad+21bl] Georges Aad et al. “Test of the universality of *tau* and *mu* lepton couplings in W-boson decays with the ATLAS detector”. In: *Nature Phys.* 17.7 (2021), pp. 813–818. DOI: 10.1038/s41567-021-01236-w. arXiv: 2007.14040 [hep-ex].

[Aad+21bm] Georges Aad et al. “The ATLAS Fast TracKer system”. In: *JINST* 16 (2021), P07006. DOI: 10.1088/1748-0221/16/07/P07006. arXiv: 2101.05078 [physics.ins-det].

[Aad+21bn] Georges Aad et al. “Two-particle azimuthal correlations in photonuclear ultraperipheral Pb+Pb collisions at 5.02 TeV with ATLAS”. In: *Phys. Rev. C* 104.1 (2021), p. 014903. DOI: 10.1103/PhysRevC.104.014903. arXiv: 2101.10771 [nucl-ex].

[Ale+21a] A. Alekou et al. “Updated physics performance of the ESSnuSB experiment: ESSnuSB collaboration”. In: *Eur. Phys. J. C* 81.12 (2021), p. 1130. DOI: 10.1140/epjc/s10052-021-09845-8. arXiv: 2107.07585 [hep-ex].

[Ale+21b] A. Alekou et al. “Updated physics performance of the ESSnuSB experiment: ESSnuSB collaboration”. In: *Eur. Phys. J. C* 81.12 (2021), p. 1130. DOI: 10.1140/epjc/s10052-021-09845-8. arXiv: 2107.07585 [hep-ex].

[Aun+21] S. Aune et al. “Timing performance of a multi-pad PICOSEC-Micromegas detector prototype”. In: *Nucl. Instrum. Meth. A* 993 (2021), p. 165076. DOI: 10.1016/j.nima.2021.165076. arXiv: 2012.00545 [physics.ins-det].

[Bor+21] J. Bortfeldt et al. “Modeling the Timing Characteristics of the PICOSEC Micromegas Detector”. In: *Nucl. Instrum. Meth. A* 993 (2021), p. 165049. DOI: 10.1016/j.nima.2021.165049. arXiv: 1901.10779 [physics.ins-det].

[Che+21] M. Chefdeville et al. “Development of Micromegas detectors with resistive anode pads”. In: *Nucl. Instrum. Meth. A* 1003 (2021), p. 165268. DOI: 10.1016/j.nima.2021.165268.

[Lei+21] A. Leisos et al. “Detection of high energy showers by the Astroneu extensive air shower array”. In: *New Astron.* 82 (2021), p. 101448. DOI: 10.1016/j.newast.2020.101448.

[Tza+21] S. E. Tzamarias et al. “Calibration Procedures for Accurate Timing and Directional Reconstruction of EAS Particle-fronts with Astroneu Stations”. In: *Instrum. Exp. Tech.* 64.1 (2021), pp. 127–140. DOI: 10.1134/S0020441220060202.

High Energy Physics - CMS

[Abb21] Abbiendi. “Status of the MUonE experiment,” in: *PoS.* (2021). DOI: https://doi.org/10.22323/1.390.0223.

[al21c] P. Asenov et al. “Study of p-type silicon MOS capacitors at HL-LHC radiation levels through irradiation with a cobalt-60 gamma source and a TCAD simulation”. In: *JINST 16 P06040* (2021). DOI: https://doi.org/10.1088/1748-0221/16/06/P06040.

[al21d] Sz. Borsanyi et al. “Leading hadronic contribution to the muon magnetic moment from lattice QCD”. In: *Nature* 593 (Apr. 2021). DOI: 10.1038/s41586-021-03418-1.

[al21e] W. Adam et al. “Beam test performance of prototype silicon detectors for the outer tracker for the phase-2 upgrade of CMS,” in: *JINST 15 (03) P03014.* (2021). DOI: https://doi:10.1088/1748-0221/15/03/p03014.

[CMS21] The Tracker group of the CMS collaboration. “Selection of the silicon sensor thickness for the Phase-2 upgrade of the CMS Outer Tracker”. In: *JOURNAL OF INSTRUMENTATION* 16.11 (Nov. 2021). DOI: 10.1088/1748-0221/16/11/P11028.

[Col21a] CMS Collaboration. “Angular analysis of the decay $B^+ \to K^*(892)^+\mu^+\mu^-$ in proton-proton collisions at $\sqrt{s} = 8\ TeV$”. In: *JOURNAL OF HIGH ENERGY PHYSICS* 4 (Apr. 2021). DOI: 10.1007/JHEP04(2021)124.

[Col21b] CMS Collaboration. "Combined searches for the production of supersymmetric top quark partners in proton-proton collisions at $\sqrt{s} = 13\ TeV$". In: *EUROPEAN PHYSICAL JOURNAL C* 81.11 (Nov. 2021). DOI: 10.1140/epjc/s10052-021-09721-5.

[Col21c] CMS Collaboration. "Comparative evaluation of analogue front-end designs for the CMS Inner Tracker at the High Luminosity LHC". In: *JOURNAL OF INSTRUMENTATION* 16.12 (Dec. 2021). DOI: 10.1088/1748-0221/16/12/P12014.

[Col21d] CMS Collaboration. "Constraints on anomalous Higgs boson couplings to vector bosons and fermions in its production and decay using the four-lepton final state". In: *PHYSICAL REVIEW D* 104.5 (Sept. 2021). DOI: 10.1103/PhysRevD.104.052004.

[Col21e] CMS Collaboration. "Constraints on the Initial State of Pb-Pb Collisions via Measurements of Z-Boson Yields and Azimuthal Anisotropy at $\sqrt{s_{NN}} = 5.02\,TeV$". In: *PHYSICAL REVIEW LETTERS* 127.10 (Aug. 2021). DOI: 10.1103/PhysRevLett.127.102002.

[Col21f] CMS Collaboration. "Correlations of azimuthal anisotropy Fourier harmonics with subevent cumulants in pPb collisions at $\sqrt{s_{NN}} = 8.16\ TeV$". In: *PHYSICAL REVIEW C* 103.1 (Jan. 2021). DOI: 10.1103/PhysRevC.103.014902.

[Col21g] CMS Collaboration. "Development and validation of HERWIG 7 tunes from CMS underlying-event measurements". In: *EUROPEAN PHYSICAL JOURNAL C* 81.4 (Apr. 2021). DOI: 10.1140/epjc/s10052-021-08949-5.

[Col21h] CMS Collaboration. "Electron and photon reconstruction and identification with the CMS experiment at the CERN LHC". In: *JOURNAL OF INSTRUMENTATION* 16.5 (May 2021). DOI: 10.1088/1748-0221/16/05/P05014.

[Col21i] CMS Collaboration. "Evidence for electroweak production of four charged leptons and two jets in proton-proton collisions at $\sqrt{s} = 13\ TeV$". In: *PHYSICS LETTERS B* 812 (Jan. 2021). DOI: 10.1016/j.physletb.2020.135992.

[Col21j] CMS Collaboration. "Evidence for Higgs boson decay to a pair of muons". In: *JOURNAL OF HIGH ENERGY PHYSICS* 1 (Jan. 2021). DOI: 10.1007/JHEP01(2021)148.

[Col21k] CMS Collaboration. "First measurement of large area jet transverse momentum spectra in heavy-ion collisions". In: *JOURNAL OF HIGH ENERGY PHYSICS* 5 (May 2021). DOI: 10.1007/JHEP05(2021)284.

[Col21l] CMS Collaboration. "First measurement of the cross section for top quark pair production with additional charm jets using dileptonic final states in pp collisions at $\sqrt{s} = 13\ TeV$". In: *PHYSICS LETTERS B* 820 (Sept. 2021). DOI: 10.1016/j.physletb.2021.136565.

[Col21m] CMS Collaboration. “Hard color-singlet exchange in dijet events in proton-proton collisions at $\sqrt{s} = 13\ TeV$”. In: *PHYSICAL REVIEW D* 104.3 (Aug. 2021). DOI: 10.1103/PhysRevD.104.032009.

[Col21n] CMS Collaboration. “In-medium modification of dijets in PbPb collisions at $\sqrt{s}(NN) = 5.02\ TeV$”. In: *JOURNAL OF HIGH ENERGY PHYSICS* 5 (May 2021). DOI: 10.1007/JHEP05(2021)116.

[Col21o] CMS Collaboration. “Measurement of b jet shapes in proton-proton collisions at $\sqrt{s} = 5.02\ TeV$”. In: *JOURNAL OF HIGH ENERGY PHYSICS* 5 (May 2021). DOI: 10.1007/JHEP05(2021)054.

[Col21p] CMS Collaboration. “Measurement of differential cross sections for Z bosons produced in association with charm jets in pp collisions at $\sqrt{s} = 13\ TeV$”. In: *JOURNAL OF HIGH ENERGY PHYSICS* 4 (Apr. 2021). DOI: 10.1007/JHEP04(2021)109.

[Col21q] CMS Collaboration. “Measurement of differential t(t)over-bar production cross sections in the full kinematic range using lepton plus jets events from proton-proton collisions at $\sqrt{s} = 13\ TeV$”. In: *PHYSICAL REVIEW D* 104.9 (Nov. 2021). DOI: 10.1103/PhysRevD.104.092013.

[Col21r] CMS Collaboration. “Measurement of differential t(t)over-bar production cross sections using top quarks at large transverse momenta in pp collisions at $\sqrt{s} = 13\ TeV$”. In: *PHYSICAL REVIEW D* 103.5 (Mar. 2021). DOI: 10.1103/PhysRevD.103.052008.

[Col21s] CMS Collaboration. “Measurement of prompt D-0 and D-0 meson azimuthal anisotropy and search for strong electric fields in PbPb collisions at $\sqrt{s_{NN}} = 5.02\ TeV$”. In: *PHYSICS LETTERS B* 816 (May 2021). DOI: 10.1016/j.physletb.2021.136253.

[Col21t] CMS Collaboration. “Measurement of prompt open-charm production cross sections in proton-proton collisions at $\sqrt{s} = 13\ TeV$”. In: *JOURNAL OF HIGH ENERGY PHYSICS* 11 (Nov. 2021). DOI: 10.1007/JHEP11(2021)225.

[Col21u] CMS Collaboration. “Measurement of single-diffractive dijet production in proton-proton collisions at $\sqrt{s} = 8\ TeV$ with the CMS and TOTEM experiments (vol 80, 1164, 2020)”. In: *EUROPEAN PHYSICAL JOURNAL C* 81.5 (May 2021). DOI: 10.1140/epjc/s10052-021-08863-w.

[Col21v] CMS Collaboration. “Measurement of the azimuthal anisotropy of Y(1S) and Y(2S) mesons in PbPb collisions at $\sqrt{s_{NN}} = 5.02\ TeV$”. In: *PHYSICS LETTERS B* 819 (Aug. 2021). DOI: 10.1016/j.physletb.2021.136385.

[Col21w] CMS Collaboration. “Measurement of the CP-violating phase phi(s) in the $B_s^0 \to J/\psi\phi(1020) \to \mu^+\mu^-K^+K^-$channel in proton-proton collisions at $\sqrt{s} = 13\ TeV$”. In: *PHYSICS LETTERS B* 816 (May 2021). DOI: 10.1016/j.physletb.2021.136188.

[Col21x] CMS Collaboration. “Measurement of the electroweak production of Z gamma and two jets in proton-proton collisions at $\sqrt{s} = 13\ TeV$ and constraints on anomalous quartic gauge couplings”. In: *PHYSICAL REVIEW D* 104.7 (Oct. 2021). DOI: 10.1103/PhysRevD.104.072001.

[Col21y] CMS Collaboration. “Measurement of the inclusive and differential Higgs boson production cross sections in the leptonic WW decay mode at $\sqrt{s} = 13\ TeV$”. In: *JOURNAL OF HIGH ENERGY PHYSICS* 3 (Mar. 2021). DOI: 10.1007/JHEP03(2021)003.

[Col21z] CMS Collaboration. “Measurement of the inclusive and differential t(t)over-bar gamma cross sections in the single-lepton channel and EFT interpretation at $\sqrt{s} = 13\ TeV$”. In: *JOURNAL OF HIGH ENERGY PHYSICS* 12 (Dec. 2021). DOI: 10.1007/JHEP12(2021)180.

[Col21aa] CMS Collaboration. “Measurement of the top quark mass using events with a single reconstructed top quark in pp collisions at $\sqrt{s} = 13\ TeV$”. In: *JOURNAL OF HIGH ENERGY PHYSICS* 12 (Dec. 2021). DOI: 10.1007/JHEP12(2021)161.

[Col21ab] CMS Collaboration. “Measurement of the W gamma Production Cross Section in Proton-Proton Collisions at $\sqrt{s} = 13\ TeV$ and Constraints on Effective Field Theory Coefficients”. In: *PHYSICAL REVIEW LETTERS* 126.25 (June 2021). DOI: 10.1103/PhysRevLett.126.252002.

[Col21ac] CMS Collaboration. “Measurement of the Z boson differential production cross section using its invisible decay mode (Z -¿ nu(nu)over-bar) in proton-proton collisions at $\sqrt{s} = 13\ TeV$”. In: *JOURNAL OF HIGH ENERGY PHYSICS* 5 (May 2021). DOI: 10.1007/JHEP05(2021)205.

[Col21ad] CMS Collaboration. “Measurements of angular distance and momentum ratio distributions in three-jet and Z plus two-jet final states in pp collisions”. In: *EUROPEAN PHYSICAL JOURNAL C* 81.9 (Sept. 2021). DOI: 10.1140/epjc/s10052-021-09570-2.

[Col21ae] CMS Collaboration. “Measurements of Higgs boson production cross sections and couplings in the diphoton decay channel at $\sqrt{s} = 13\ TeV$”. In: *JOURNAL OF HIGH ENERGY PHYSICS* 7 (July 2021). DOI: 10.1007/JHEP07(2021)027.

[Col21af] CMS Collaboration. “Measurements of pp -¿ ZZ production cross sections and constraints on anomalous triple gauge couplings at $\sqrt{s} = 13\ TeV$”. In: *EUROPEAN PHYSICAL JOURNAL C* 81.3 (Mar. 2021). DOI: 10.1140/epjc/s10052-020-08817-8.

[Col21ag] CMS Collaboration. “Measurements of production cross sections of polarized same-sign W boson pairs in association with two jets in proton-proton collisions at $\sqrt{s} = 13\ TeV$”. In: *PHYSICS LETTERS B* 812 (Jan. 2021). DOI: 10.1016/j.physletb.2020.136018.

[Col21ah] CMS Collaboration. "Measurements of production cross sections of the Higgs boson in the four-lepton final state in proton-proton collisions at $\sqrt{s} = 13\ TeV$". In: *EUROPEAN PHYSICAL JOURNAL C* 81.6 (June 2021). DOI: 10.1140/epjc/s10052-021-09200-x.

[Col21ai] CMS Collaboration. "Measurements of the differential cross sections of the production of Z plus jets and gamma plus jets and of Z boson emission collinear with a jet in pp collisions at $\sqrt{s} = 13\ TeV$". In: *JOURNAL OF HIGH ENERGY PHYSICS* 5 (May 2021). DOI: 10.1007/JHEP05(2021)285.

[Col21aj] CMS Collaboration. "Measurements of the Electroweak Diboson Production Cross Sections in Proton-Proton Collisions at $\sqrt{s} = 5.02\ TeV$ Using Leptonic Decays". In: *PHYSICAL REVIEW LETTERS* 127.9 (Nov. 2021). DOI: 10.1103/PhysRevLett.127.191801.

[Col21ak] CMS Collaboration. "Measurements of the pp -¿ W-+/-gamma gamma and pp -¿ Z gamma gamma cross sections at $\sqrt{s} = 13\ TeV$ and limits on anomalous quartic gauge couplings". In: *JOURNAL OF HIGH ENERGY PHYSICS* 10 (Oct. 2021). DOI: 10.1007/JHEP10(2021)174.

[Col21al] CMS Collaboration. "MUSiC: a model-unspecific search for new physics in proton-proton collisions at $\sqrt{s} = 13\ TeV$". In: *EUROPEAN PHYSICAL JOURNAL C* 81.7 (July 2021). DOI: 10.1140/epjc/s10052-021-09236-z.

[Col21am] CMS Collaboration. "Observation of a New Excited Beauty Strange Baryon Decaying to $\Xi_b^- \pi^+ \pi^-$". In: *PHYSICAL REVIEW LETTERS* 126.25 (June 2021). DOI: 10.1103/PhysRevLett.126.252003.

[Col21an] CMS Collaboration. "Observation of Forward Neutron Multiplicity Dependence of Dimuon Acoplanarity in Ultraperipheral Pb-Pb Collisions at $\sqrt{s_{NN}} = 5.02\ TeV$". In: *PHYSICAL REVIEW LETTERS* 127.12 (Sept. 2021). DOI: 10.1103/PhysRevLett.127.122001.

[Col21ao] CMS Collaboration. "Observation of tW production in the single-lepton channel in pp collisions at $\sqrt{s} = 13\ TeV$". In: *JOURNAL OF HIGH ENERGY PHYSICS* 11 (Nov. 2021). DOI: 10.1007/JHEP11(2021)111.

[Col21ap] CMS Collaboration. "Performance of the CMS muon trigger system in proton-proton collisions at $\sqrt{s} = 13\ TeV$". In: *JOURNAL OF INSTRUMENTATION* 16.7 (July 2021). DOI: 10.1088/1748-0221/16/07/P07001.

[Col21aq] CMS Collaboration. "Precision luminosity measurement in proton-proton collisions at root $\sqrt{s} = 13\ TeV$ in 2015 and 2016 at CMS". In: *EUROPEAN PHYSICAL JOURNAL C* 81.9 (Sept. 2021). DOI: 10.1140/epjc/s10052-021-09538-2.

[Col21ar] CMS Collaboration. "Probing effective field theory operators in the associated production of top quarks with a Z boson in multilepton final states at $\sqrt{s} = 13\,TeV$". In: *JOURNAL OF HIGH ENERGY PHYSICS* 12 (Dec. 2021). DOI: 10.1007/JHEP12(2021)083.

[Col21as] CMS Collaboration. "Search for a heavy Higgs boson decaying into two lighter Higgs bosons in the tau tau bb final state at $\sqrt{s} = 13\,TeV$". In: *JOURNAL OF HIGH ENERGY PHYSICS* 11 (Nov. 2021). DOI: 10.1007/JHEP11(2021)057.

[Col21at] CMS Collaboration. "Search for a heavy resonance decaying to a top quark and a W boson at $\sqrt{s} = 13\,TeV$ in the fully hadronic final state". In: *JOURNAL OF HIGH ENERGY PHYSICS* 12 (Dec. 2021). DOI: 10.1007/JHEP12(2021)106.

[Col21au] CMS Collaboration. "Search for a heavy vector resonance decaying to a Z boson and a Higgs boson in proton-proton collisions at $\sqrt{s} = 13\,TeV$". In: *EUROPEAN PHYSICAL JOURNAL C* 81.8 (Aug. 2021). DOI: 10.1140/epjc/s10052-021-09348-6.

[Col21av] CMS Collaboration. "Search for charged Higgs bosons produced in vector boson fusion processes and decaying into vector boson pairs in proton-proton collisions at $\sqrt{s} = 13\,TeV$". In: *EUROPEAN PHYSICAL JOURNAL C* 81.8 (Aug. 2021). DOI: 10.1140/epjc/s10052-021-09472-3.

[Col21aw] CMS Collaboration. "Search for chargino-neutralino production in events with Higgs and W bosons using 137 fb(-1) of proton-proton collisions at $\sqrt{s} = 13\,TeV$". In: *JOURNAL OF HIGH ENERGY PHYSICS* 10 (Oct. 2021). DOI: 10.1007/JHEP10(2021)045.

[Col21ax] CMS Collaboration. "Search for dark matter produced in association with a leptonically decaying Z boson in proton-proton collisions at $\sqrt{s} = 13\,TeV$". In: *EUROPEAN PHYSICAL JOURNAL C* 81.1 (Jan. 2021). DOI: 10.1140/epjc/s10052-020-08739-5.

[Col21ay] CMS Collaboration. "Search for dark matter produced in association with avleptonically decaying Z boson in proton-proton collisions at $\sqrt{s} = 13\,TeV$ (vol 81, 13, 2021)". In: *EUROPEAN PHYSICAL JOURNAL C* 81.4 (Apr. 2021). DOI: 10.1140/epjc/s10052-021-08959-3.

[Col21az] CMS Collaboration. "Search for dark photons in Higgs boson production via vector boson fusion in proton-proton collisions at $\sqrt{s} = 13\,TeV$". In: *JOURNAL OF HIGH ENERGY PHYSICS* 3 (Mar. 2021). DOI: 10.1007/JHEP03(2021)011.

[Col21ba] CMS Collaboration. "Search for lepton-flavor violating decays of the Higgs boson in the mu tau and e tau final states in proton-proton collisions at $\sqrt{s} = 13\,TeV$". In: *PHYSICAL REVIEW D* 104.3 (Aug. 2021). DOI: 10.1103/PhysRevD.104.032013.

[Col21bb] CMS Collaboration. "Search for Long-Lived Particles Decaying in the CMS End Cap Muon Detectors in Proton-Proton Collisions at $\sqrt{s} = 13\ TeV$". In: *PHYSICAL REVIEW LETTERS* 127.26 (Dec. 2021). DOI: 10.1103/PhysRevLett.127.261804.

[Col21bc] CMS Collaboration. "Search for long-lived particles decaying to jets with displaced vertices in proton-proton collisions at $\sqrt{s} = 13TeV$". In: *PHYSICAL REVIEW D* 104.5 (Sept. 2021). DOI: 10.1103/PhysRevD.104.052011.

[Col21bd] CMS Collaboration. "Search for long-lived particles using displaced jets in proton-proton collisions at $\sqrt{s} = 13\ TeV$". In: *PHYSICAL REVIEW D* 104.1 (July 2021). DOI: 10.1103/PhysRevD.104.012015.

[Col21be] CMS Collaboration. "Search for new particles in events with energetic jets and large missing transverse momentum in proton-proton collisions at $\sqrt{s} = 13\ TeV$". In: *JOURNAL OF HIGH ENERGY PHYSICS* 11 (Nov. 2021). DOI: 10.1007/JHEP11(2021)153.

[Col21bf] CMS Collaboration. "Search for new physics in top quark production with additional leptons in proton-proton collisions at $\sqrt{s} = 13\ TeV$ using effective field theory". In: *JOURNAL OF HIGH ENERGY PHYSICS* 3 (Mar. 2021). DOI: 10.1007/JHEP03(2021)095.

[Col21bg] CMS Collaboration. "Search for nonresonant Higgs boson pair production in final states with two bottom quarks and two photons in proton-proton collisions at $\sqrt{s} = 13\ TeV$". In: *JOURNAL OF HIGH ENERGY PHYSICS* 3 (Mar. 2021). DOI: 10.1007/JHEP03(2021)257.

[Col21bh] CMS Collaboration. "Search for resonant and nonresonant new phenomena in high-mass dilepton final states at $\sqrt{s} = 13\ TeV$". In: *JOURNAL OF HIGH ENERGY PHYSICS* 7 (July 2021). DOI: 10.1007/JHEP07(2021)208.

[Col21bi] CMS Collaboration. "Search for singly and pair-produced leptoquarks coupling to third-generation fermions in proton-proton collisions at $\sqrt{s} = 13\ TeV$". In: *PHYSICS LETTERS B* 819 (Aug. 2021). DOI: 10.1016/j.physletb.2021.136446.

[Col21bj] CMS Collaboration. "Search for supersymmetry in final states with two oppositely charged same-flavor leptons and missing transverse momentum in proton-proton collisions at $\sqrt{s} = 13\ TeV$". In: *JOURNAL OF HIGH ENERGY PHYSICS* 4 (Apr. 2021). DOI: 10.1007/JHEP04(2021)123.

[Col21bk] CMS Collaboration. "Search for the lepton flavor violating decay tau -¿ 3 mu in proton-proton collisions at $\sqrt{s} = 13\ TeV$". In: *JOURNAL OF HIGH ENERGY PHYSICS* 1 (Jan. 2021). DOI: 10.1007/JHEP01(2021)163.

[Col21bl] CMS Collaboration. "Search for the rare decay of the W boson into a pion and a photon in proton-proton collisions at $\sqrt{s} = 13\ TeV$". In: *PHYSICS LETTERS B* 819 (Aug. 2021). DOI: 10.1016/j.physletb.2021.136409.

[Col21bm] CMS Collaboration. "Search for top squark pair production using dilepton final states in pp collision data collected at $\sqrt{s} = 13\ TeV$". In: *EUROPEAN PHYSICAL JOURNAL C* 81.1 (Jan. 2021). DOI: 10.1140/epjc/s10052-020-08701-5.

[Col21bn] CMS Collaboration. "Search for top squark production in fully hadronic final states in proton-proton collisions at $\sqrt{s} = 13\ TeV$". In: *PHYSICAL REVIEW D* 104.5 (Sept. 2021). DOI: 10.1103/PhysRevD.104.052001.

[Col21bo] CMS Collaboration. "Search for top squarks in final states with two top quarks and several light-flavor jets in proton-proton collisions at $\sqrt{s} = 13\ TeV$". In: *PHYSICAL REVIEW D* 104.3 (Aug. 2021). DOI: 10.1103/PhysRevD.104.032006.

[Col21bp] CMS Collaboration. "Search for W ' bosons decaying to a top and a bottom quark at $\sqrt{s} = 13\ TeV$ in the hadronic final state". In: *PHYSICS LETTERS B* 820 (Sept. 2021). DOI: 10.1016/j.physletb.2021.136535.

[Col21bq] CMS Collaboration. "Studies of charm and beauty hadron long-range correlations in pp and pPb collisions at LHC energies". In: *PHYSICS LETTERS B* 813 (Feb. 2021). DOI: 10.1016/j.physletb.2020.136036.

[Col21br] CMS Collaboration. "Study of Drell-Yan dimuon production in proton-lead collisions at $\sqrt{s_{NN}} = 8.16\ TeV$". In: *JOURNAL OF HIGH ENERGY PHYSICS* 5 (May 2021). DOI: 10.1007/JHEP05(2021)182.

[Col21bs] CMS Collaboration. "Study of p-type silicon MOS capacitors at HL-LHC radiation levels through irradiation with a cobalt-60 gamma source and a TOAD simulation". In: *JOURNAL OF INSTRUMENTATION* 16.6 (June 2021). DOI: 10.1088/1748-0221/16/06/P06040.

[Col21bt] CMS Collaboration. "Study of Z boson plus jets events using variables sensitive to double-parton scattering in pp collisions at $sqrts 13\ TeV$". In: *JOURNAL OF HIGH ENERGY PHYSICS* 10 (Oct. 2021). DOI: 10.1007/JHEP10(2021)176.

[Col21bu] CMS Collaboration. "The CMS Phase-1 pixel detector upgrade". In: *JOURNAL OF INSTRUMENTATION* 16.2 (Feb. 2021). DOI: 10.1088/1748-0221/16/02/P02027.

[Col21bv] CMS Collaboration. "The very forward CASTOR calorimeter of the CMS experiment". In: *JOURNAL OF INSTRUMENTATION* 16.2 (Feb. 2021). DOI: 10.1088/1748-0221/16/02/P02010.

[G21] Anagnostou G. “Searching in 2-Dimensional mass space for final states with 2 invisible particles”. In: *J. High Energ. Phys. 2021, 112* (2021). DOI: https://doi.org/10.1007/JHEP07(2021)112.

High Energy Physics - Additional experimental activities

High Energy Physics - Theory

[AFN21a] M. Axenides, E. Floratos, and S. Nicolis. “The arithmetic geometry of AdS2 and its continuum limit”. In: *Symmetry, Integrability and Geometry: Methods and Applications (SIGMA)* 17 (2021). cited By 0. DOI: 10.3842/SIGMA.2021.004. URL: https://www.scopus.com/inward/record.uri?eid=2-s2.0-85104712364&doi=10.3842%2fSIGMA.2021.004&partnerID=40&md5=e755a4df27b4d20d390df01066a3395c.

[Axe+21b] M. Axenides et al. “M-Theory as a Dynamical System Generator”. In: cited By 0. 2021, pp. 73–89. DOI: 10.1007/978-3-030-70795-8_6. URL: https://www.scopus.com/inward/record.uri?eid=2-s2.0-85122015947&doi=10.1007%2f978-3-030-70795-8_6&partnerID=40&md5=b49265c9b4ec0607838851cef41dda56.

[Axe+21c] Minos Axenides et al. “Cascade of instabilities in the classical limit of the Berenstein-Maldacena-Nastase matrix model”. In: *Phys. Rev. D* 104.10 (2021), p. 106002. DOI: 10.1103/PhysRevD.104.106002. arXiv: 2109.01088 [hep-th].

[Bev+21a] G. Bevilacqua et al. “Progress on 2—loop Amplitude Reduction”. In: *J. Phys. Conf. Ser.* 2105.5 (2021), p. 012010. DOI: 10.1088/1742-6596/2105/1/012010.

[CPS21a] D. D. Canko, C. G. Papadopoulos, and N. Syrrakos. “Analytic Representation of All Planar Two-loop Five-point Master Integrals with One Off-shell Leg”. In: *Acta Phys. Polon. B* 52.8 (2021), pp. 1091–1098. DOI: 10.5506/APhysPolB.52.1091.

[CPS21b] D. D. Canko, C. G. Papadopoulos, and N. Syrrakos. “Simplified Differential Equations for Master Integrals at N^3LO”. In: *Acta Phys. Polon. B* 52.8 (2021), pp. 879–887. DOI: 10.5506/APhysPolB.52.879.

[Can+21] D. D. Canko et al. “Progress on Feynman Integrals for $2 \to 3$ scattering at NNLO”. In: *J. Phys. Conf. Ser.* 2105.4 (2021), p. 012009. DOI: 10.1088/1742-6596/2105/1/012009.

[FI21a] E. G. Floratos and J. Iliopoulos. “On Some Geometrical Properties of Gauge Theories”. In: *Acta Phys. Polon. B* 52.6-7 (2021), p. 745. DOI: 10.5506/APhysPolB.52.745.

[FI21b] E.G. Floratos and J. Iliopoulos. "ON SOME GEOMETRICAL PROPERTIES of GAUGE THEORIES". In: *Acta Physica Polonica B* 52.6 (2021). cited By 0, pp. 745–762. DOI: 10.5506/APHYSPOLB.52.745. URL: https://www.scopus.com/inward/record.uri?eid=2-s2.0-85109572836&doi=10.5506%2fAPHYSPOLB.52.745&partnerID=40&md5=94314784a0820ddac05ff523e245e4df.

[KMP21a] D. Katsinis, I. Mitsoulas, and G. Pastras. "The dressing method as non linear superposition in sigma models". In: *Journal of High Energy Physics* 2021.3 (2021). cited By 0. DOI: 10.1007/JHEP03(2021)024. URL: https://www.scopus.com/inward/record.uri?eid=2-s2.0-85102046630&doi=10.1007%2fJHEP03%282021%29024&partnerID=40&md5=9859b18a7607f732af7b92d1f6674b95.

[Kat21] Dimitrios Katsinis. "Entanglement entropy and gravity". PhD thesis. Athens Natl. Capodistrian U., 2021. DOI: 10.12681/eadd/49954.

[Kon21] S. Konitopoulos. "Closed algebras for higher rank, non-Abelian tensor gauge fields". In: *Nuclear Physics B* 963 (2021). cited By 0. DOI: 10.1016/j.nuclphysb.2020.115285. URL: https://www.scopus.com/inward/record.uri?eid=2-s2.0-85098137571&doi=10.1016%2fj.nuclphysb.2020.115285&partnerID=40&md5=522581dd6c0b12226c79eefefed30958.

[Kon+21] S. Konitopoulos et al. "Dark gravitational sectors on a generalized scalar-tensor vector bundle model and cosmological applications". In: *Physical Review D* 104.6 (2021). cited By 1. DOI: 10.1103/PhysRevD.104.064018. URL: https://www.scopus.com/inward/record.uri?eid=2-s2.0-85114900378&doi=10.1103%2fPhysRevD.104.064018&partnerID=40&md5=05d12eeca17f3195979b01242142

[PF21] A. Pavlidis and E. Floratos. "Quantum-Fourier-transform-based quantum arithmetic with qudits". In: *Physical Review A* 103.3 (2021). cited By 0. DOI: 10.1103/PhysRevA.103.032417. URL: https://www.scopus.com/inward/record.uri?eid=2-s2.0-85103658427&doi=10.1103%2fPhysRevA.103.032417&partnerID=40&md5=b61f0ec4619ad70cc9ee09094a558df8.

[Sav21b] George Savvidy. "Maximally Chaotic Dynamical System of Infinite Dimensionality". In: (May 2021). arXiv: 2105.12968 [nlin.CD].

[Syr21a] Nikolaos Syrrakos. "One-loop Feynman integrals for $2 \to 3$ scattering involving many scales including internal masses". In: *JHEP* 10 (2021), p. 041. DOI: 10.1007/JHEP10(2021)041. arXiv: 2107.02106 [hep-ph].

[Syr21c] Nikolaos Syrrakos. "Pentagon integrals to arbitrary order in the dimensional regulator". In: *JHEP* 06 (2021), p. 037. DOI: 10.1007/JHEP06(2021)037. arXiv: 2012.10635 [hep-ph].

Astroparticle Physics

[Age+21a] Michel Ageron et al. "Indirect dark matter searches with neutrinos from the Galactic Centre region with the ANTARES and KM3NeT telescopes". In: *PoS* ICRC2021 (2021), p. 537. DOI: 10.22323/1.395.0537.

[Age+21b] Michel Ageron et al. "PMT gain calibration and monitoring based on highly compressed hit information in KM3NeT". In: *JINST* 16.09 (2021), p. C09011. DOI: 10.1088/1748-0221/16/09/C09011. arXiv: 2108.11467 [astro-ph.IM].

[Aie+21a] S. Aiello et al. "Sensitivity to light sterile neutrino mixing parameters with KM3NeT/ORCA". In: *JHEP* 10 (2021), p. 180. DOI: 10.1007/JHEP10(2021)180. arXiv: 2107.00344 [hep-ex].

[Aie+21b] S. Aiello et al. "The KM3NeT potential for the next core-collapse supernova observation with neutrinos". In: *Eur. Phys. J. C* 81.5 (2021), p. 445. DOI: 10.1140/epjc/s10052-021-09187-5. arXiv: 2102.05977 [astro-ph.HE].

[Aie+21c] Sebastiano Aiello et al. "Architecture and performance of the KM3NeT front-end firmware". In: *J. Astron. Telesc. Instrum. Syst.* 7.1 (2021), p. 016001. DOI: 10.1117/1.JATIS.7.1.016001.

[Cir+21] Marco Circella et al. "Draw me a Neutrino: the first KM3NeT art contest". In: *PoS* ICRC2021 (2021), p. 1400. DOI: 10.22323/1.395.1400.

[D T+21] Dídac D. Tortosa et al. "KM3NeT Detection Unit Line Fit reconstruction using positioning sensors data". In: *JINST* 16.09 (2021), p. C09023. DOI: 10.1088/1748-0221/16/09/C09023. arXiv: 2109.04914 [astro-ph.IM].

[Man+21] Jerzy Manczak et al. "Neutrino non-standard interactions with the KM3NeT/ORCA detector". In: *PoS* ICRC2021 (2021), p. 1165. DOI: 10.22323/1.395.1165.

[Mar+21a] Antonio Marinelli et al. "KM3NeT/ARCA expectations in view of a novel multimessenger study of starburst galaxies". In: *JINST* 16.12 (2021), p. C12016. DOI: 10.1088/1748-0221/16/12/C12016. arXiv: 2108.00176 [astro-ph.HE].

[Nau+21] Lodewijk Nauta et al. "First neutrino oscillation measurement in KM3NeT/ORCA". In: *PoS* ICRC2021 (2021), p. 1123. DOI: 10.22323/1.395.1123.

[Sam+21] Dorothea Samtleben et al. "The Calibration Units of KM3NeT". In: *PoS* ICRC2021 (2021), p. 1096. DOI: 10.22323/1.395.1096.

[Sin+21a] Anna Sinopoulou et al. "Atmospheric neutrinos with the first detection units of KM3NeT-ARCA". In: *PoS* ICRC2021 (2021), p. 1134. DOI: 10.22323/1.395.1134.

[Sin+21b] Anna Sinopoulou et al. "Atmospheric neutrinos with the first detection units of KM3NeT/ARCA". In: *JINST* 16.11 (2021), p. C11015. DOI: 10.1088/1748-0221/16/11/C11015. arXiv: 2107.12721 [hep-ex].

[Sot+21] Alfonso Garcia Soto et al. "Sensitivity estimates for diffuse, point-like, and extended neutrino sources with KM3NeT/ARCA". In: *JINST* 16.09 (2021), p. C09030. DOI: 10.1088/1748-0221/16/09/C09030. arXiv: 2107.13050 [astro-ph.IM].

[Sta+21] Dimitris Stavropoulos et al. "Atmospheric neutrinos from the first KM3NeT/ORCA data and prospects for measuring the atmospheric neutrino flux". In: *PoS* ICRC2021 (2021), p. 1125. DOI: 10.22323/1.395.1125.

Nuclear Physics - Theory

[al21a] P. Vasileiou et al. "Experimental study of the nuclear structure of 180Hf: Preliminary results". In: *Proceedings of the 29th Annual Symposium of the Hellenic Nuclear Physics Society*. HNPS Advances in Nuclear Physics. 2021.

[al21b] A. Zyriliou et al. "Nuclear structure investigations in Yb isotopes". In: *Proceedings of the 29th Annual Symposium of the Hellenic Nuclear Physics Society*. HNPS Advances in Nuclear Physics. 2021.

[Bon+21a] D. Bonatsos et al. "Connecting the proxy-SU(3) symmetry to the shell model". In: *The European Physical Journal Web of Conferences* 252 (2021), p. 02004. DOI: 10.1051/epjconf/202125202004.

[Bon+21b] D. Bonatsos et al. "Shell model foundations of the proxy-SU(3) symmetry: Nucleon pairs creating nuclear deformation". In: *HNPS Advances in Nuclear Physics*. 2021.

[Bon+21c] D. Bonatsos et al. "Unified Picture of Nucleon Pairs Playing Leading Roles in Nuclear Collectivity." In: *Bulgarian Journal of Physics* 48.5-6 (2021), p. 441.

[Bon+21d] Dennis Bonatsos et al. "Energy differences of ground state and $\gamma 1$ bands as a hallmark of collective behavior". In: *Nuclear Physics A* 1009 (2021), p. 122158. DOI: 10.1016/j.nuclphysa.2021.122158.

[Mar21a] Andriana Martinou. "A mechanism for shape coexistence". In: *The European Physical Journal Web of Conferences* 252 (2021). Ed. by A. Pakou et al., p. 02005. DOI: 10.1051/epjconf/202125202005.

[Mar21b] Andriana Martinou. "The L-projection of the shell model SU(3) wave functions". In: *Bulgarian Journal of Physics* 48 (2021), p. 557.

[Mar21c] Andriana Martinou. "The microscopic origin of the Interacting Boson Model". In: *Proceedings of the 29th Annual Symposium of the Hellenic Nuclear Physics Society*. HNPS Advances in Nuclear Physics. 2021.

[Mar+21b] Andriana Martinou et al. "Highest weight irreducible representations favored by nuclear forces within SU(3)-symmetric fermionic systems". In: *The European Physical Journal Web of Conferences* 252 (2021). Ed. by A. Pakou et al., p. 02006. DOI: 10.1051/epjconf/202125202006.

[Mar+21c] Andriana Martinou et al. "The islands of shape coexistence within the Elliott and the proxy-SU(3) Models". In: *European Physical Journal A* 57 (2021), p. 84. DOI: 10.1140/epja/s10050-021-00396-w.

[Mar+21d] Andriana Martinou et al. "Why nuclear forces favor the highest weight irreducible representations of the fermionic SU(3) symmetry". In: *European Physical Journal A* (2021). DOI: 10.1140/epja/s10050-021-00395-x.

[Mer+21] T.J. Mertzimekis et al. "Experimental investigations of nuclear structure around A=180". In: *Bulgarian Journal of Physics* 48 (2021), p. 625.

[Per21] Spyridon Peroulis. *Electric quadrupole transitions in Algebraic Nuclear Models*. 2021. DOI: 10.26240/HEAL.NTUA.21869.

[SHB21] Hadi Sobhani, Hassan Hassanabadi, and Dennis Bonatsos. "Resolution of the spin paradox in the Nilsson model". In: *The European Physical Journal Plus* 136.4 (2021), p. 398. DOI: 10.1140/epjp/s13360-021-01300-7.

[Sob+21] Hadi Sobhani et al. "An analytical description of the parity-doublet structure in an odd-A nucleus". In: *Nuclear Physics A* 1013 (2021), p. 122224. DOI: 10.1016/j.nuclphysa.2021.122224.

[Vas+21b] P. Vasileiou et al. "Experimental investigation of the nuclear structure in the neutron-rich 180Hf". In: *Bulgarian Journal of Physics* 48 (2021), p. 618.

[Zyr+21] A. Zyriliou et al. "Reviewing nuclear structure properties of even-even Yb isotopes". In: *Bulgarian Journal of Physics* 48 (2021), p. 608.

Nuclear Physics - Experimental

[Geo+21a] E. Georgali et al. "Cross-section measurements of the $^{156}\mathrm{Dy}(n, 2n)^{155}\mathrm{Dy}$ reaction at neutron energies higher than 17 MeV". In: *Phys. Rev. C* 104 (6 2021), p. 064603. DOI: 10.1103/PhysRevC.104.064603. URL: https://link.aps.org/doi/10.1103/PhysRevC.104.064603.

[Geo+21b] E. Georgali et al. “Using GEANT4 Monte Carlo simulations to resolve low energy γ-ray spectra: The study of 164Hog+m decay using a broad energy HPGe detector”. In: *Nuclear Instruments and Methods in Physics Research Section A: Accelerators, Spectrometers, Detectors and Associated Equipment* 985 (2021), p. 164711. ISSN: 0168-9002. DOI: https://doi.org/10.1016/j.nima.2020.164711. URL: https://www.sciencedirect.com/science/article/pii/S0168900220311086.

[Har+21a] S. Harissopulos et al. “Cross section measurements of proton capture reactions on Sr isotopes for astrophysics applications”. In: *Phys. Rev. C* 104 (2 2021), p. 025804. DOI: 10.1103/PhysRevC.104.025804. URL: https://link.aps.org/doi/10.1103/PhysRevC.104.025804.

[Har+21b] S. Harissopulos et al. “The Tandem Accelerator Laboratory of NCSR ”Demokritos”: current status and perspectives”. In: *The European Physical Journal Plus* 136.6 (2021), p. 617. ISSN: 2190-5444. DOI: 10.1140/epjp/s13360-021-01596-5. URL: https://doi.org/10.1140/epjp/s13360-021-01596-5.

[Kol+21] Konstantinos Kollias et al. “Dissolution and sorption mechanisms at the aluminosilicate and carbonate mineral-AMD (Acid Mine Drainage) interface”. In: *Applied Geochemistry* 131 (2021), p. 105027. ISSN: 0883-2927. DOI: https://doi.org/10.1016/j.apgeochem.2021.105027. URL: https://www.sciencedirect.com/science/article/pii/S0883292721001591.

[Mic+21a] V. Michalopoulou et al. “Erratum to: Measurement of the $^{232}Th(n, f)$ cross section with quasi-monoenergetic neutron beams in the energy range 2β€“18 MeV”. In: *The European Physical Journal A* 57.11 (2021), p. 306. ISSN: 1434-601X. DOI: 10.1140/epja/s10050-021-00613-6. URL: https://doi.org/10.1140/epja/s10050-021-00613-6.

[Mic+21b] V. Michalopoulou et al. “Measurement of the $^{232}Th(n, f)$ cross section with quasi-monoenergetic neutron beams in the energy range 2β€“18 MeV”. In: *The European Physical Journal A* 57.9 (2021), p. 277. ISSN: 1434-601X. DOI: 10.1140/epja/s10050-021-00590-w. URL: https://doi.org/10.1140/epja/s10050-021-00590-w.

[VAD21] E. Vagena, M. Axiotis, and P. Dimitriou. “Systematics of the semimicroscopic proton-nucleus optical potential at low energies relevant for nuclear astrophysics”. In: *Phys. Rev. C* 103 (4 2021), p. 045806. DOI: 10.1103/PhysRevC.103.045806. URL: https://link.aps.org/doi/10.1103/PhysRevC.103.045806.

[Vas+21a] P. Vasileiou et al. “An investigation of radiative proton–capture reactions in the Cd–In mass region”. In: *Nuclear Physics A* 1015 (2021), p. 122298. ISSN: 0375-9474. DOI: https://doi.org/10.1016/j.nuclphysa.2021.122298. URL: https://www.sciencedirect.com/science/article/pii/S0375947421001639.

X-Ray Spectrometry

[Ayr+21a] Vibha Ayri et al. "Experimental evidence for onset of L1–L3M5 transition at Z = 75 through measurements of fluorescence and Coster–Kronig yields for W and Re". In: *J. Anal. At. Spectrom.* 36 (2 2021), pp. 380–389. DOI: 10.1039/D0JA00455C. URL: http://dx.doi.org/10.1039/D0JA00455C.

[Ayr+21b] Vibha Ayri et al. "Experimental L-series x ray production cross sections for Re by tuning synchrotron radiation across its Li (i=1–3) sub-shell ionization thresholds". In: *Radiation Physics and Chemistry* 188 (2021), p. 109599. ISSN: 0969-806X. DOI: https://doi.org/10.1016/j.radphyschem.2021.109599. URL: https://www.sciencedirect.com/science/article/pii/S0969806X21002498.

[Ayr+21c] Vibha Ayri et al. "Measurements of L x-ray intensity ratios for 75Re at incident photon energies across its Li (i=1-3) edge energies". In: *AIP Conference Proceedings* 2352.1 (Aug. 2021), p. 050004. ISSN: 0094-243X. DOI: 10.1063/5.0052425. eprint: https://pubs.aip.org/aip/acp/article-pdf/doi/10.1063/5.0052425/14232316/050004_1_online.pdf. URL: https://doi.org/10.1063/5.0052425.

[Bre+21] Hariclia Brecoulaki et al. "Re-presenting in colours at the 'Palace of Nestor': Original polychromy and painting materials". In: *Representations: Material and immaterial modes of communication in the Bronze Age Aegean*. Ed. by JohnEditor Bennet. Vol. 3. Oxbow Books, 2021, pp. 53–106. URL: https://hdl.handle.net/10442/18774.

[Gek+21] Georgia Geka et al. "CuO/PMMA Polymer Nanocomposites as Novel Resist Materials for E-Beam Lithography". In: *Nanomaterials* 11.3 (2021). ISSN: 2079-4991. DOI: 10.3390/nano11030762. URL: https://www.mdpi.com/2079-4991/11/3/762.

[Gin+21] Maria Gini et al. "Inter-laboratory comparison of ED-XRF/PIXE analytical techniques in the elemental analysis of filter-deposited multi-elemental certified reference materials representative of ambient particulate matter". In: *Science of The Total Environment* 780 (2021), p. 146449. ISSN: 0048-9697. DOI: https://doi.org/10.1016/j.scitotenv.2021.146449. URL: https://www.sciencedirect.com/science/article/pii/S0048969721015175.

[Har+21c] S. Harissopulos et al. "The Tandem Accelerator Laboratory of NCSR "Demokritos": current status and perspectives". In: *The European Physical Journal Plus* 136.6 (2021), p. 617. ISSN: 2190-5444. DOI: 10.1140/epjp/s13360-021-01596-5. URL: https://doi.org/10.1140/epjp/s13360-021-01596-5.

[Kau+21a] Sandeep Kaur et al. “Experimental validation of theoretically predicted cut-off of L1–L3M4,5 transitions at Z = 50 through measurements of fluorescence and Coster–Kronig yields for Sn and Sb”. In: *Metrologia* 58.3 (2021), p. 035002. DOI: 10.1088/1681-7575/abe988. URL: https://dx.doi.org/10.1088/1681-7575/abe988.

[Kau+21b] Sandeep Kaur et al. “Measurements of L x-ray intensity ratios for 51Sb at incident photon energies across its Li(i=1-3) edge energies”. In: *AIP Conference Proceedings* 2352.1 (Aug. 2021), p. 050002. ISSN: 0094-243X. DOI: 10.1063/5.0052413. eprint: https://pubs.aip.org/aip/acp/article-pdf/doi/10.1063/5.0052413/14234084/050002_1_online.pdf. URL: https://doi.org/10.1063/5.0052413.

[Kla+21] N.K. Kladouri et al. “Bronze votive pins from the sanctuary of Athena Alea at Tegea, Arcadia, Greece, ca. 9th-7th BCE: A microscopic and compositional study using portable micro X-ray fluorescence spectrometry (micro-XRF)”. In: *Journal of Archaeological Science: Reports* 37 (2021), p. 102975. ISSN: 2352-409X. DOI: https://doi.org/10.1016/j.jasrep.2021.102975. URL: https://www.sciencedirect.com/science/article/pii/S2352409X21001875.

[Les+21] Diah Dwiana Lestiani et al. “Selected elements characterization of fine particulate matter PM2.5 using synchrotron radiation XRF”. In: *AIP Conference Proceedings* 2381.1 (Nov. 2021), p. 020035. ISSN: 0094-243X. DOI: 10.1063/5.0066285. eprint: https://pubs.aip.org/aip/acp/article-pdf/doi/10.1063/5.0066285/13717584/020035_1_online.pdf. URL: https://doi.org/10.1063/5.0066285.

[Mih+21] Iva Božičević Mihalić et al. “Multivariate analysis of PIXE + XRF and PIXE spectral images”. In: *J. Anal. At. Spectrom.* 36 (3 2021), pp. 654–667. DOI: 10.1039/D0JA00529K. URL: http://dx.doi.org/10.1039/D0JA00529K.

[Tas+21] Nikoleta Tasiouli et al. “Study and Conservation of a 19th Century Printed Silk Scarf from the Collection of the National Historical Museum of Greece”. In: *Archaeology* 9 (2021), pp. 56–67. ISSN: 2352-838X. DOI: 10.5923/j.archaeology.20210901.11. URL: http://article.sapub.org/10.5923.j.archaeology.20210901.11.html.